GUIDELINES FOR DESIGNING REINFORCEMENT INTERVENTIONS WITH THE RESISTO 5.9 SYSTEM

VERSION 01 - 17/06/2022

Translation in English from the original report in Italian provided by RubiconEX S.r.l.

TABLE OF CONTENTS

LIST OF TABLES

LIST OF FIGURES

1 FOREWORD

A numerical-experimental study was conducted at Fondazione EUCENTRE, Pavia, in order to assess the in-plane seismic behaviour of an innovative modular steel reinforcement system for load-bearing masonry (Resisto 5.9) designed by Progetto Sisma s.r.l.. The main purpose of the research concerns the evaluation of the seismic performance of existing load-bearing masonry walls and buildings reinforced with the proposed system.

The results of the research provided initial indications for the structural design of the system, summarised in this document.

2 REINFORCEMENT SYSTEM: DESCRIPTION OF THE SYSTEM

2.1 Description of the Resisto 5.9 reinforcement system

Resisto 5.9 is a modular steel consolidation system for existing masonry buildings. The reinforcement system is integrated with thermal cladding, as illustrated in Figure 2.1.

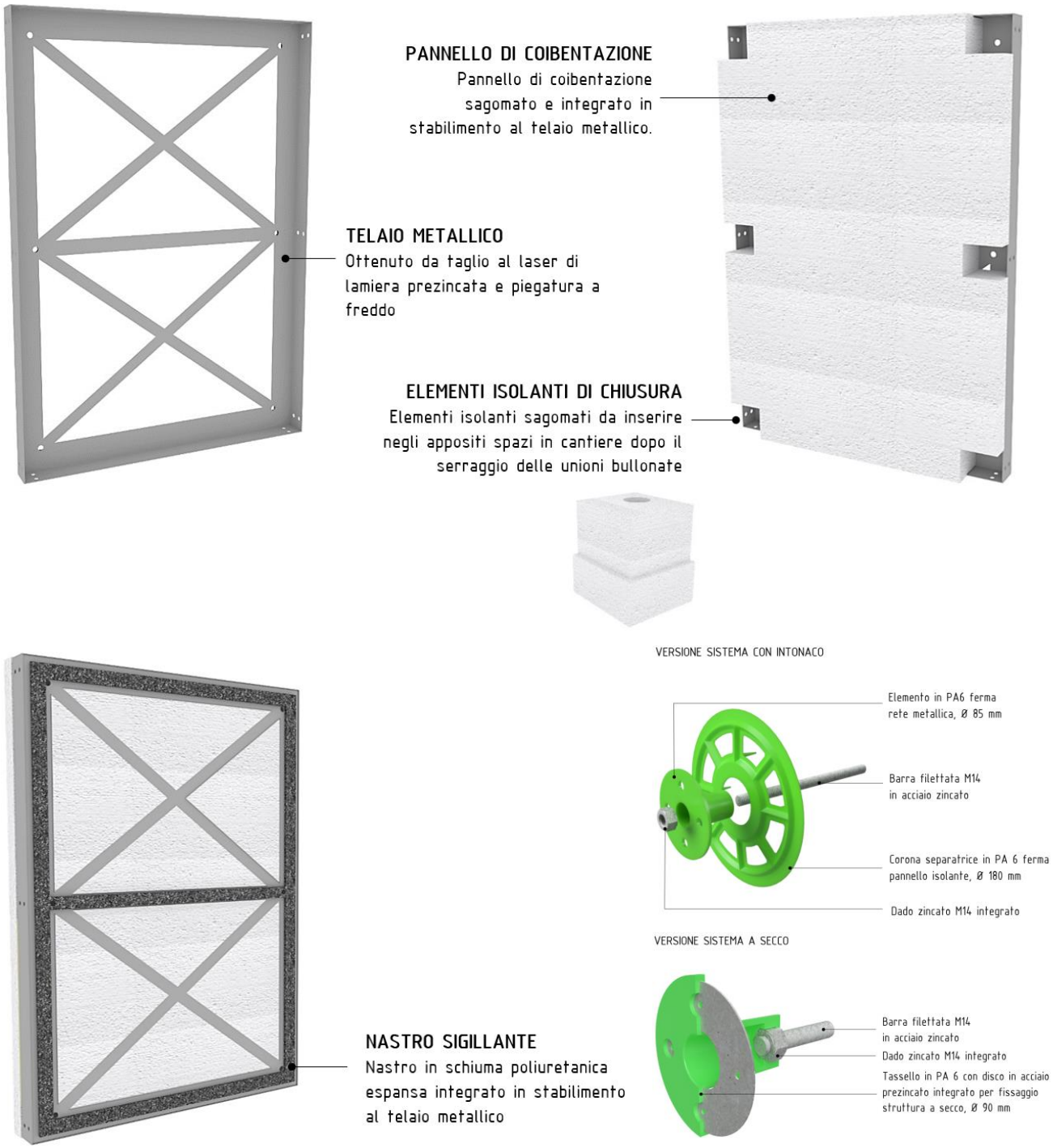

Figure 2.1 Reinforcement system with thermal cladding

The reinforcement system is intended to guarantee:

- An increase in the degree of connection between orthogonal walls, encouraging building box action of the building;
- Enhanced connection between walls and horizontal structures;
- A reduced chance of out-of-plane overturning of walls;
- Effective absorption of unopposed horizontal thrust;
- Improved distribution of seismic actions between the pier elements of the building;
- Improvement of the seismic performance of pier elements and coupling beams.

The system consists of suitably interconnected steel elements (frames) that are connected to masonry. The metal frames, obtained by the cold folding and laser cutting of 3 mm thick galvanised S250GD+Z structural steel (yield strength of steel f_y=250 MPa, tensile strength of steel f_u=330 MPa), are rectangular in shape (except for special completion pieces) with standard dimensions of 1150 mm x 1500 mm, consisting of an L-shaped cross-section frame measuring 88 mm x 80 mm, horizontal beams 50 mm wide and diagonal bracing that is 40 mm wide. Holes along the frame enable anchoring to masonry and the connection of modules (Figure 2.2).

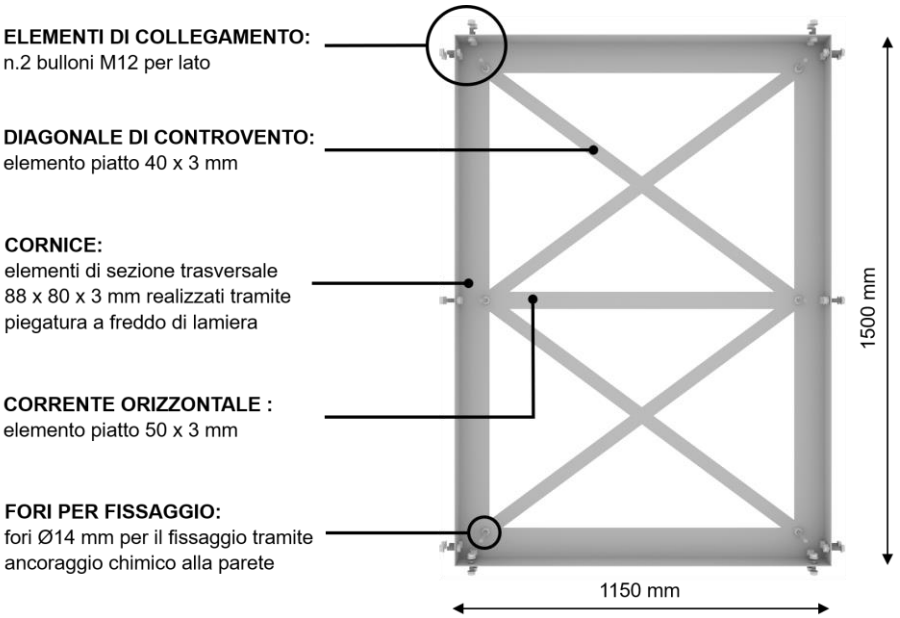

Figure 2.2 Base module of the reinforcement system.

The modules must be adhesive-laid onto the external surface of the wall, aligned and connected to masonry by means of non pass-through anchors of equal pitch (between 700 and 1000 mm). Anchoring must be chemical and requires the injection of a specific resin into holes of suitable diameter and depth (according to the anchor manufacturer's specifications) followed by the insertion of class 8.8 M14 steel threaded bars, to which the metal frames are fastened by means of M14 class 8 nuts and washers. Each module is also connected to any adjacent ones by means of class 8.8 steel bolts and M12 class 8 nuts and washers (Figure 2.3).

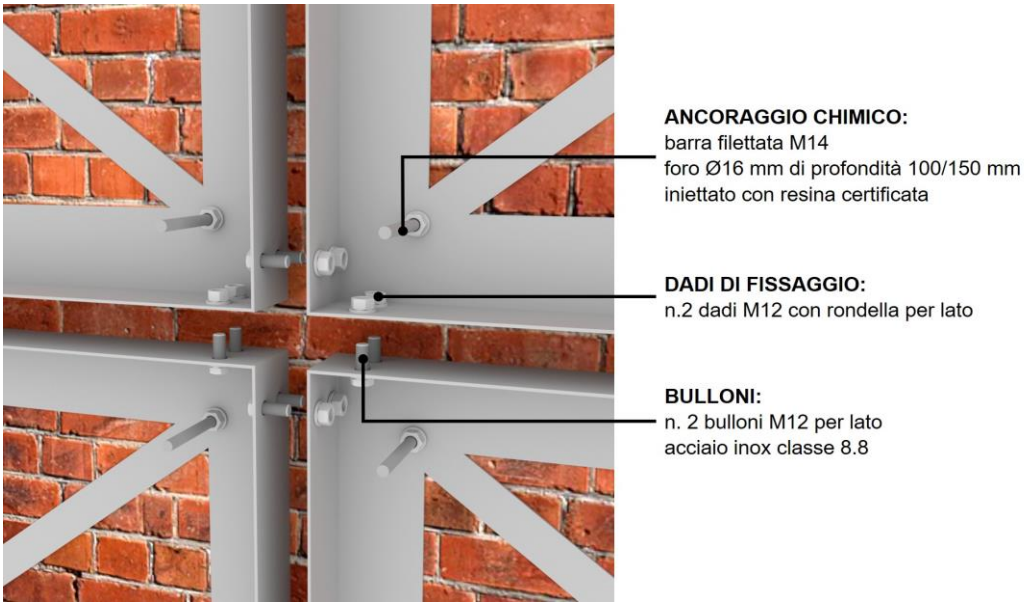

Figure 2.3 Diagram of the system for the connection of steel modules and anchoring to masonry wall.

Finally, the system is completed by metal plate corner profiles for the connection of metal modules on all the building's masonry façades and to achieve a continuous and global structural framing (Figure 2.4).

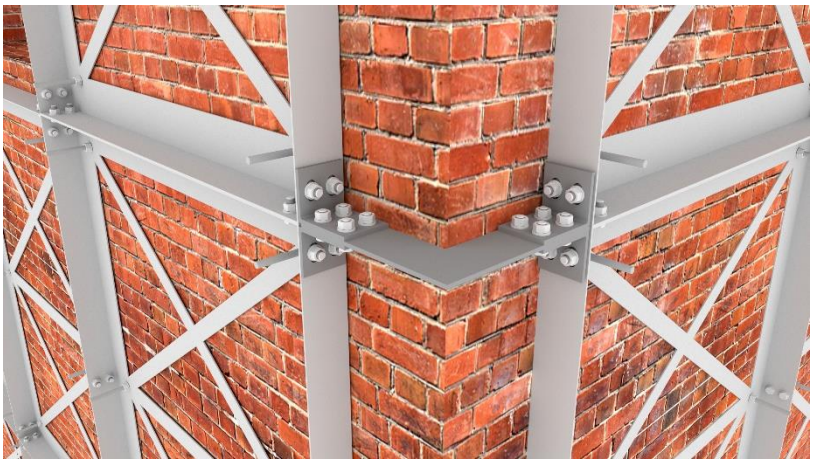

Figure 2.4 Diagram of the three-dimensional connection system between the reinforcement frames at the intersection of damaged masonry walls.

Frames must be positioned to ensure the continuity of reinforcing elements vertically, horizontally and diagonally. The distance between the first frame from the free edge of masonry, for both corners and openings, must be around 10-15 cm. Figure 2.5 shows an example of the application of the reinforcement system on a wall with openings and a gable, by coupling standard modules and suitably sized special pieces.

Figure 2.5 Example of the application of the reinforcement on a wall with openings.

Application of the reinforcement system involves the following steps:

- Identification of the position of the anchoring holes by temporarily positioning the modular elements against the wall (using suitable shims such as wooden slats);
- Drilling of holes (after removal of the metal module from the wall), taking care not to use the hammer function of the drill to avoid local damage to the masonry (mortar joints, brick edges);
- Repositioning of the metal module;
- Injection of the chemical anchor, in the quantity recommended by the manufacturer, according to the diameter and depth of the holes, in such a way as to as far as possible avoid (during bar section insertion) leakage of material that could leak between the masonry and the metal frame;
- Insertion of the bar sections into the holes, according to the chemical anchor manufacturer's instructions (turning the section inside the hole to ensure adherence between the resin and the thread of the bar), paying particular attention to their perfect orthogonality with respect to the wall surface;
- Fixing of the metal module to the wall by means of washers and bolts (also with partial tightening), after waiting no less than the setting time of the chemical anchor recommended by the manufacturer;
- Connection of the metal modules by means of bolts and nuts;
- Verification of the tightening of all connections according to the design instructions.

3 LEGISLATIVE FRAMEWORK

The Resisto 5.9 modular steel system is an integrated intervention that aims to improve the seismic performance and enhance the energy efficiency of existing buildings. In its application as reinforcement of load-bearing masonry buildings, the system combines aspects of novelty and originality to such an extent that there is to date neither established literature on the subject nor specific regulatory references.

In structural terms, the purpose of the Resisto 5.9 System is the seismic improvement/updating of bearing masonry buildings pursuant to §§ 8.4.2 and 8.4.3 of Technical Standard for Construction NTC 2018, and it is generally implemented as a global intervention, in order to requalify the structure as a whole. This objective may be pursued by improving the performance levels of local mechanisms/kinematics (or “mode I”, for example out-of-plane overturning of façades), or by acting on global mechanisms (or “mode II”, linked to the behaviour of the entire building's structural elements within their own plane), as stated in § 8.7.1 of NTC 2018 and in §§ C8.7.1, C8.7.1.2 (Local Mechanisms – seismic response analysis methods and verification criteria) and C8.7.1.3 (Global Mechanisms – seismic response analysis methods and verification criteria) of Circular 7/2019 of NTC2018.

In some particular cases, the system can also be used as a local intervention pursuant to § 8.4.1 of the Technical Standards for Construction NTC 2018, applied to single masonry portions or elements (individual walls, for example), in order to reduce the vulnerability of the structure when subjected to local mechanisms/kinematics.

3.1 Use of the Resisto 5.9 reinforcement system in the context of NTC 2018

The national and international frameworks do not contain adverse indications as to the use of this modular system as a reinforcement solution for load-bearing masonry. Reinforcement is in fact a special metal bracing system applied directly to masonry.

In the national regulatory context (NTC 2018 and its Circular), § 8.7.4 of the NTC 2018 “Criteria and types of intervention” provides general indications on the aspects to be evaluated and taken care of in the implementation of interventions. The corresponding § C8.7.4.1 “Criteria for consolidation interventions on masonry buildings” of the NTC 2018 Circular goes into more detail, provides further indications and reads as follows:

> *“This chapter provides general criteria for the consolidation of masonry buildings, with reference to some commonly used techniques, with reference to some commonly used techniques. The following criteria and techniques are indicative and not exhaustive and do not exclude the use of unmentioned intervention techniques, innovative methodologies or particular solutions that the designer identifies as suitable for the specific case. Attention must be paid to the execution phase of interventions in order to avoid compromising their effectiveness. In addition to interventions aimed at remedying deficiencies with respect to non-seismic actions, those that generally induce the greatest benefits with respect to seismic actions concern:*
>
> *1. The formation of floor diaphragms at floor level and possibly in the roof pitches.*
>
> *2. The connections of walls to each other and to floor diaphragms.*
>
> *3. The connections in the wall thickness in the presence of multiple façades.*
>
> *4. The increase of seismic strength of walls.*
>
> *5. The containment of thrusts and the consolidation of arches and vaults.*
>
> *Below are some indicative technical solutions for some of the above improvements.*
>
> *(…)*
>
> ***4. Increased capacity of walls***
>
> *(…)*

Walls may be reinforced by means of integrative cooperating structural elements installed on the surface; such elements may, for example, be made of steel (reticular structures consisting of plates/ tapes) or wood (panelling). Suitable connections must enable the cooperation of existing walls and the reinforcement.

(…)"

National standards therefore allow the use of integrative collaborative structural elements arranged on the surface and expressly indicate those *"made of steel with reticular structures consisting of plates and tapes"*, a solution into which the Resisto 5.9 reinforcement system falls.

3.2 Identification, qualification and acceptance of the Resisto 5.9 reinforcement system

As described in detail in the previous § 2.1, the modular system is manufactured by the cold folding of thin galvanised steel class S250GD+Z sheets.

The steel elements used (profiles and bolts) are standardized in NTC 2018, with reference to § 4.2 and § 11.3, the sub-section of which § 11.3.4 gives specific guidance for steelwork structures. In particular, § 11.3 also provides reference for the evaluation of the mechanical properties of the steel and bolts used in the reinforcement system and for the material identification, qualification and acceptance procedures. With regards to anchoring on masonry, reference can be made to EAD Guidelines 330076-00-0604 (EOTA 2014) and Technical Reports TR-053 (EOTA 2016a) and TR-054 (EOTA 2016b).

For the structural design and verification of steel elements and bolted connections, the regulatory reference is § 4.2 in the case of non-seismic actions and § 7.5 for seismic actions.

3.2.1 On-site acceptance of the Resisto 5.9 system according to NTC 2018

The following concerns on-site acceptance according to NTC 2018 of the components that make up the modular steel system for reinforcing masonry elements of existing load-bearing masonry buildings, called Resisto 5.9, designed and manufactured by Progetto Sisma s.r.l.

The system consists of modular steel elements (frames) that are suitably interconnected to each other by bolted joints and connected to the masonry by means of chemical anchoring. The metal frames are obtained by the cold folding and laser cutting of 3 mm thick galvanised S250GD+Z structural steel sheets. The steel of the frames has a CE marking and is processed at certified Processing Centres.

Holes along the frame enable anchoring to masonry and the connection of modules. Each module is connected to any adjacent ones by means of M12 steel bolts and nuts, class 8.8 and class 8 respectively, all of them CE-marked. Moreover, the steel modules are connected to the masonry through chemical anchoring using CE-marked resins of class 8.8 M14 threaded bars in accordance with EAD Guidelines 330076-00-0604 (EOTA 2014) and Technical Reports TR-053 (EOTA 2016a) and TR-054 (EOTA 2016b) and subsequent fastening using M14 nuts and washers made of class 8 steel.

The application of the system is completed with CE-marked thermal cladding.

From a regulatory perspective, the Resisto 5.9 reinforcement system is among those listed in §C8.7.4.1 "Criteria for consolidation interventions on masonry buildings" of the NTC 2018 Circular (point 4., fifth paragraph) which reads as follows: *"Walls may be reinforced by means of integrative cooperating structural elements installed on the surface; such elements may, for example, be made of steel (reticular structures consisting of plates/ tapes) or wood (panelling). Suitable connections must enable the cooperation of existing walls and the reinforcement."*

The system thus described is produced on a project-specific basis for each installation. The reinforcement of masonry with the modular system is therefore a prototype in its own right, whose functioning is certified by appropriate calculations based on the methods of Construction Science and Technology in accordance with the indications of the Technical Standards for Construction and cannot therefore be considered a standard product.

4 ANALYSIS AND VERIFICATION CRITERIA FOR THE DESIGN OF REINFORCEMENT OF EXISTING MASONRY BUILDINGS WITH THE RESISTO 5.9 SYSTEM

The purpose of the Resisto 5.9 System is the seismic improvement/updating of bearing masonry buildings pursuant to §§ 8.4.2 and 8.4.3 of Technical Standard for Construction NTC 2018, and it is generally implemented as a global intervention, in order to requalify the structure as a whole.

This objective may be pursued by improving the performance levels of local mechanisms/kinematics (or “mode I”, for example out-of-plane overturning of façades), or by acting on global mechanisms (or “mode II”, linked to the behaviour of the entire building's structural elements within their own plane), as stated in § 8.7.1 of NTC 2018 and in §§ C8.7.1, C8.7.1.2 (Local Mechanisms – seismic response analysis methods and verification criteria) and C8.7.1.3 (Global Mechanisms – seismic response analysis methods and verification criteria) of the NTC 2018 Circular.

Application of the Resisto 5.9 reinforcement system can certainly contribute to increasing the performance of masonry walls with respect to “Mode I” collapse mechanisms. The modular metal frame, which is connected to the masonry by means of widespread anchoring points arranged on individual walls, undoubtedly has first and foremost a “stitching” effect, which effectively counteracts the occurrence of cracks. In addition, the metal connections (distributed at regular intervals along the height of the building) between the reinforcement frames of the perimeter walls provide a three-dimensional “caging” effect, resulting in the “containment” of the individual walls and counteracting out-of-plane overturning mechanisms. Thus, a “box” action of the construction is guaranteed, which justifies the designer to also consider a global response of the construction, governed by “mode II” mechanisms.

4.1 Calculation method and verification criteria for the reinforcement system

The calculation and verification procedure to be adopted typically consists of the following steps.

1) Identify the possible formation in the building, or in a portion of the building, of local mechanisms/kinematics (such as out-of-plane overturning of façades/wall portions) and, if the formation of one or more mechanisms is possible, evaluate the seismic performance of the masonry portions affected by the corresponding kinematics, in the unreinforced (as-is) and reinforced with the Resisto 5.9 system configurations (see § 5).
2) In all cases, assess and verify the global response of the building to horizontal seismic actions, considering the behaviour of the walls for actions in their own mean plane, in the unreinforced (as-is) and reinforced configurations with the Resisto 5.9 system (see § 6).

It is clear that it is first necessary to understand in which situations it is actually necessary to assess local mechanisms and when it is instead sufficient to carry out only a global verification of the building, accompanied by a local out-of-plane vertical bending verification of individual walls. This depends on the type of masonry buildings being considered. A simplification that can generally be adopted concerns the distinction between “modern” and “non-modern” existing buildings, as defined here.

“Modern” buildings: Masonry buildings that have effective connections between floors/roofing and walls, e.g. due to the presence of reinforced concrete floor kerbs, and sufficiently rigid horizontal structures in their own plane.

“Non-modern buildings”: masonry buildings in which there are no effective connections between floors/roofing and walls (absence of reinforced concrete kerbs) and which are characterised by horizontal structures that are not rigid in their own plane, in which it is therefore possible for local mechanisms/kinematics to form, such as the out-of-plane overturning of façades/partitions.

In the case of “modern” buildings, it will generally be possible to limit oneself to performing only the global verification, together with a local out-of-plane buckling verification of individual walls, while in the case of “non-modern” buildings it will be more appropriate to perform both the verification of local mechanisms and the global verification.

Obviously, this is only a general indication: particular and specific cases will require ad hoc evaluations.

From the analysis of the local mechanisms and the global response of the building, as specified in the following §§ 5 and 6, the capacity values are obtained for the different limit states considered (DLS and LSLS in the case of local mechanism analysis; OLS, DLS, LSLS and CPLS in the case of global analysis), in terms of PGA.

In particular, putting forward the symbolism used below, with $PGA^C_{L,SLi}$ and $PGA^C_{G,SLi}$ we identify the capacitive values of PGA to the i-th limit state considered associated, respectively, with the local mechanisms and the global response and with PGA^C_{SLi} the critical capacity value for the building under consideration, defined as in Table 4.1.

With particular reference to the LSLS, it is put forward that the verification of local mechanisms is carried out by means of the simplified procedure with behaviour factor referred to in § C8.7.1.2.1.7 of Circular 7/2019, adopting, in addition to the proposed value *q* = 2, the value *q* = 1. For justification of the reasons for this choice, please refer to the following § 5.1.4.

Table 4.1. Definition of the capacitive PGA at the different limit states considered (PGA^C_{SLi})

Limit state	$\boldsymbol{PGA^C_{SLi}}$
OLS	$PGA^C_{SLO} = PGA^C_{G,SLO}$
DLS	$PGA^C_{SLD} = min\{PGA^C_{L,SLD}; PGA^C_{G,SLD}\}$
LSLS	$PGA^C_{G,SLV} \geq PGA^C_{L,SLV(q=1)} \implies \begin{cases} PGA^C_{G,SLV} \geq PGA^C_{L,SLV(q=2)} \implies PGA^C_{SLV} = PGA^C_{L,SLV(q=2)} \\ PGA^C_{G,SLV} < PGA^C_{L,SLV(q=2)} \implies PGA^C_{SLV} = PGA^C_{G,SLV} \end{cases}$ $PGA^C_{G,SLV} < PGA^C_{L,SLV(q=1)} \implies PGA^C_{SLV} = PGA^C_{G,SLV}$
CPLS	$PGA^C_{SLC} = PGA^C_{G,SLC}$

The capacity return period $T^C_{R,SLi}$ at each i-th limit state (defined as specified below) is defined as that corresponding to the obtained PGA^C_{SLi}.

For each i-th limit state considered, the capacity value of PGA, PGA^C_{SLi}, must be compared with the corresponding demand value, PGA^D_{SLi}, evaluated for the associated exceedance probability $P_{V_{R,SLi}}$, defining the corresponding safety index $\zeta_{E,SLi}$:

$$\zeta_{E,SLi} = \frac{PGA^C_{SLi}}{PGA^D_{SLi}} \quad (1)$$

The parameters introduced above can be assessed with reference to both the *ante-operam* configuration (unreinforced building: PGA^C_{SLi}, $\zeta_{E,SLi}$ and $T^C_{R,SLi}$) *post-operam* (building reinforced with the Resisto 5.9 system: $PGA^C_{r,SLi}$, $\zeta_{Er,SLi}$ and $T^C_{Rr,SLi}$): with the values obtained, it is possible to assess the seismic risk class of the building (SISMABONUS) in the two configurations.

In the following §§ 5 and 6 considerations and contributions related to the evaluation of the seismic performance of buildings reinforced with the Resisto 5.9 system are highlighted in **bold red**.

5 LOCAL MECHANISMS

As stated in § C8.7.1.2 of the NTC 2018 Circular, partial collapses can occur in masonry buildings due to loss of equilibrium of masonry portions as a result of seismic shaking. Local mechanisms are activated in walls predominantly by actions perpendicular to their mean plane. Local mechanisms include, for example, critical issues related to the out-of-plane rotation/overturning of walls and to the presence of thrusting elements (such as arches, vaults or struts), but also to the disconnection of floors and roofing from the masonry walls that support them in the absence of an adequate connection (for example, in the absence of reinforced concrete kerbs, chains or other elements that withstand tensile stress coupled to the masonry and effective bonding between perpendicular walls).

The identification of local mechanisms may be obtained by means of specific modelling, for example with continuous or discrete elements, or prefigured by the designer based on historical knowledge of the structure or the seismic behaviour of similar structures or on the basis of the survey of the cracking conditions already present, even of non-seismic origin.

The recurring shapes in which local mechanisms manifest themselves, identified and classified for different types of buildings on the basis of past experience, are reported in guidelines and scientific publications and are a useful reference for defining collapse modes. Cited here as an example is Beolchini et al. (2007), referred to extensively below.

Verification of most of the aforementioned mechanisms can be performed through the analysis of rigid body kinematics, accurately identifying the elements considered vulnerable due to their position and slenderness. The calculation method typically consists of the following steps.

- Transformation of a part of the building into a labile system (kinematic chain) through the identification of rigid bodies, defined by fracture planes that can be hypothesised due to the low tensile strength of the masonry, capable of rotating or creep between them (damage and collapse mechanism).
- Evaluation by means of linear kinematic analysis of the horizontal load multiplier α_0 involving activation of the mechanism, defined as the ratio between the results of the overturning moment and stabilizing moment attributable to the horizontal forces applied and the masses involved in the kinematics.
- Evaluation (if necessary) by means of non-linear kinematic analysis of the evolution of the horizontal load multiplier α as the displacement d of a control point of the kinematic chain increases (usually chosen near the centre of gravity of the masses) until the horizontal seismic force is cancelled and consequent construction of the capacity curve α-d of the kinematic chain.
- Transformation of the α-d curve (in the case of non-linear analysis) into a capacity curve a-d of an equivalent single-degree-of-freedom oscillator, i.e. into accelerations a and spectral displacements d, with evaluation of the ultimate displacement due to mechanism collapse or the mechanism activation multiplier α_0 (in the case of linear analysis) into the corresponding spectral acceleration a_0.
- Safety check.

The calculation methods described below assume significance only in cases where a certain monolithicity of the masonry is guaranteed, whereas they are not considered to be applicable in cases where the masonry undergoes point collapses or disintegrations.

The following assumptions are made for application of the method:

- Zero tensile strength of the masonry
- Absence of creep between the blocks;
- Infinite compressive strength of the masonry;
- Walls initially constrained with continuity to the transverse walls.

For a more realistic simulation, it is possible to consider in the calculation, albeit in approximate form:

- Creep between the blocks, considering the presence of friction (generally, only when using particularly advanced applications);
- The quality of the connection between walls and between walls and horizontal structures;
- The presence of metal chains or other elements that withstand tensile stress that offer a stabilizing contribution, counteracting activation of the mechanism;
- The limited compressive strength of the masonry, considering a position suitably set back with respect to the section edge of the hinges connecting the blocks.

The effect of the reinforcement system may be duly taken into account in the calculation, including the stabilizing contributions specifically related to the characteristics of the reinforcement (typically, horizontal or vertical forces, concentrated at the elements of the modular wall frame or at its connections with those of the orthogonal perimeter walls, depending on the type of mechanism considered) in the equilibrium equation describing each specific kinematic motion.

In addition to manual calculation for the analysis and verification of local mechanisms, dedicated software and/or spreadsheets could be used (capable of handling the stabilizing contributions mentioned above in the case of the reinforced configuration). These applications make it possible to carry out either a linear or non-linear kinematic analysis, as appropriate.

It should be noted that, for the purposes of verifying the effectiveness of the reinforcement of the building, verification by linear analysis alone is considered sufficient since it is indispensable in order to be able to evaluate the global response of the building to seismic actions (as specified above) that the local mechanism does not activate: for this purpose, it is therefore not so much the evaluation of the evolution of the local mechanisms (from activation to collapse) that is relevant but only the verification of the inhibition of activation.

5.1 Linear kinematic analysis

Linear kinematic analysis requires the definition of only the horizontal load multiplier α_0 leading to the activation of the local damage mechanism and can be used to perform both verification at DLS (activation of the local mechanism) and at LSLS (in the latter case through the simplified behaviour factor q method).

5.1.1 Capacity evaluation

As an indication (please refer to the following sections for detailed discussion of the individual local mechanisms), as indicated in § C8.7.1.2.1 of Circular 7/2019, it is first necessary for the purposes of the calculation to identify the magnitude and point of application of all the forces involved in the equilibrium of the system of rigid blocks constituting the identified kinematic chain, thus considering:

- The self-weights of the blocks, applied at their centre of gravity;
- The vertical loads carried by them (self-weights and overloads of floors and roofing, other wall elements not considered in the structural model);
- Any external forces (e.g. those transmitted by metal chains);
- Any internal forces (e.g. attritive actions linked to interlocking between the masonry segments in the areas where the walls intersect).

The seismic action acting on the system can therefore be represented by:

- A system of horizontal forces proportional (through a coefficient α) to the self-weights and the vertical loads carried;
- A system of horizontal forces induced by any masses that do not weigh directly on the blocks involved in the mechanism but whose inertial seismic action would act on them because they are not effectively transmitted to other parts of the building (e.g. a floor or a roof which, although weighing on the element of the kinematic chain only partially, could exert a horizontal seismic action on it proportional to the whole mass if not retained at the other end).

It should be remembered that the assumption of the rigid block scheme allows the forces acting on a block to be represented by their resultant applied at the centre of gravity of the block itself, simplifying the treatment of the problem.

Once a virtual rotation θ_k has been assigned to the generic block k, it is possible to determine (as a function of this and the geometry of the structure) the system of displacements of the points of application of the various applied forces. The multiplier α_0 is then obtained by applying the Principle of Virtual Work, in terms of displacements, by equating the total work performed by the external forces and the internal forces applied to the system at the act of virtual motion, through the following expression:

$$\alpha_0 = \frac{\sum_{k=1}^{N} P_k \delta_{P_{y,k}} - \sum_{k=1}^{m} F_k \delta_{F_k} + L_i}{\sum_{k=1}^{N} (P_k + Q_k) \delta_{PQ_{x,k}}} \tag{2}$$

where:

N is the number of blocks of which the kinematic chain consists;

m is the number of external forces, assumed to be independent of the seismic action (therefore, not associated with masses), applied to the different blocks;

P_k is the resultant of the weight forces applied to the k-th block (the block's self-weight, applied at its centre of gravity, added to the other weights carried);

Q_k is the resultant of the weight forces not weighing on the k-th block but whose mass generates a horizontal seismic force on it, since it is not effectively transmitted to other parts of the building;

F_k is the generic external force applied to one of the blocks; these forces may favour activation of the mechanism (e.g. vaulting thrusts) or hinder it (e.g. contrasting arches, i.e. attritive forces that develop in the presence of parts of the construction not involved in the mechanism);

$\delta_{P_{y,k}}$ is the virtual vertical displacement of the centre of gravity of the self-weight and load-bearing forces P_k acting on the k-th block, assumed positive if upwards;

δ_{F_k} is the virtual displacement of the point of application of the external force F_k, projected in the direction of the external force (of positive or negative sign depending on whether it favours or opposes the mechanism: hence, the negative sign in the expression);

$\delta_{PQ_{x,k}}$ is the virtual horizontal displacement of the centre of gravity of the horizontal forces $\alpha(P_k + Q_k)$ acting on the k-th block, assuming the positive direction of the seismic action activating the mechanism;

L_i is the total work of any internal forces (creep with friction in the presence of bonding between the blocks of the mechanism, due to translational or torsional relative motions; deformation in the plane of floors or roofs that are connected but not rigid; elongation of a chain; etc.).

When evaluating the collapse mechanism under the condition of masonry building reinforcement using the Resisto 5.9 system, the work of the internal forces associated with the deformation of the metal elements of the modular frame must be counted in the term L_i, as specified below for each kinematic motion considered.

The multiplier α_0 obtained in this way represents an excess estimate of the actual static collapse multiplier (corresponding to activation of the mechanism in the dynamic field) and can be estimated as the lowest of the multipliers obtained for all the mechanisms selected as possible from those recurring for similar configurations, taking into account realistic static and kinematic conditions for each of them. In this sense, the geometric shape of the portions of masonry involved in the kinematic chain (and the position of the hinges) should derive from a minimisation process within each mechanism class, also referring to attritive models with rigid blocks (identification of the correct mechanism). A classic example is the attritive forces that may develop along the height of the zone of (partially) effective bonding between a wall that bends out of its mid-plane (simple overturning) and the orthogonal walls (unless there is already an evident detachment from the orthogonal spine walls or they are totally unbonded), the resultant of which may be estimated as an approximation using the expression [C8.7.1.2].

According to the instructions in § C8.7.1.2.1.3 below, once the participating mass fraction e^* has been defined as:

$$e^* = \frac{\left[\sum_{k=1}^{N}(P_k + Q_k)\delta_{PQ_{x,k}}\right]^2}{\sum_{k=1}^{N}(P_k + Q_k) \cdot \sum_{k=1}^{N}(P_k + Q_k)\delta_{PQ_{x,k}}^2} \tag{3}$$

the activation multiplier of the mulitiplier α_0 can be transformed into the corresponding spectral acceleration a_0 of the equivalent single-degree-of-freedom oscillator:

$$a_0 = \frac{\alpha_0 g}{e^* FC}. \tag{4}$$

Being g acceleration of gravity and FC the confidence factor relative to the LC level of knowledge defined. In the case where an infinite compressive strength of the masonry is assumed in the calculation of α_0 (see above), a value of the confidence factor FC = 1.35 (corresponding to a knowledge level LC1) can be assumed as a precautionary measure; in the case where its actual (limited) value f_m is taken into account, FC can be defined in relation to the level of knowledge actually achieved (LC1, LC2 or LC3).

It should be noted that, set out in this way, the calculation assumes that the behaviour of the mechanism, prior to its activation, can be considered infinitely rigid. This assumption is admissible in the case of out-of-plane mechanisms of masonry walls initially constrained with continuity to the transverse walls since the former, prior to the activation of the mechanism itself, are not characterised by an autonomous dynamic behaviour.

5.1.2 Evaluation of demand

As recommended in § C8.7.1.2.1.4 of Circular 7/2019, it is necessary for the verification of local mechanisms to correctly assess the dynamic interaction effects with the building in relation to its dynamic characteristics (eigenfrequencies) and the elevation z at which the elements subject to verification are located (modal shapes).

For determination of the response spectra at the different elevations of the building, reference may be made in particular to § C7.2.3 above, in which a simplified analytical formulation is provided, valid for non-structural elements, installations and local mechanisms (and which is applied here specifically to the latter), which allows the acceleration spectrum $S_{ez}(T, \xi, z)$ to be evaluated at an elevation z considered significant based on the dynamic properties of the main structure and on the values of the response spectrum at the base of the building, calculated at the building's own construction periods.

This formulation, given below in its most general form, allows the contribution made by all vibration modes deemed significant to be taken into account. It provides for identification in advance of all the vibration modes (and their relative periods) which are significant for the non-structural element, system or local mechanism under examination, also in relation to its position on the plan (the summation in the following formula is extended to these modes, identified by the subscript "k").

$$S_{ez}(T, \xi, z) = \sqrt{\sum_k \left(S_{ez,k}(T, \xi, z)\right)^2} \ (\geq S_e(T, \xi)\ per\ T > T_1) \tag{5}$$

$$S_{ez,k}(T, \xi, z) = \begin{cases} \dfrac{1.1\xi_k^{-0.5}\eta(\xi)a_{z,k}(z)}{1 + \left[1.1\xi_k^{-0.5}\eta(\xi) - 1\right]\left(1 - \dfrac{T}{aT_k}\right)^{1.6}} & per\ T < aT_k \\ 1.1\xi_k^{-0.5}\eta(\xi)a_{z,k}(z) & per\ aT_k \leq T < bT_k \\ \dfrac{1.1\xi_k^{-0.5}\eta(\xi)a_{z,k}(z)}{1 + \left[1.1\xi_k^{-0.5}\eta(\xi) - 1\right]\left(\dfrac{T}{bT_k} - 1\right)^{1.2}} & per\ T \geq bT_k \end{cases} \tag{6}$$

$$a_{z,k}(z) = S_e(T_k, \xi_k)|\gamma_k \psi_k(z)|\sqrt{1 + 0.0004\xi_k^2}\ . \tag{7}$$

In the above expressions:

$S_e(T, \xi)$ is the elastic ground response spectrum, evaluated for the equivalent period T and the equivalent viscous damping ξ of the considered mechanism.

$S_{ez,k}$ is the contribution to the floor response spectrum provided by the k-th mode of the main structure of its period T_k and equivalent damping ξ_k, (in percentage), defined by the following expression:

a and b are coefficients defining the maximum amplification range of the floor spectrum, which can be taken to be 0.8 and 1.1 respectively;

γ_k is the k-th modal participation coefficient of the construction;

$\psi_k(z)$ is the value of the k-th modal form at elevation z, at the position in the plan where the local mechanism to be verified is located;

η is the factor that alters the elastic spectrum for values of the damping coefficient ξ other than 5%, defined by the expression [3.2.4] of § 3.2.3.2.1 of NTC 2018:

$$\eta = \sqrt{10/(5 + \xi)} \geq 0.55$$

$a_{z,k}(z)$ is the contribution of the k-th mode to the maximum plane acceleration.

The maximum acceleration $a_z(z)$ at elevation z is then defined by the expression:

$$a_z(z) = \sqrt{\sum_k \left(a_{z,k}(z)\right)^2} \tag{8}$$

while the contribution to the spectral acceleration peak provided by the k-mo mode at T_k is:

$$S_{ez,k}(T, \xi, z) = 1.1\xi_k^{-0.5}\eta(\xi)a_{z,k}(z)\ . \tag{9}$$

In view of this general formulation, the same § C7.2.3 Circular 7/2019 specifies that it is generally sufficient in the verification of local mechanisms in multi-storey buildings to refer only to the first mode of vibration in the verification direction, since this is the one that induces the most significant displacement demand. In the absence of more accurate evaluations, the period T_1 can be estimated for masonry constructions as a function of the height H of the construction measured from the foundation plane using the formula in § C7.3.2:

$$T_1 = 0.05 \cdot H^{3/4}. \tag{10}$$

In the case of structures with masses distributed substantially uniformly along the height, if one assumes the first linear modal shape and normalises it with respect to the displacement at the top of the building, the modal participation factor can be approximated as a function of the number n of floors of the building using the formula:

$$\gamma_1 = \frac{3n}{2n + 1}\,. \tag{11}$$

For sufficiently regular structures, and in any case in the absence of more accurate evaluations, the component of the first modal shape $\psi_1(z)$ in the direction and at the z-elevation considered can be defined approximately as:

$$\psi_1(z) = \frac{z}{H}\,. \tag{12}$$

In particular, in the evaluation of local mechanisms, *z* is assumed to be equal to the centre of gravity, with respect to the building foundation, of the constraint lines between the blocks affected by the kinematics and the rest of the structure. Specific indications regarding the definition of the parameter *z* will be given in the discussion of the individual mechanisms below.

5.1.3 Verification at DLS

In the case of local mechanisms, activation of the kinematics involves the opening of cracks, a condition which may still be far from actual overturning and which is conventionally identified as corresponding to DLS. Although, in general, the presence of details of a cracking pattern does not necessarily indicate the activation of a failure mechanism, in the case of masonry elements that are not effectively connected to the rest of the construction due to the absence of chains, bonding with orthogonal walls and/or connections with horizontal diaphragms, vulnerability to this limit state may be high.

According to § C8.7.1.2.1.5 of Circular 7/2019, the verification at DLS can be carried out in terms of the acceleration of activation of the mechanism.

In particular, on the assumption that the portion of the structure constituted by the system of rigid bodies considered (kinematic chain) has infinitely rigid behaviour until activation of the kinematic motion, this is activated when the maximum acceleration at elevation z at which the local mechanism under consideration $a_{z,DLS}$ equals the acceleration a_0 corresponding to the activation multiplier α_0:

$$a_{z,SLD} = a_0 = \frac{\alpha_0 g}{e^* FC}. \tag{13}$$

If the plastic hinge around which the collapse kinematics develops is activated at the base of the construction, at the elevation of the foundation plane, the following can be assumed, referring to the anchoring point of the base spectrum (as defined in § 3.2.3.2.1 of NTC 2018):

$$a_{z,SLD} = a_{g,SLD} \cdot S_{SLD} \tag{14}$$

from which, combining the relations (13) and (14) it follows that:

$$a_{g,SLD} = \frac{a_0}{S_{SLD}}. \tag{15}$$

If, on the other hand, the portion of the building affected by the kinematics is not in contact with the foundation but is located at a higher elevation, amplification of the seismic acceleration with respect to the ground must be taken into account. In this case, referring to the simplified formulation proposed by Circular 7/2019 referred to in § 5.1.2 above, considering only the first mode as significant and adopting a damping ξ = 5% for local mechanisms (unless more accurate evaluations are made, depending on the geometry and constraint conditions), the following can be assumed:

$$a_{z,SLD} = S_{e.SLD}(T_1, \xi)|\gamma_1 \psi_1(z)|\sqrt{1 + 0.0004\xi^2} \tag{16}$$

Combining the relations (13) and (16) it follows that:

$$S_{e,SLD}(T_1, \xi) = \frac{a_0}{|\gamma_1 \psi_1(z)|\sqrt{1 + 0.0004\xi^2}} \tag{17}$$

Using the formulas of the base spectrum (as a function of the values of the fundamental period T_1 and the reference periods T_B, T_C and T_D) it is then possible to determine the value of the reference ground acceleration $a_{g,DLS}$ corresponding to the spectral ordinate defined through the (17), also varying the parameters $T_{R,DLS}$ and $F_{0,DLS}$.

For verification purposes, in both cases it is necessary to finally compare the value of $a_{g,DLS}$ obtained with that of the reference ground acceleration $a_{g(DLS)}$ evaluated for the probability of exceedance $P_{V_{R,SLD}}$ at DLS (63%), as defined in § 3.2 of NTC 2018.

Contrary to what is indicated in Circular 7/2019, it is considered that the verification must be carried out not simply in terms of reference ground acceleration a_g (defined in conditions of rigid ground and horizontal topographic surface), but of $PGA = a_g \cdot S$ (*peak ground acceleration* or spectral ordinate in acceleration at the anchoring point), that is the maximum acceleration at the foundation laying plane, including any local amplification (stratigraphic and topographic).

Taking the above and using superscripts C and D to identify the values of the parameters introduced below corresponding, respectively, to capacity and demand and subscript "L" to identify the values associated with a local mechanism, for verification purposes it is necessary to determine the capacity return period $T^C_{RL,SLD}$ (or, dually,, the associated exceedance probability, assuming the reference period is kept constant for the building considered V_R), for which:

- The value of the acceleration response spectrum at the anchoring point $a_g \cdot S$, corresponds to the acceleration of activation of the kinematics a_0 in the event that it develops around a plastic hinge activated at the base of the construction;
- The value of the spectral ordinate for the fundamental period T_1 corresponds to the value resulting from the expression (17).

Having then determined the values of PGA of capacity, $PGA^C_{L.SLD}$, corresponding to the return period $T^C_{RL.SLD}$, and of demand, PGA^D_{SLD}, corresponding to the return period $T^D_{R,SLD}$ associated with the probability of exceedance $P_{V_{R,SLD}}$ = 63% in the reference period V_R ($T^D_{R,SLD}$ = 50 years times V_R = 50 years), it is possible to define the safety index of the local mechanism at the DLS, $\zeta_{EL,SLD}$:

$$\zeta_{EL,SLD} = \frac{PGA^C_{L,SLD}}{PGA^D_{SLD}} \tag{18}$$

5.1.4 Simplified verification at LSLS with behaviour factor

Pursuant to § C8.7.1.2.1.7 of Circular 7/2019, the verification at LSLS, in addition to the displacement thresholds identified on the capacity curve (and, therefore, by means of non-linear kinematic analysis, according to the indications of § C8.7.1.2.1.6), can also be carried out by adopting a linear method, considering only the mechanism activation multiplier and using a behaviour factor q. This simplification can be convenient in particular for complex mechanisms, identified by also taking into account the contribution of friction and interaction with other elements of the construction, for which performing a non-linear kinematic analysis would be problematic.

In particular, the ground acceleration $a_{g,LSLS}$ can be calculated by multiplying the ground acceleration $a_{g,DLS}$ assessed for the DLS by the procedures described in the previous § 0, by a behaviour factor q:

$$a_{g,SLV} = q \cdot a_{g,SLD} \tag{19}$$

The value of $a_{g,LSLS}$ thus obtained must then be compared with the reference ground acceleration value $a_{g(LSLS)}$, assessed for the probability of exceedance $P_{V_{R,SLV}}$ at LSLS in the reference life (10%), as defined in § 3.2 of NTC 2018.

Recalling what was stated in the previous § 0 in relation to verification to DLS, it is considered more correct to also carry out the LSLS verification in terms of PGA instead of a_g. . Referring to the criterion proposed by Circular 7/2019, summarised in the previous (19), we therefore define the capacity value PGA at LSLS, $PGA^C_{L,SLV}$, as:

$$PGA^C_{L,SLV} = q \cdot PGA^C_{L,SLD} \tag{20}$$

and we proceed by determining the value of the capacity return period $T^C_{RL,SLV}$ (or, dually,, the associated exceedance probability, assuming the reference period is kept constant for the building

considered V_R) for which the value of the acceleration response spectrum at the anchoring point, $a_g \cdot S$, corresponds to $PGA^C_{L,SLV}$.

Having then assessed the demand of PGA at LSLS, PGA^D_{SLV}, corresponding to the return period $T^D_{R,SLV}$ associated with the probability of exceedance $P_{V_{R,SLV}}$ = 10% in the reference period V_R ($T^D_{R,SLV}$ = 475 years times V_R = 50 years), it is possible to define the safety index of the local mechanism at the LSLS $\zeta_{EL,SLV}$:

$$\zeta_{EL,SLV} = \frac{PGA^C_{L,SLV}}{PGA^D_{SLV}} \tag{21}$$

In the absence of more accurate evaluations, which take into account the type of mechanism and the thickness of the walls, still according to the indications of Circular 7/2019 at § C8.7.1.2.1.7, q = 2 may be assumed. Nevertheless, it is considered that, proceeding in this way, verification of the mechanism at LSLS may be satisfied under certain conditions even where the kinematics has been activated. Since, wanting to ensure a global response of the building, it is absolutely necessary to inhibit activation of kinematics, it is considered that the verification at this limit state, again using the (21), must also be carried out assuming q = 1.

5.2 Local mechanisms considered

The following is a discussion of the most significant local mechanisms that may affect single-façade monolithic masonry buildings, for which the Resisto 5.9 reinforcement system is to be used:

- Simple overturning;
- Compound overturning;
- Vertical bending;
- Horizontal bending;
- Gable overturning.

As explained in more detail below, it is considered that the compound overturning mechanism cannot be activated in buildings reinforced with the Resisto 5.9 system, given the characteristics of the system itself and is only mentioned here for completeness.

On “non-modern” load-bearing masonry buildings (as classified in the previous § 4.1) all the verifications for the mechanisms listed above must generally be carried out considering all the possible modes of collapse, also in terms of the number of consecutive floors involved in the kinematics, while on “modern” buildings (again with reference to the classification given in § 4.1) only verifications for the vertical inter-floor bending mechanism (for all floors) may be carried out. Obviously, depending on the characteristics of the specific construction under investigation (constraint conditions corresponding to the degree of wall-to-wall and masonry-to-horizontal structure bonding), the number of cases to be considered may vary on a case-by-case basis.

The activation multiplier α_0 associated with each mechanism considered (and for each of the different possible collapse modes) must be defined as the minimum among those corresponding to different possible (realistic) static and kinematic conditions of the system of rigid blocks involved in the kinematics (dimensions of the rigid blocks, position of the hinges, etc.). The critical multiplier for the building is then defined as the minimum among those associated with the different types of mechanism.

Finally, both the pre-intervention situation and the reinforced situation must be assessed.

The presence of the Resisto 5.9 reinforcement system (which is intended to be continuous on all the façades of the building) can be taken into account in the calculation, including the appropriate stabilizing contributions specifically related to the characteristics of the reinforcement (typically, horizontal or vertical forces, concentrated at the elements of the modular wall frame or at its connections with those arranged on the orthogonal perimeter walls, depending on the type of mechanism considered), in the equilibrium equation describing each specific kinematic motion.

Information is given in the following sections regarding the criteria to be adopted for definition of the different stabilizing contributions to be considered in the evaluation of the mechanisms. Please refer to Appendix A for the calculation of the magnitude of these contributions based on the geometry of the metal frames, the characteristics of the bolted connections and the properties of the materials, in compliance with the requirements of NTC 2018 and the indications of Circular 7/2019.

5.2.1 Simple overturning

Simple overturning of external walls of masonry buildings occurs when the wall hit by the seismic action is free at the top and not abutted by the walls orthogonal to it. Even if the latter have an unsatisfactory quality, the collapse occurs first in the wall normal to the seismic action. The constraint conditions that make this mechanism possible are the absence of an effective connection of perpendicular walls and of connecting devices, such as kerbs or chains, at the head of the overturning wall.

The mechanism manifests itself through the rigid rotation of entire façades or portions of walls with respect to axes that are predominantly horizontal at their base and that run through the masonry structure stressed by out-of-plane actions. It may concern different geometries of the wall under examination in relation to a detected crack pattern (vertical cracks present at the intersection between the area from the roof to the top of the wall and the walls orthogonal to it) or to the presence of openings in the wall (doors and windows) which affect its progression. It may also affect one or more floors of the building, depending on the manner and quality of the connection between the floors and the masonry at the various levels of the structure. In these cases, consider the possibility that the overturning may involve different levels of the wall, evaluating the critical collapse multiplier as the lower of those resulting from the calculation for different positions of the cylindrical hinge.

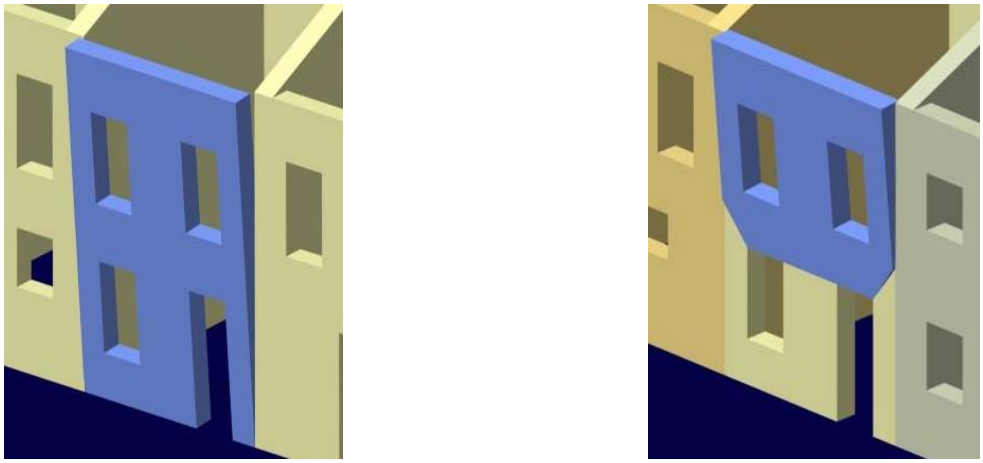

Figure 5.1 Simple overturning mode of multi-storey masonry wall (from Beolchini et al. 2007).

The calculation referring to the case of multi-storey wall overturning is shown below, remembering that the mechanism should be analysed assuming the position of the hinge at all levels of the building and identifying the configuration associated with the lowest activation multiplier α_0 as critical.

5.2.1.1 Unreinforced condition

Considering the kinematic chain associated with the mechanism, we identify the forces involved and the position of the corresponding application points with respect to the plastic hinge, as illustrated in Figure 5.3a:

n is the number of planes affected by the kinematics;

W_i is the self-weight of the wall in the i-th plane;

F_{Vi} is the vertical component of the thrust of arches or vaults on the wall in the i-th plane;

F_{Hi} is the horizontal component of the thrust of arches or vaults on the wall in the i-th plane;

P_{Si} is the weight of the floor acting on the wall in the i-th floor, calculated from the area of influence;

P_H represents the static horizontal force transmitted from the roof to the top of the wall.

T_i is the maximum value of the action in any elements that withstand tensile stress (metal tie rods/reinforced concrete kerbs) at the head of the wall in the i-th plane;

s_i is the thickness of the wall at the i-th plane;

h_i is the height of the wall in the i-th plane with respect to the hinge B;

h_{Vi} is the height of the point of application of the thrust of arches or vaults at the i-th plane with respect to the hinge B;

d_i is the horizontal distance from hinge B of the point where the floor load is applied to the wall in the i-th plane;

d_{Vi} are the horizontal distances from hinge B of the application points of F_{Vi};

y_{Gi} is the height of the centre of gravity of the wall at the i-th plane with respect to the hinge B;

α is the multiplier of the horizontal forces.

Under the condition of activation of the mechanism, that is assuming an infinite virtual rotation of the plastic hinge, it is possible to express the virtual displacements of the points of application of the forces involved with respect to the geometric parameters identified above. The overturning M_R and stabilizing M_S moments are then derived using the following relationships (22) and (23).

$$M_R = \alpha\left[\sum_{i=1}^{n} W_i y_{Gi} + \sum_{i=1}^{n} F_{Vi} h_{Vi} + \sum_{i=1}^{n} P_{Si} h_i\right] + \sum_{i=1}^{n} F_{Hi} h_{Vi} + P_H h_n \tag{22}$$

$$M_S = \sum_{i=1}^{n} W_i \frac{s_i}{2} + \sum_{i=1}^{n} F_{Vi} d_{Vi} + \sum_{i=1}^{n} P_{Si} d_i + \sum_{i=1}^{n} T_i h_i \tag{23}$$

By imposing the equilibrium between the overturning moment and stabilizing moment, the value of the multiplier can be determined α_0 in the kinematic activation condition:

$$\alpha_0 = \frac{\sum_{i=1}^{n} W_i \frac{s_i}{2} + \sum_{i=1}^{n} F_{Vi} d_{Vi} + \sum_{i=1}^{n} P_{Si} d_i + \sum_{i=1}^{n} T_i h_i - \sum_{i=1}^{n} F_{Hi} h_{Vi} - P_H h_n}{\sum_{i=1}^{n} W_i y_{Gi} + \sum_{i=1}^{n} F_{Vi} h_{Vi} + \sum_{i=1}^{n} P_{Si} h_i} \tag{24}$$

5.2.1.2 Condition reinforced with the Resisto 5.9 system

In the reinforced condition of the building, it is assumed that an additional contribution to the stabilizing moment is considered, represented by a system of horizontal forces F_{roj} at each of the two reinforced perimeter bracing walls, at the elevation h_{rj} with respect to the hinge B of each of the n_{ro} levels of the reinforcement arranged in the portion of the wall affected by the kinematics, as illustrated in Figure 5.3b.

Each level of horizontal reinforcement of the wall under verification can in fact be equated to a metal framing of the masonry, which transmits the stresses resulting from the activation and evolution of the kinematics to the orthogonal walls (through the connections).

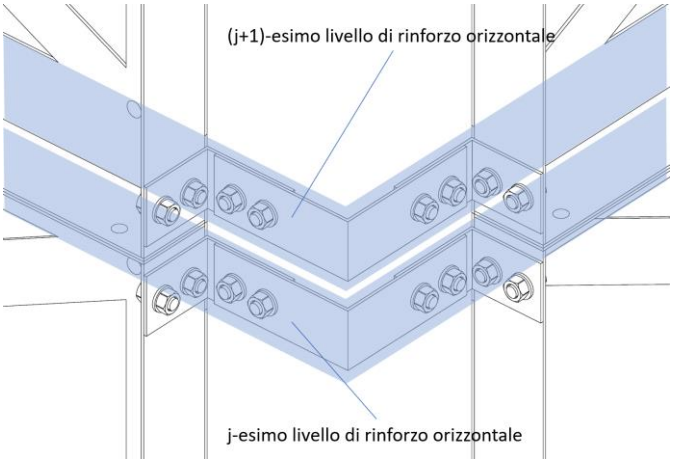

Figure 5.2 Detail of the connection system between the metal frames of two façade walls and identification of the horizontal reinforcement levels considered for calculation purposes.

The value of the force F_{roj} is assumed to be the maximum force that can be withstood by the connection between the reinforcement system of the wall under consideration and those of the bracing walls, which can be evaluated as the minimum between:

- The tensile strength of the bolted connection between the frame framing element and the plate, to be assessed according to the number of bolts, the tensile strength of the individual bolt and the puncture strength of the plate;
- The tensile strength of the plate;
- The shear strength of the bolted connection between the plates, to be evaluated as a function of the number of bolts, the shear strength of the individual bolt, the tensile strength of the cross-section of the plate weakened by the holes, and the bearing strength of the plate.

The stabilizing moment of the reinforced wall $M_{S,r}$ results, by changing the (23):

$$M_{S,r} = \sum_{i=1}^{n} W_i \frac{s_i}{2} + \sum_{i=1}^{n} F_{Vi} d_{Vi} + \sum_{i=1}^{n} P_{Si} d_i + \sum_{i=1}^{n} T_i h_i + \mathbf{2} \sum_{\boldsymbol{j=1}}^{\boldsymbol{n_{ro}}} \boldsymbol{F_{roj} h_{rj}} \tag{25}$$

By imposing equality between (22) and (25) we then derive the corresponding value of the $\alpha_{0,r}$ activation multiplier.

$$\alpha_{0,r} = \frac{\sum_{i=1}^{n} W_i \frac{s_i}{2} + \sum_{i=1}^{n} F_{Vi} d_{Vi} + \sum_{i=1}^{n} P_{Si} d_i + \sum_{i=1}^{n} T_i h_i + \mathbf{2} \sum_{\boldsymbol{j=1}}^{\boldsymbol{n_{ro}}} \boldsymbol{F_{roj} h_{rj}} - \sum_{i=1}^{n} F_{Hi} h_{Vi} - P_H h_n}{\sum_{i=1}^{n} W_i y_{Gi} + \sum_{i=1}^{n} F_{Vi} h_{Vi} + \sum_{i=1}^{n} P_{Si} h_i} \tag{26}$$

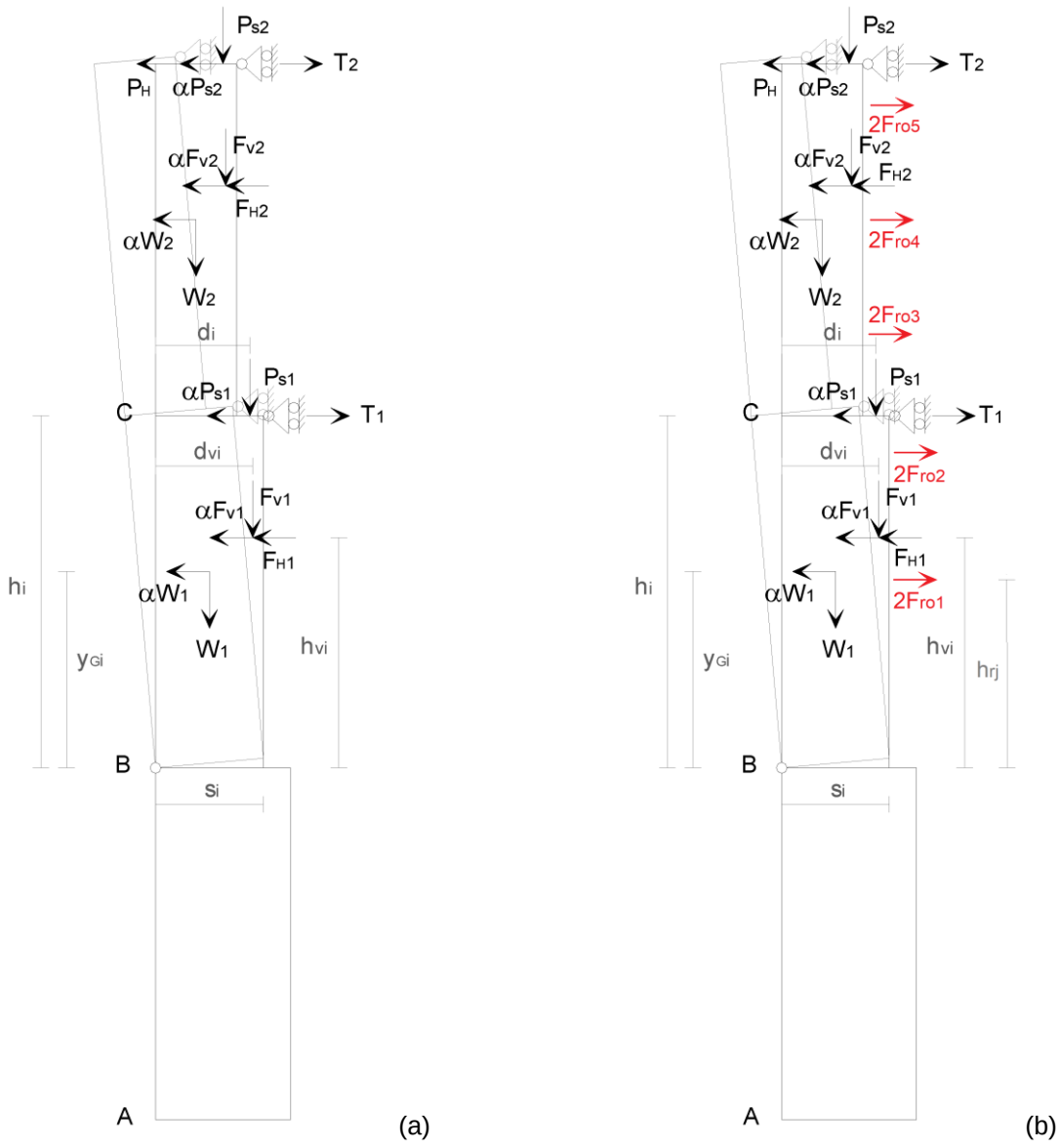

Figure 5.3 Calculation scheme for the simple overturning mechanism: (a) unreinforced wall; (b) reinforced wall (modified from Beolchini et al. 2007).

5.2.2 Compound overturning

Compound overturning refers to a set of situations in which the overturning of the wall normal to the seismic action is accompanied by the dragging of parts of the masonry structures belonging to the bracing walls (the external/internal walls perpendicular to the one in question). The constraint conditions that make this mechanism possible are therefore an effective connection between the wall hit by the earthquake and those orthogonal to it, such as kerbs or chains, at the head of the overturning wall.

Compound overturning may involve one or more levels of the wall, depending on the presence of connection to the different horizontal structures and different geometries of the macro-element, in relation to the quality of the masonry of the bracing wall and the presence of openings in it, as well as the type of the overlying horizontal structures (if rigid, double diagonal detached wedges may be defined).

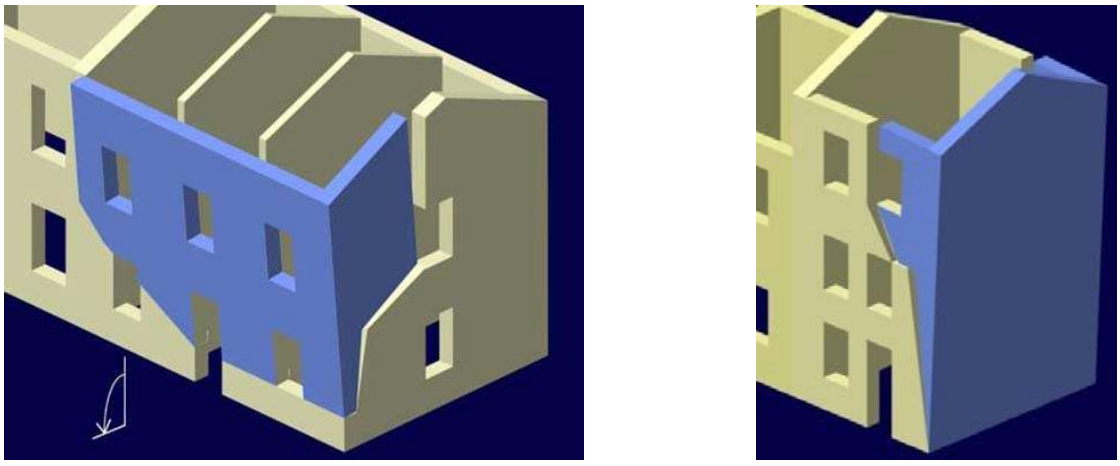

Figure 5.4 Compound overturning mode of multi-storey masonry wall (from Beolchini et al. 2007).

It is considered that this type of mechanism cannot be activated in buildings reinforced with the Resisto 5.9 system, given the "bridling" effect of the wall texture guaranteed by the diffusion and regularity of the anchoring of the metal frames, which counteract the formation of diagonal cracks in the walls orthogonal to the one under verification and therefore the detachment of the wedges.

5.2.3 Vertical bending

This is rather common situation in masonry buildings represented by walls constrained at the extremities and free in the central area such as, for example, in the case of a building provided with a top kerb (or metal tie rods or hoops) but lacking effective connections between the masonry and the intermediate floors, or in the case of the portion of a wall between two floors that are well connected to it. In these conditions, the presence of a connection device at the top prevents the wall from overturning outwards, but it may still collapse due to vertical instability under the effect of horizontal shaking.

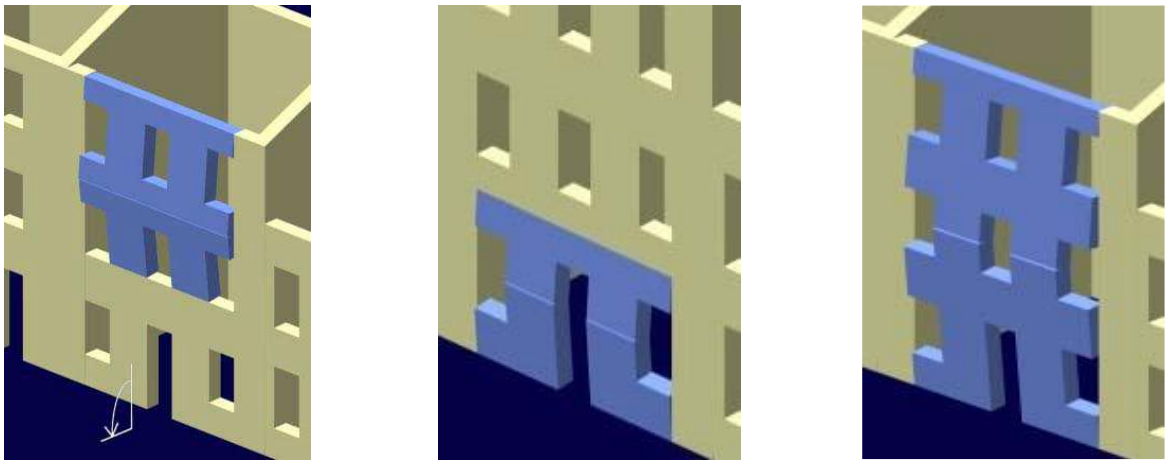

Figure 5.5 Overturning mode by vertical bending (from Beolchini et al. 2007).

In fact, the masonry structure, built by overlapping stone blocks or brick elements bound by simple contact or by means of a layer of mortar generally characterised by limited if not poor tensile strength, withstands the bending stresses induced by actions orthogonal to its plane only as long as the resultant of the normal stresses remains within the cross-section of the wall. If this is not the case, a horizontal cylindrical hinge is activated in the wall, around which the two blocks formed in the masonry rotate reciprocally, thus triggering a vertical bending kinematics.

The vertical bending mechanism of a wall may affect one or more floors of the building, depending on the presence of constraints on the horizontal structures and different geometries of the macro-elements, determined by the presence of openings or localised thrusts. The calculation referring to the case of vertical bending of a multi-storey wall is given here as an example. In general, the number of storeys involved in the kinematics obviously depends on the degree of bonding (effectiveness of the connection, to be evaluated on the basis of the construction details adopted) between intermediate floors and masonry. Once the calculation scheme compatible with the characteristics of the structure under verification has been identified, remember that the mechanism should be analysed by varying the height of the plastic hinge along the height of the portion of wall affected by the kinematics and identifying the configuration associated with the lowest activation multiplier α_0 as critical.

5.2.3.1 Unreinforced condition

Considering the kinematic chain associated with the mechanism, we identify the forces involved and the position of the corresponding application points with respect to the plastic hinges. Figure 5.6 shows, by way of example, a calculation scheme referring to a three-storey wall, with different masonry thicknesses at the first and subsequent levels, which assumes the formation of the plastic hinge at an elevation between the first and second horizontal structure.

n is the number of planes affected by the kinematics;

W_i is the self-weight of the i-th body in which the portion of the wall involved in the kinematics is divided by the plastic hinge;

F_{Vi} is the vertical component of the thrust of arches or vaults on the wall in the i-th plane;

F_{Hi} is the horizontal component of the thrust of arches or vaults on the wall in the i-th plane;

P_{Si} is the weight of the floor acting on the wall in the i-th floor, calculated from the area of influence;

N is the weight transmitted to body 2 by the masonry and floors of the upper levels;

T_i is the maximum value of the action of the metal tie rods that may be present at the floor level of the i-th floor;

s_i is the thickness of the wall in the i-th plane;

h_i is the height of the i-th body;

h_{Pi} is the vertical distance of the point of application of the load transmitted by the i-th floor from the reduction pole of the body on which it is discharged;

x_{Gi} is the horizontal distance of the centre of gravity of the i-th body from its reduction pole (hinge A for body 1 and carriage B for body 2);

y_{Gi} is the vertical distance of the centre of gravity of the i-th body from its reduction pole (hinge A for body 1 and carriage B for body 2);

h_{Vi} is the vertical distance of the point of application of the thrust of arches or vaults to the i-th plane from the pole of reduction of the body on which it discharges;

d is the horizontal distance of the point of application of the load N transmitted to the wall from the upper floors in relation to carriage B;

d_{Vi} is the horizontal distance of the point of application of the thrust of arches or vaults to the i-th plane from the pole of reduction of the body on which it discharges;

a_i is the horizontal distance of the point of application of the load transmitted by the i-th floor from the reduction pole of the body on which it is discharged;

α is the multiplier of the horizontal forces.

With reference to the static scheme of Figure 5.6a, the generalised displacements of the rigid body system are expressed by the following relations:

$$(u_{01}; v_{01}; \theta_1) = (u_A; v_A; \psi) = (0; 0; 1)$$
$$(u_{02}; v_{02}; \theta_2) = (u_B; v_B; \varphi) = (0; s_2; -h_1/h_2) \quad (27)$$

Applying the Principle of Virtual Work results in:

$$\alpha[W_1\delta_{1x} + W_2\delta_{2x} + F_{V1}\delta_{V1x} + F_{V2}\delta_{V2x} + F_{V3}\delta_{V3x} + P_{S1}\delta_{P1x} + P_{S2}\delta_{P2x}] +$$
$$F_{H1}\delta_{V1x} + F_{H2}\delta_{V2x} + F_{H3}\delta_{V3x} - W_1\delta_{1y} - W_2\delta_{2y} - F_{V1}\delta_{V1y} - F_{V2}\delta_{V2y} - \quad (28)$$
$$F_{V3}\delta_{V3y} - N\delta_{Ny} - P_{S1}\delta_{P1y} - P_{S2}\delta_{P2y} - P_{S3}\delta_{P3y} - T_1\delta_{P1x} - T_2\delta_{P2x} = 0$$

Upon activation of the kinematics, according to scheme in Figure 5.6 and taking into account (27), the virtual displacements of the points of application of the forces in the respective direction of action result as:

$$\delta_{1x} = y_{G1} \qquad \delta_{V3x} = \frac{h_1}{h_2}h_{V3} = -\delta_{h3} \qquad \delta_{1y} = x_{G1} \qquad \delta_{V3y} = s_2 + \frac{h_1}{h_2}d_{V3}$$
$$\delta_{2x} = \frac{h_1}{h_2}y_{G2} \qquad \delta_{P1x} = h_{P1} \qquad \delta_{2y} = s_2 + \frac{h_1}{h_2}x_{G2} \qquad \delta_{P1y} = a_1 \quad (29)$$
$$\delta_{V1x} = h_{V1} = -\delta_{h1} \qquad \delta_{P2x} = \frac{h_1}{h_2}h_{P3} \qquad \delta_{V1y} = d_{V1} \qquad \delta_{P2y} = s_2 + \frac{h_1}{h_2}a_2$$
$$\delta_{V2x} = \frac{h_1}{h_2}h_{V2} = -\delta_{h2} \qquad \delta_{Ny} = s_2 + \frac{h_1}{h_2}d \qquad \delta_{V2y} = s_2 + \frac{h_1}{h_2}d_{V2} \qquad \delta_{P3y} = s_2 + \frac{h_1}{h_2}a_3$$

Substituting into the expression (28) the (29) and explicating with respect to α, we obtain the value α_0 of the multiplier in the kinematic activation condition:

$$\alpha_0 = \frac{E}{W_1 y_{G1} + F_{V1}h_{V1} + P_{S1}h_{P1} + (W_2 y_{G2} + F_{V2}h_{V2} + F_{V3}h_{V3} + P_{S2}h_{P3})\frac{h_1}{h_2}} \quad (30)$$

The term E at the numerator of the previous relation (30) represents the expression (31):

$$E = W_1 x_{G1} + W_2\left(s_2 + x_{G2}\frac{h_1}{h_2}\right) + F_{V1}d_{V1} + (F_{V2} + F_{V3})s_2 + F_{V2}\frac{h_1}{h_2}d_{V2} + F_{V3}\frac{h_1}{h_2}d_{V3} + P_{s1}a_1 +$$
$$+(P_{S2} + P_{S3})\left(s_2 + a_2\frac{h_1}{h_2}\right) + N\left(s_2 + d\frac{h_1}{h_2}\right) + T_1 h_{P1} - F_{H1}h_{V1} - (F_{H2}h_{V2} + F_{H3}h_{V3} - T_2 h_{P3})\frac{h_1}{h_2} \quad (31)$$

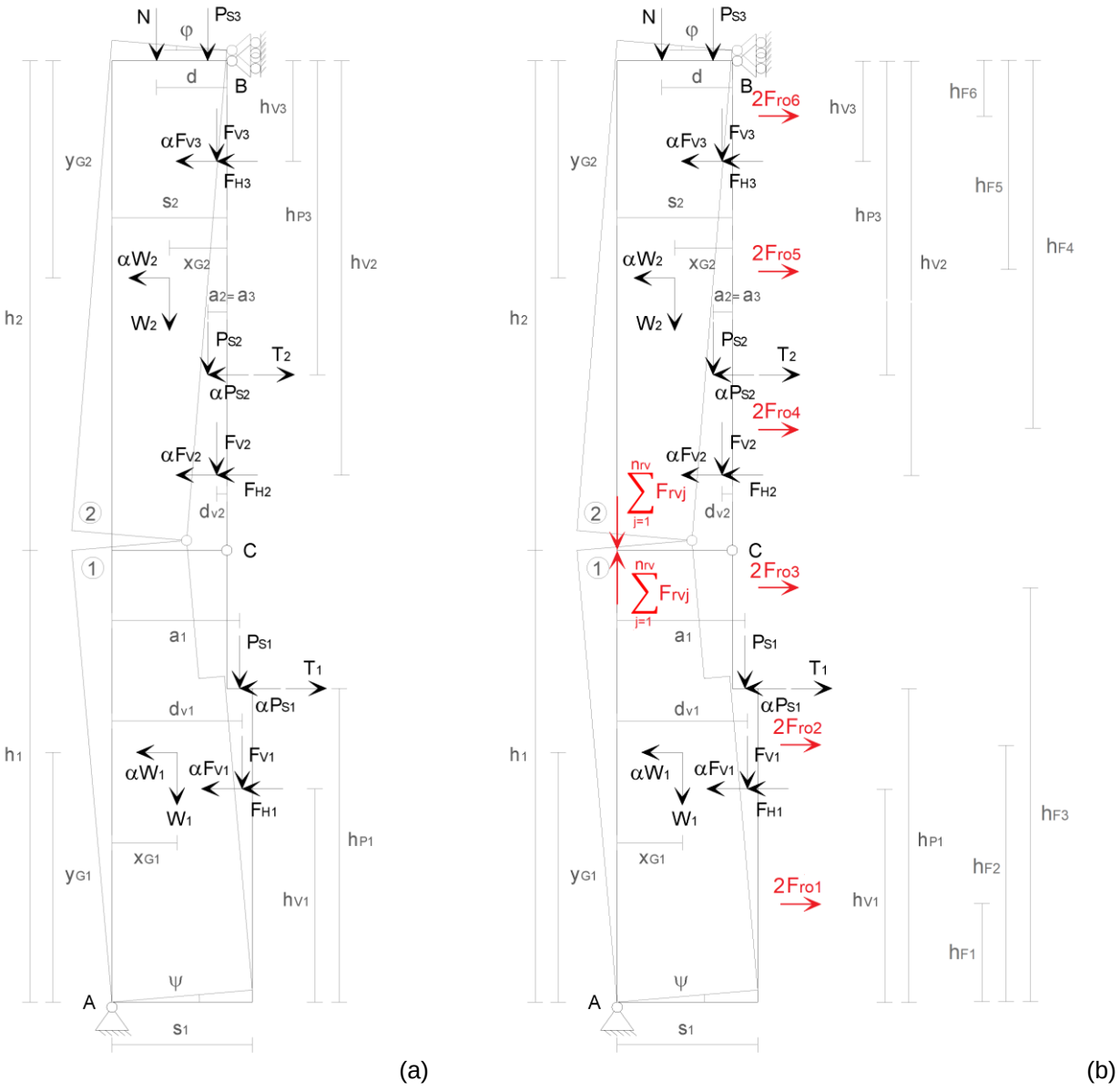

Figure 5.6 Calculation scheme for the vertical bending mechanism: (a) unreinforced wall; (b) reinforced wall (modified from Beolchini et al. 2007).

We would like to reiterate that the calculation presented here, expressed by the relations from (28) to (31), corresponds to the specific case illustrated in Figure 5.6a: it therefore has no general validity but is an example only and should be adapted to the specific case studied, depending on the number of floors of the portion of the wall affected by the kinematics, the thickness of the masonry at the various levels and the varying position of the cylindrical hinge C along the height of the wall itself.

5.2.3.2 Condition reinforced with the Resisto 5.9 system

In the reinforced configuration of the building, the presence of the vertical metal elements of the Resisto 5.9 modular system, which are continuous along the entire height of the masonry wall, contributes to counteracting the activation of the kinematics.

To evaluate the activation multiplier under reinforced conditions $\alpha_{0,r}$, the contributions of a system of vertical forces F_{rvj}, and a system of horizontal forces F_{roj} must be taken into account in the calculation.

Each force F_{rvj} is considered to be acting in the metal elements of the j-th of the n_{rv} vertical reinforcement positions arranged along the horizontal development of the wall. Its value is assumed

to be equal to the maximum tensile force that can be withstood by the system, based on its characteristics, and is therefore evaluated as the lesser of:

- The tensile strength of the vertical member (only the uprights that are continuous from the base to the top of the wall, excluding from the calculation those interrupted by the presence of any openings, are considered in correspondence of the section of contact between two metal modules);
- The tensile strength of the bolted connection between the frame modules, to be assessed according to the number of bolts, the tensile strength of the individual bolt and the puncture strength of the plate;
- the strength in the vertical direction of the anchoring system between the reinforcement and masonry.

The maximum vertical force that can be withstood by each anchoring is assumed to be the lesser of:

- The shear strength of the anchoring (to be determined by appropriate in situ tests or from the epoxy resin manufacturer's data sheets);
- The bearing strength of the member at the section weakened by the hole for the anchoring bar section.

The strength in the vertical direction of the anchoring system between the reinforcement and masonry is therefore determined by multiplying the strength of the single anchor by the smallest number $n_{a,min}$ of anchors present in the two rigid bodies into which the portion of wall involved in the kinematics is divided by the plastic hinge C. Unlike the previous ones, this contribution therefore varies as the position of the plastic hinge C varies along the height of the portion of wall considered.

With reference to the calculation scheme of Figure 5.6b, two vertical n_{rv} forces F_{rvj} equal to the resultant of the forces are considered to act on rigid bodies 1 and 2 participating in the kinematic motion, at the outer (reinforced) side of the wall and at the height of the cylindrical plastic hinge C.

Each force F_{roj} is instead assumed to be applied at the height of the j-th level of the n_{ro} horizontal reinforcement placed in the wall, at a vertical distance h_{Fj} from the reduction pole of the rigid body to which the reinforcement level refers, based on the height of the plastic hinge C. Its value is assumed to be equal to that of the maximum force supportable by the connection between the reinforcement system of the wall under verification and those of the bracing walls (see previous 5.2.1.2). With reference to the calculation scheme of Figure 5.6b, it is assumed in the example considered that there are 6 different levels of horizontal reinforcement along the wall elevation.

Indicating with δ_{F1y} and δ_{F2y} the vertical virtual displacements of the points of application of the forces F_{rvj} acting on the two rigid bodies participating in the kinematics and with δ_{Fjx} the horizontal virtual displacements of the forces $F_{roj}$and applying the Principle of Virtual Work, we have:

$$\begin{aligned}&\alpha[W_1\delta_{1x} + W_2\delta_{2x} + F_{V1}\delta_{V1x} + F_{V2}\delta_{V2x} + F_{V3}\delta_{V3x} + P_{S1}\delta_{P1x} + P_{S2}\delta_{P2x}] + F_{H1}\delta_{V1x} + F_{H2}\delta_{V2x}\\ &F_{H3}\delta_{V3x} - W_1\delta_{1y} - W_2\delta_{2y} - F_{V1}\delta_{V1y} - F_{V2}\delta_{V2y} - F_{V3}\delta_{V3y} - N\delta_{Ny} - P_{S1}\delta_{P1y} - P_{S2}\delta_{P2y}\\ &-P_{S3}\delta_{P3y} - T_1\delta_{P1x} - T_2\delta_{P2x} + \sum_{j=1}^{n_{rv}} \boldsymbol{F_{rvj}\delta_{F1y}} - \sum_{j=1}^{n_{rv}} \boldsymbol{F_{rvj}\delta_{F2y}} - \mathbf{2}\sum_{j=1}^{n_{ro}} \boldsymbol{F_{roj}\delta_{Fjx}} = 0\end{aligned} \tag{32}$$

Taking into account (27), with geometric considerations entirely analogous to those that led to the definition of (29), it is possible to determine the virtual displacements of the points of application of the forces which, under the condition of activation of the kinematics (infinitesimal rotations of the plastic hinges) are respectively equal to:

$$\delta_{F1y} = 0\,;\ \delta_{F2y} = s_2\left(1 + \frac{h_1}{h_2}\right);\ \delta_{Fjx} = \begin{cases} h_{Fj} & j = 1,2,3 \\ \dfrac{h_1}{h_2}h_{Fj} & j = 4,5,6 \end{cases} \tag{33}$$

Substituting into (32) the (29) and (33) and explicating with respect to α it is thus possible to determine the value of the activation multiplier under reinforced conditions $\alpha_{0,r}$ (the calculation is omitted, for the sake of brevity, bearing in mind that the calculation schemes in Figure 5.6 are only examples, since they refer to a specific case and are therefore not general).

5.2.4 Horizontal bending

The horizontal bending mechanism may occur at masonry panels that are effectively constrained to the orthogonal walls but not restrained at the top side by any device, subject to horizontal overhead actions (inertial forces associated with self-weights and borne loads, action due to the presence of a pushing roof). Under these conditions, the structural response can be expressed through a horizontal arc discharge effect in the thickness of the masonry.

The phenomenon of horizontal arc discharge in masonry assumes that the horizontal forces discharged on the wall hit by the seismic action reach the walls orthogonal to it in terms of a resultant action R which, at the masonry intersections, is divided into an orthogonal T component and an H component parallel to the façade wall. In the event that elements that withstand tensile stress are present in the walls orthogonal to the one under verification (such as, for example, metal tie rods or reinforced concrete floor kerbs) that are capable of effectively counteracting the T component that the ideal arc transmits to them, the arc effect may be activated and thus, under boundary conditions, the horizontal bending collapse mechanism may occur. In the absence of such devices, the collapse of the wall develops instead according to a simple overturning mechanism.

In the equilibrium boundary condition, the kinematic mechanism is activated by the formation in the thickness of the masonry of three plastic hinges: one in an intermediate position and the others at the ends of the horizontal arc, near the intersection between the wall under examination and the walls orthogonal to it, in correspondence with the elements that withstand tensile stress that counteract the T pull.

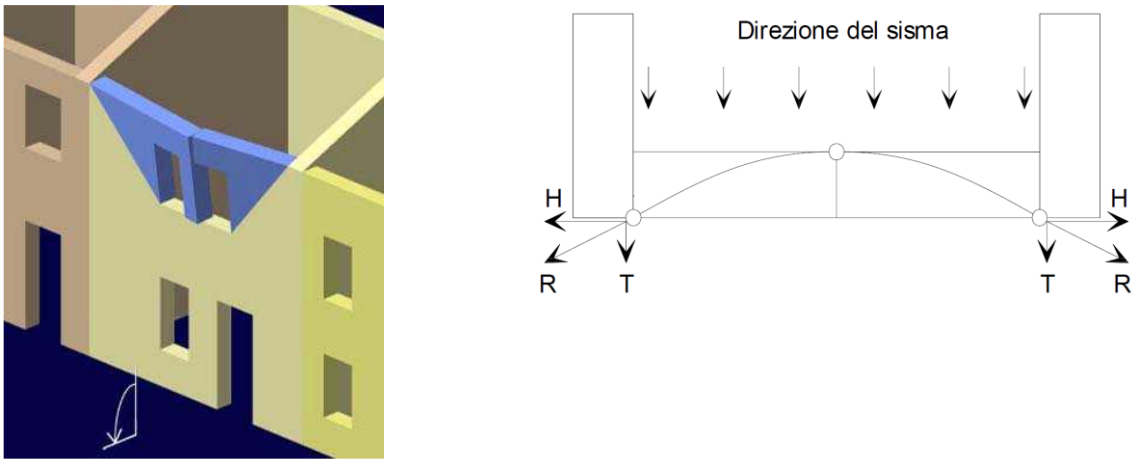

Figure 5.7 Overturning mode by horizontal bending (from Beolchini et al. 2007).

In particular, activation of the collapse mechanism occurs when the wall does not find contrasting structural elements capable of providing a reaction equal and opposite to the thrust component H. If the façade wall is not effectively confined with respect to displacements parallel to its plane (since it belongs, for example, to isolated or corner buildings), the displacement of the upwind walls, due to the H thrust, determines the instability of the kinematic chain constituted by the bodies involved in the mechanism and the consequent collapse: the masonry arch segments between the pairs of plastic hinges may undergo progressive rotations in the horizontal plane until the three hinges align. In this boundary condition, the isostatic scheme of the three-hinged arch becomes labile and wall collapse occurs. The evaluation of the multiplier α of the horizontal loads that triggers the described kinematics can be evaluated in this case by applying the Principle of Virtual Work. A different condition is represented by a wall that is effectively confined because it is restrained by the continuity of the wall (e.g. if the façade belongs to a cell that is interlocked in a row). In this case, the mechanism

may manifest itself as a result of plastic hinge formation due to compression crisis of the material. The condition just described foresees that the thrusts of the arch are completely balanced by the adjoining walls and that the stress state in the thickness of the wall under examination determines the possibility of crushing the masonry subjected to compressive stresses, in the keystone and at the reins of the ideal arch, with consequent activation of the mechanism. In this case, the analysis proceeds through the evaluation of the tension state generated in the masonry upon the application of the loads acting on the system and the comparison with the reference tension at break of the material (this second case is not considered here, for the sake of brevity).

5.2.4.1 Unreinforced condition

With reference to the unconfined masonry wall condition, some simplification must be introduced in the definition of the calculation scheme in order to make the procedure for assessing the activation multiplier α_0 easier. The collapse mechanism foresees the formation of two oblique cylindrical hinges and a vertical hinge delimiting the macro-elements. Each of the two identified bodies, under near-collapse conditions, can rotate around each of these oblique hinges and both rotate reciprocally with respect to the vertical element that separates them. In this kinematic motion, the points belonging to the two bodies undergo displacements defined by:

- One component in a direction parallel to the plane of the wall, which tends to move the two macro-elements apart;
- One in the vertical direction pointing upwards;
- One component in the direction orthogonal to the wall that highlights the overturning.

The actions that oppose these displacements are represented by the reaction to the thrust H of the horizontal arch, by the bracing walls, and by the stabilizing effect of the vertical loads.

However, the effects of displacements in the vertical direction are less significant than those occurring in the direction of the wall plane which, due to the interaction between the two bodies, accumulate in the reciprocal movement of the two macro-elements. It is therefore considered legitimate to disregard them. The simplification allows the examination of the plane problem represented by the static scheme illustrated in Figure 5.8, referring to the plane with respect to which the horizontal bending of the wall structure occurs, avoiding the analysis of a spatial problem.

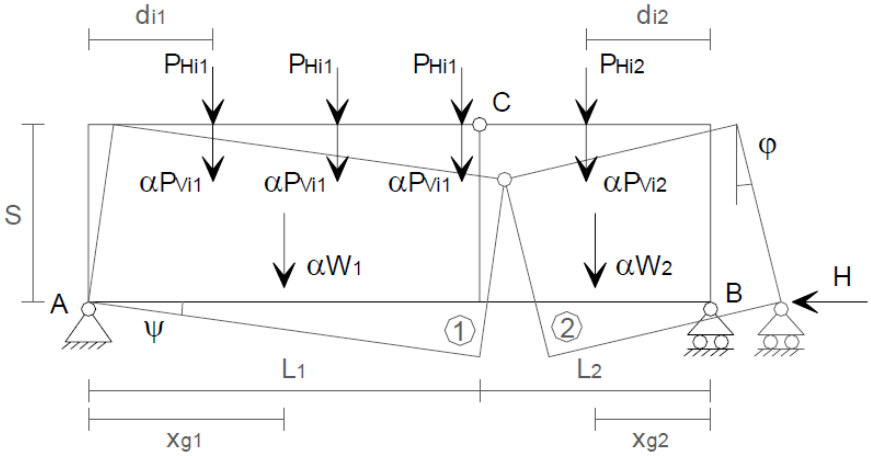

Figure 5.8 Calculation scheme (from Beolchini et al. 2007).

After assessing the dimensions and geometry of the macro-elements, the constraint conditions and the loads acting on the system, represented by the horizontal actions (due to the earthquake or static thrusts) and the containment action H of the bracing walls, the virtual displacements of the points of application of the forces are calculated by assigning a unit virtual rotation ψ = -1 to body 1.

W_i is the self-weight of the i-th macro-element participating in the kinematics;

P_{Vi1} is the i-th vertical load transmitted at the head of macro-element 1;

P_{Vi2} is the i-th vertical load transmitted at the head of macro-element 2;

P_{Hi1} is the i-th static thrust transmitted by the roof overhead macro-element 1;

P_{Hi2} is the i-th static thrust transmitted by the roof overhead macro-element 2;

H is the maximum value of the reaction that can be withstood by the bracing wall, or walls, in cooperation with any other devices that can withstand tensile stress capable of counteracting the horizontal thrust of the arch (such as, for example, metal tie rods and/or reinforced concrete kerbs);

s is the thickness of the wall;

L_i is the length of the i-th macro-element;

d_{i1} is the horizontal distance of the point of application of the i-th load acting at the head of macro-element 1 with respect to the corresponding reduction pole (hinge A);

d_{i2} is the horizontal distance of the point of application of the i-th load acting at the head of macro-element 2 with respect to the corresponding reduction pole (carriage B);

x_{Gi} is the horizontal distance of the centre of gravity of the i-th macro-element from its reduction pole (hinge A for body 1 and carriage B for body 2);

α is the multiplier of the horizontal forces.

By imposing the congruence conditions on the virtual displacements of the two macro-elements, the generalised displacement parameters can be determined to describe the kinematics. Points A for macro-element 1 and B for macro-element 2 are set as reduction poles, respectively, and the congruence conditions are defined:

$$u_A = 0; v_A = 0; \theta_1 = -1; v_A = 0 \tag{34}$$

By imposing further constraint conditions:

$$u_{C1} = u_{C2}; v_{C1} = v_{C2} \tag{35}$$

We derive:

$$\begin{cases} u_{C1} = s \\ v_{C1} = -L_1 \end{cases} \quad \begin{cases} u_{C2} = u_B - \varphi s \\ v_{C2} = -\varphi L_2 \end{cases} \Rightarrow \begin{cases} \varphi = L_1/L_2 \\ u_B = s(1 + L_1/L_2) \end{cases} \tag{36}$$

Finally, the generalised displacements of the rigid body system are determined:

$$\begin{aligned} &(u_{01}; v_{01}; \theta_1) = (u_A; v_A; \psi) = (0; 0; 1) \\ &(u_{02}; v_{02}; \theta_2) = (u_B; v_B; \varphi) = (s(1 + L_1/L_2); 0; L_1/L_2) \end{aligned} \tag{37}$$

Applying the Principle of Virtual Work results in:

$$\alpha \left[W_1 \delta_{1y} + W_2 \delta_{2y} + \sum_i P_{Vi1} \delta_{Pi1y} + \sum_i P_{Vi2} \delta_{Pi2y} \right] - \sum_i P_{Hi1} \delta_{Pi1y} - \sum_i P_{Hi2} \delta_{Pi2y} - H \delta_{Hx} = 0 \tag{38}$$

In the condition of activation of the kinematics, according to scheme in Figure 5.8 and taking into account (35),(36) and (37), the virtual displacements of the points of application of the forces in the respective direction of action result as:

$$\delta_{1y} = x_{G1} \quad \delta_{2y} = \frac{L_1}{L_2} x_{G2} \quad \delta_{Pi1y} = d_{i1} = -\delta_{hi1} \quad \delta_{Pi2y} = \frac{L_1}{L_2} d_{i2} = -\delta_{hi2} \quad \delta_{Hx} = s\left(1 + \frac{L_1}{L_2}\right) \tag{39}$$

Substituting into the expression (38) the (39) and explicating with respect to α, we obtain the value α_0 of the multiplier in the kinematic activation condition:

$$\alpha_0 = \frac{Hs\left(1+\frac{L_1}{L_2}\right) - \sum_i P_{Hi1} d_{i1} - \sum_i P_{Hi2} \frac{L_1}{L_2} d_{i2}}{W_1 x_{G1} + W_2 \frac{L_1}{L_2} x_{G2} + \sum_i P_{Vi1} d_{i1} + \sum_i P_{Vi2} \frac{L_1}{L_2} d_{i2}} \quad (40)$$

For the evaluation of the value of the force H (see above), one can make use of the simple diagram in Figure 5.9 which depicts a portion of the bracing wall to which the wall in Figure 5.8, orthogonal to it, is restrained. The boundary force H is calculated considering the equilibrium boundary conditions at the overturning of the bracing wall.

The stabilizing and overturning moments with respect to pole A are respectively:

$$M_{S(A)} = W\frac{S_c}{2} + F_V d_V + P_S d + Th \quad (41)$$

$$M_{R(A)} = Hh_H + F_H h_V + P_H h \quad (42)$$

By imposing equilibrium between the two moments and explicating with respect to H, we obtain:

$$H = \frac{\left(W\frac{S_c}{2} + F_V d_V + P_S d + Th - F_H h_V - P_H h\right)}{h_H} \quad (43)$$

In the previous expressions, the terms take on their usual meaning, with weights and actions transmitted by the horizontal structures evaluated by prefixing a suitable length, dependent on the conditions of the masonry of the bracing wall called upon to withstand the thrust. Note that the equilibrium equation does not include terms related to the inertia of the vertical loads, as the seismic action is parallel to the bracing itself.

The height $h_H = h - \theta b$ is calculated after fixing the height b of the two masonry bodies involved in the kinematics; the parameter θ is 0.50 in the case of a rectangular masonry beam and 0.33 if the mass involved is triangular.

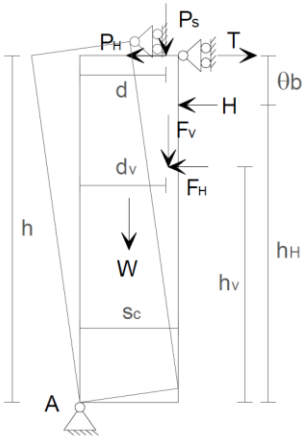

Figure 5.9 Calculation scheme (from Beolchini et al. 2007).

The calculation, as described here, must be repeated as the position of the vertical cylindrical hinge varies along the development of the façade wall (e.g. assuming a discrete step considered reasonable), so that the "critical" configuration of the kinematic chain is identified as the one associated with the lowest value of α_0.

5.2.4.2 Condition reinforced with the Resisto 5.9 system

In the reinforced configuration of the building, the presence of the horizontal metal elements of the modular system contributes to a significant increase in the force H_r that can be withstood by the bracing wall and thus counteracts the activation of the kinematics. In particular, by modifying (43), the force H_r can be evaluated by means of the following expression, in which the summation is understood to extend to all n_{ro} continuous horizontal reinforcement levels (therefore excluding from the calculation those interrupted by the presence of any openings) of the entire façade wall affected by the kinematics:

$$H_r = \frac{\left(W\frac{S_c}{2} + F_V d_V + P_S d + Th + \sum_{j=1}^{n_{ro}} \boldsymbol{F_{roj} h_{roj}} - F_H h_V - P_H h\right)}{h_H} \quad (44)$$

In which F_{roj}, the maximum horizontal force that can be withstood by the j-th level of continuous horizontal reinforcement (at elevation h_{roj} with respect to the foundation) is to be assessed as the minimum between:

- The tensile strength of the gross cross-section and the cross-section weakened by the holes, with reference to the minimum horizontal section member (between plate and L-profile) identified along the development of the reinforcement at the level considered (to be assessed on the basis of the arrangement of the modules, conditioned by the geometry of the wall and, in particular, the presence of openings);
- The tensile strength of the bolted connection between the frame modules, to be assessed according to the number of bolts, the tensile strength of the individual bolt and the puncture strength of the plate;
- The strength in the horizontal direction of the anchoring system between the reinforcement and masonry;
- The strength of the connection between the frames of the different walls (see above 5.2.1.2).

The strength in the horizontal direction of the anchoring system between the reinforcement and masonry is determined by multiplying the strength of the single anchor (see previous 5.2.3.2) by the smallest number $n_{a,min}$ of anchors present in the two rigid bodies into which the portion of wall involved in the kinematics is divided by the plastic hinge C. Unlike the previous ones, this contribution therefore varies as the geometry of the rigid bodies considered varies.

Considering the increase in the horizontal force that can be withstood by the bracing wall ($H_r - H$)guaranteed by the bracing system, (40) is then changed to the following expression (45):

$$\alpha_{0,r} = \frac{\boldsymbol{H_r s}\left(\mathbf{1}+\frac{\boldsymbol{L_1}}{\boldsymbol{L_2}}\right) - \sum_i P_{Hi1} d_{i1} - \sum_i P_{Hi2} \frac{L_1}{L_2} d_{i2}}{W_1 x_{G1} + W_2 \frac{L_1}{L_2} x_{G2} + \sum_i P_{Vi1} d_{i1} + \sum_i P_{Vi2} \frac{L_1}{L_2} d_{i2}} \tag{45}$$

5.2.5 Gable overturning

5.2.5.1 Unreinforced condition

The overturning of the gable wall (typically as a result of the cyclic hammering action of a large ridge beam in the absence of an effective connection of the wall to the roof) activates an out-of-plane bending mechanism characterised by the formation of wedge-shaped wall macro-elements rotating around oblique cylindrical hinges, as illustrated in Figure 5.10(a).

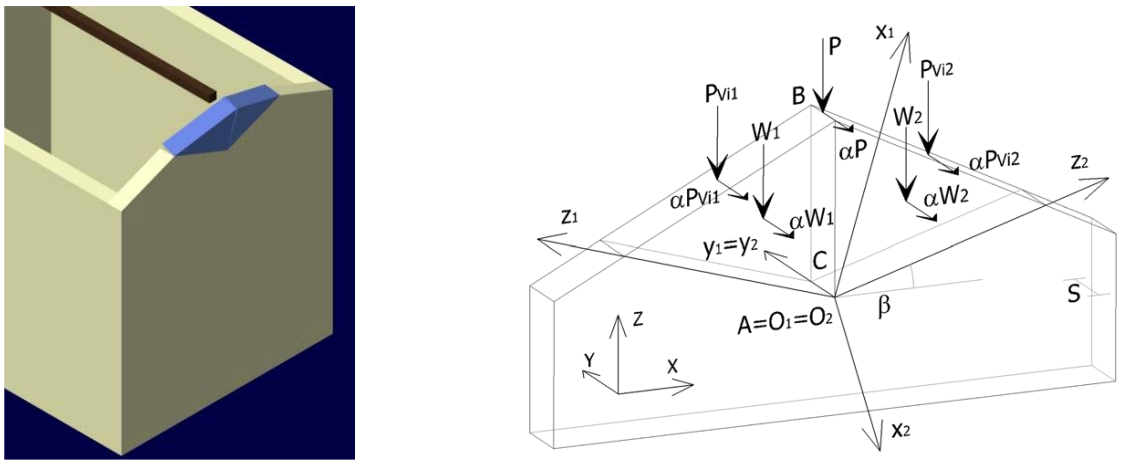

Figure 5.10 Overturning mode of the gable wall (a); “general” calculation sheet for variable inclination of oblique hinges with respect to the horizontal plane (b) (from Beolchini et al. 2007).

In order to define the geometry of the bodies involved in the kinematic motion, it is necessary to fix the angle of inclination β of the oblique hinges with respect to the horizontal, as depicted in Figure 5.10 (b). It should be noted in this regard that the smaller the angle β is, the more the overturning mechanism of the gable wall can be likened to a simple overturning mechanism around a horizontal

cylindrical hinge at its base. On the contrary, the more the cylindrical hinges assume a vertical course, the closer the kinematic motion approaches that of horizontal bending, according to the schematization adopted in the previous § 5.2.4. The geometry of the macro-elements is obviously also conditioned by the possible presence of openings near the roof.

Keeping in mind that we are considering the problem of the structural reinforcement of existing constructions made of blocks or solid bricks, with a typically regular masonry bond, it is assumed that we can limit treatment to the first case only, i.e. (assuming β = 0) to a simple overturning mode of the gable wall around a horizontal cylindrical hinge activated at its base. Please refer to Beolchini et al. (2007) for a more general treatment of the problem.

Please refer to the "simplified" calculation scheme in Figure 5.11, in which:

n is the number of vertical loads transmitted at the head of the gable wall by the roof (excluding the load transmitted by the ridge beam);

W is the self-weight of the gable wall;

P is the vertical load transmitted by the ridge beam;

P_{Vi} is the i-th vertical load transmitted to the gable wall from the roof;

s is the thickness of the gable wall;

h is the maximum height (at the ridge) of the gable wall;

h_{Vi} is the height of the point of application of the i-th vertical load transmitted at the head of the gable wall with respect to the hinge C at the base;

y_G is the height of the centre of gravity of the gable wall in relation to the hinge C at the base;

d_P is the retraction of the point of application of the vertical load transmitted by the ridge beam with respect to the external surface of the gable wall;

d_{Vi} is the retraction of the point of application of the i-th vertical load transmitted at the head of the gable wall with respect to its external surface;

α is the multiplier of the horizontal forces.

Under the condition of activation of the mechanism, that is assuming an infinite virtual rotation of the plastic hinge C, it is possible to express the virtual displacements of the points of application of the forces involved with respect to the geometric parameters identified above. The overturning M_R and stabilizing M_S moments are then derived using the following relationships (46) and (47).

$$M_R = \alpha \left[W y_G + P h + \sum_{i=1}^{n} P_{Vi} h_{Vi} \right] \tag{46}$$

$$M_S = W \frac{s}{2} + P d_P + \sum_{i=1}^{n} P_{Vi} d_{Vi} \tag{47}$$

By imposing the equilibrium between the overturning moment and stabilizing moment, the value of the multiplier can thus be determined α_0 in the kinematic activation condition:

$$\alpha_0 = \frac{W \frac{s}{2} + P d_P + \sum_{i=1}^{n} P_{Vi} d_{Vi}}{W y_G + P h + \sum_{i=1}^{n} P_{Vi} h_{Vi}} \tag{48}$$

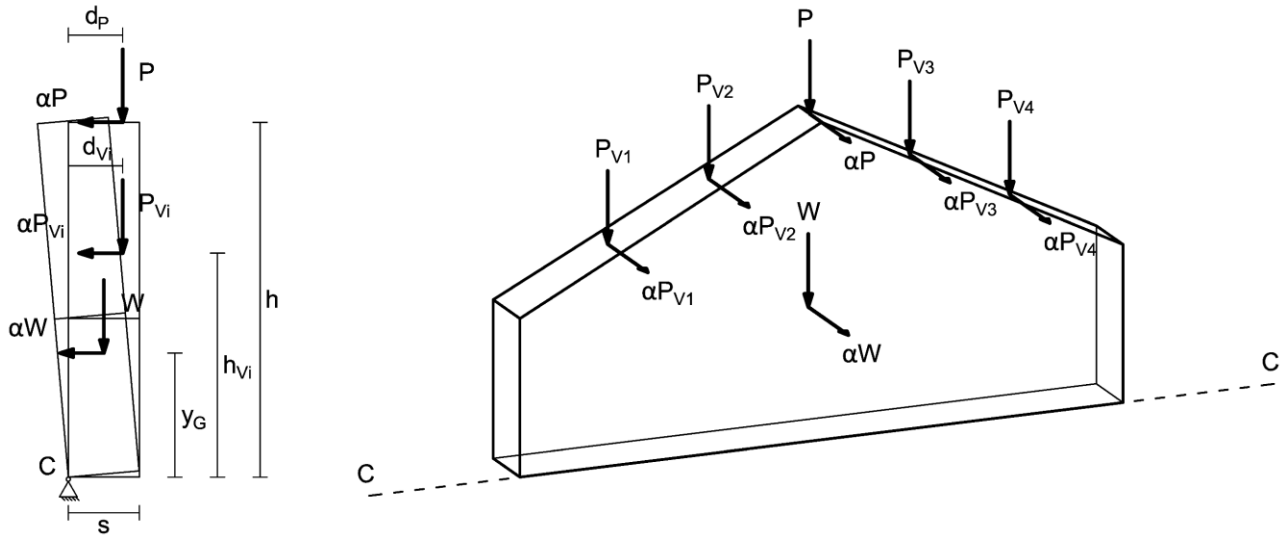

Figure 5.11 “Simplified” calculation sheet

5.2.5.2 *Condition reinforced with the Resisto 5.9 system*

Reinforcement of the gable wall by means of the Resisto 5.9 system, with the same overturning moment M_R, offers an increase in the stabilizing moment M_S that counteracts the activation of the kinematism. In particular, it is assumed that only the contribution of the vertical metal uprights constituted by the framing elements of the modular frames (disregarding the contribution offered by any vertical plates) is considered in the calculation.

The stabilizing moment contribution offered by the gable reinforcement as a whole is defined as a function of the number n_{rt} of vertical uprights and the contribution $M_{S,r}$ of each upright, evaluated as the minimum between the resistant moment of the L-profile and the moment corresponding to the tensile strength of the bolted connection between the reinforcing elements at the base of the gable wall and the modular frames arranged at the lower level (in turn defined as a function of the geometry of the connection and the lower of the tensile strength of the individual bolt and the puncture strength of the plate). Noting $M_{S,r}$ it is therefore possible to define the activation multiplier of the kinematic mechanism $\alpha_{0,r}$ for the reinforced wall, assuming the overturning moment is unchanged M_R:

$$M_S = W\frac{S}{2} + Pd_P + \sum_{i=1}^{n} P_{Vi}d_{Vi} + \boldsymbol{n_{rt} \cdot M_{S,r}} \tag{49}$$

$$\alpha_{0,r} = \frac{W\frac{S}{2} + Pd_P + \sum_{i=1}^{n} P_{Vi}d_{Vi} + \boldsymbol{n_{rt} \cdot M_{S,r}}}{Wy_G + Ph + \sum_{i=1}^{n} P_{Vi}h_{Vi}} \tag{50}$$

5.3 Calculation example

Verification of the local mechanisms of the perimeter wall of the south façade of a two-storey, above ground residential building in load-bearing solid brick and lime mortar (Figure 5.12) is considered below.

Figure 5.12 Identification of the wall under verification in the building considered.

It is assumed that the building is located in the Municipality of Cavezzo (MO), in a site characterised by type B subsoil and topographical category T1. The seismic parameters relative to the site, assuming a nominal life of the building V_N of 50 years and a class of use C_u = 1, are given in Table 5.1. A damping of 5% is assumed in the definition of the elastic response spectrum.

Table 5.1. Seismic parameters for the reference site

LIMIT STATE	a_g [g]	F_o [-]	T_C^* [s]	S_S [-]	S_T [-]	C_C [-]	S [-]	T_B [s]	T_C [s]	T_D [s]
OLS	*0.040*	*2.566*	*0.250*	*1.200*	*1.000*	*1.451*	*1.200*	*0.121*	*0.363*	*1.758*
DLS	0.051	2.496	0.268	1.200	1.000	1.432	1.200	0.128	0.383	1.803
LSLS	0.150	2.588	0.269	1.200	1.000	1.431	1.200	0.128	0.385	2.201
SLC	*0.202*	*2.535*	*0.276*	*1.195*	*1.000*	*1.423*	*1.195*	*0.131*	*0.393*	*2.409*

The geometry of the wall, characterised by full-head masonry bond with a thickness of 25 cm, is schematized in Figure 5.13 (in which the dashed line identifies the extrados height of the intermediate floor).

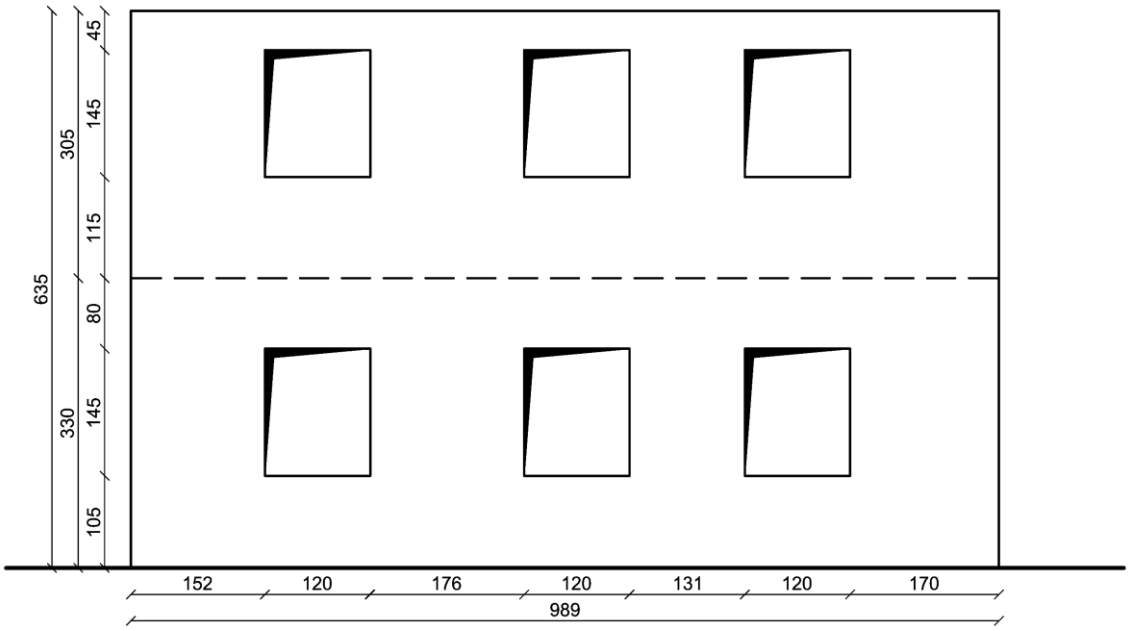

Figure 5.13 Geometry of the wall under verification (measurements in [cm]).

The specific weight of the masonry is assumed to be equal to 18 kN/m^3. The floors, assumed to be made on both levels of the building with wooden beams and single-layer floorboard, are warped in a north-south direction with a net span of 4.0 m (influence span 2.0 m), with reference to the wall under verification; on the first level there is a terracotta floor on a light screed and a thin bed of mortar. The roof pitch resting on the wall, with 0.8 m overhanging eaves, has a wooden joist and batten structure and a roof covering of brick tiles. On the whole, with reference to the “seismic” combination of loads and considering a variable overload of 2.0 kN/m^2 on the first floor, the load transmitted by the floors on the first and second levels is equivalent, depending on the mechanism considered (see below) to a load uniformly distributed along the longitudinal development of the wall equal to 4.2 kN/m and 3.8 kN/m respectively.

It should also be noted that, to simplify calculation, all the loads (and therefore, in addition to the self-weight of the rigid bodies involved in the kinematic motion, also the loads transmitted by the floors or by the overlying portion of the wall) are considered to be applied to the centre of the wall thickness.

Figure 5.14 illustrates the solution adopted for wall reinforcement using the Resisto 5.9 modular system. In particular, the reinforcement solution foresees the coupling of the frames to floor metal kerbs, at the level of each horizontal structure, realised by means of special C-section elements with a height of 20 cm, with the other geometric dimensions corresponding to those of the frame elements of the modular system.

Given the dimensions given in Figure 5.14 and the details illustrated Figure A.2 in Appendix A, it is possible to identify the position of the horizontal and vertical reinforcement lines to be considered in the evaluation of the different mechanisms, based on the indications given in the previous paragraphs. In particular, in Figure 5.15 below, the vertical and horizontal continuous reinforcement lines in the wall are identified in full strokes (12 and 6 respectively). The additional connection dimensions of the modular frame to the bracing of the bracing walls (14 in all) are also identified in dashes. Finally, it is possible to identify the position of the modular system anchoring to the masonry at the continuous, horizontal and vertical reinforcement lines.

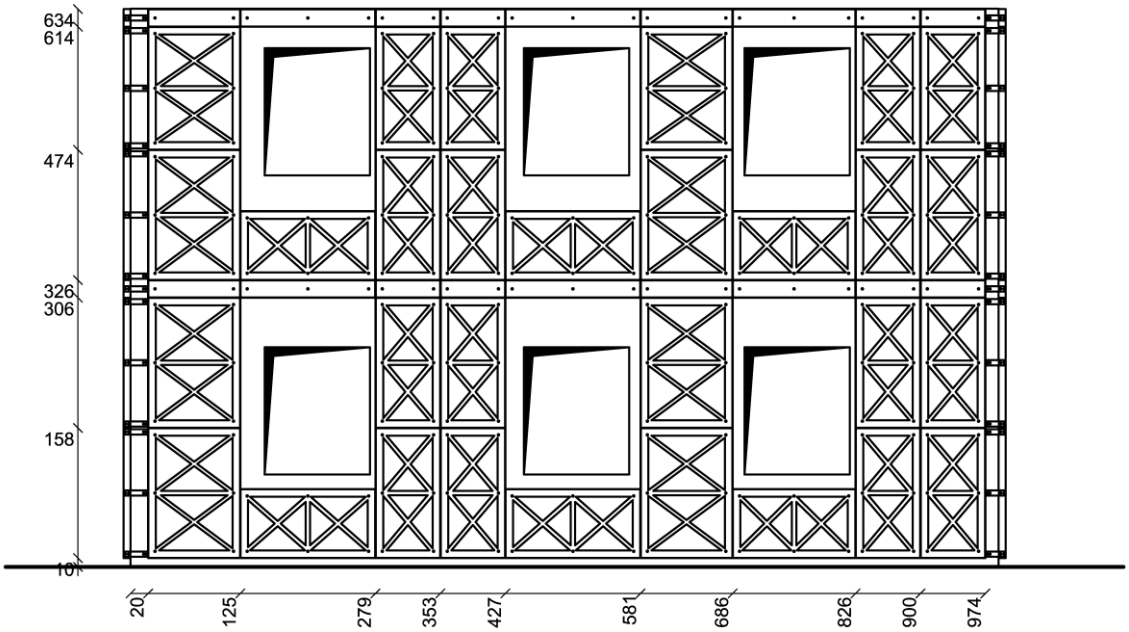

Figure 5.14 Scheme of wall reinforcement using the Resisto 5.9 system (dimensions in [cm]).

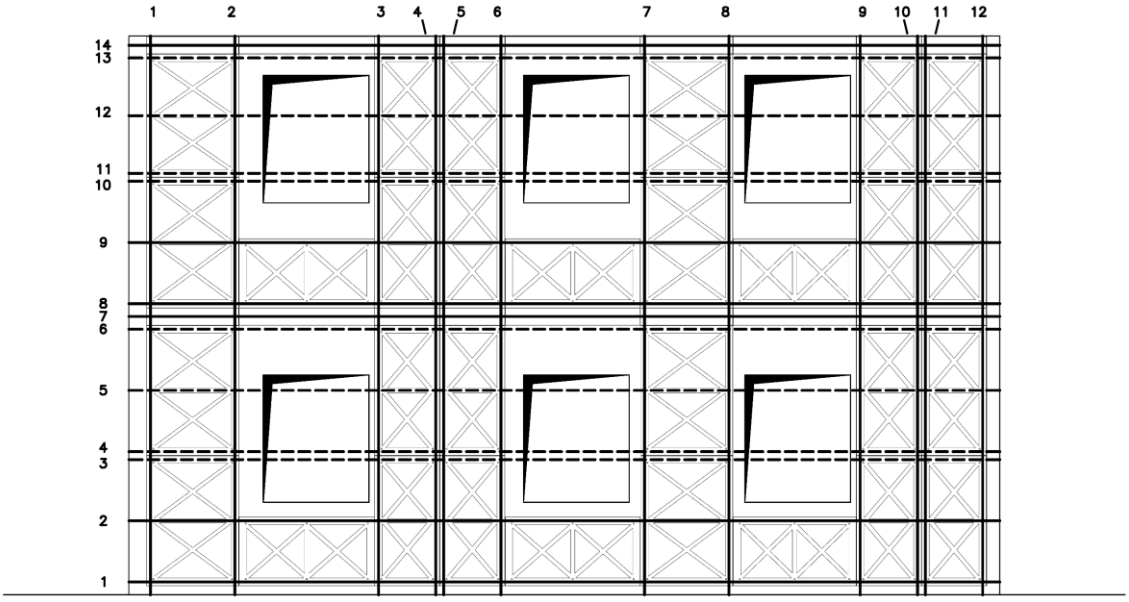

Figure 5.15 Identification of continuous reinforcement and connection lines considered in the calculation.

Table 5.2 shows the position h_r of the connections between the modular reinforcement systems arranged in correspondence with the wall under verification and the bracing walls; the horizontal lines of continuous wall reinforcement (not interrupted by openings), are indicated by "*". With regard to this distinction, please note that, while in the evaluation of simple overturning and vertical bending mechanisms (§§ 5.2.3.2 and 5.2.3.2) all connections between the metal reinforcement frames of

orthogonal walls are considered, in the evaluation of the horizontal bending mechanism (§ 5.2.4.2) only continuous horizontal reinforcement lines are considered. In particular, the position h_r is defined by the height in relation to the wall base of the centre of gravity of the bolted frame-frame connection.

Table 5.3 shows the height h_a (in relation to the base) and the position d_a (in relation to the left edge of the wall) of the anchoring placed at the vertical and horizontal reinforcement lines, respectively. With reference to the vertical and horizontal bending mechanisms, as specified in the previous §§ 5.2.3.2 and 5.2.4.2, as the position of the intermediate cylindrical hinge C varies, the position of the anchoring conditions the definition of the maximum force that can be withstood by the reinforcement line, through the parameter $n_{a,min}$, number of anchors less than those present in the two rigid bodies involved in the kinematic mechanism.

Table 5.2. Position of connections between modular perimeter wall reinforcement systems

position	h_r [m]
1	0.145 *
2	0.840 *
3	1.535
4	1.625
5	2.320
6	3.015
7	3.160 *
8	3.305 *
9	4.000 *
10	4.695
11	4.785
12	5.440
13	6.095
14	6.240 *

Table 5.3. Position of the anchors of the modular reinforcement system to the masonry

h_a [m]	d_a [m]
0.178	0.278
0.840	1.172
1.502	1.328
1.658	2.020
2.320	2.712
2.982	2.868
3.160	3.452
3.338	3.608
4.000	4.192
4.662	4.348
4.818	5.040
5.440	5.732
6.062	5.888
6.240	6.782
-	6.938
-	7.560
-	8.182
-	8.338
-	8.922
-	9.078
-	9.662

All the possible local mechanisms for the wall (simple overturning, vertical bending and horizontal bending) are analysed below, taking into consideration, when necessary, different collapse modes (kinematics) in the hypothesis of an ineffective wall-wall and masonry-roofing bonding. With regard to this last aspect, please note that there are no reinforced concrete horizontal structure kerbs in the building. It is also assumed that the level of knowledge of the work is LC2 and, consequently, a confidence factor CF = 1.2 is adopted. Finally, the simplifying hypothesis of infinite compressive strength of the masonry is adopted in the calculation.

By way of example, it can be useful to preface this detailed evaluation with the calculation of the activation multiplier α_0 of the local mechanisms of simple overturning and vertical bending of a single-storey blind wall, with dimensions corresponding to those of the ground floor of the wall under verification (length 9.89 m, height 3.30 m, thickness 0.25 m). Reinforcement of the wall, in this case, is realised (again adopting the floor kerb solution) by using the "base" module of the modular system (dimensions 1050 x 1480 mm; see Figure A.1). As shown in Figure 5.16, there are 7 and 18 continuous horizontal and vertical reinforcement lines in the wall, respectively. For the purposes of calculation, it should be noted that the former are positioned at the same h_r dimensions as those shown in Table 5.2.

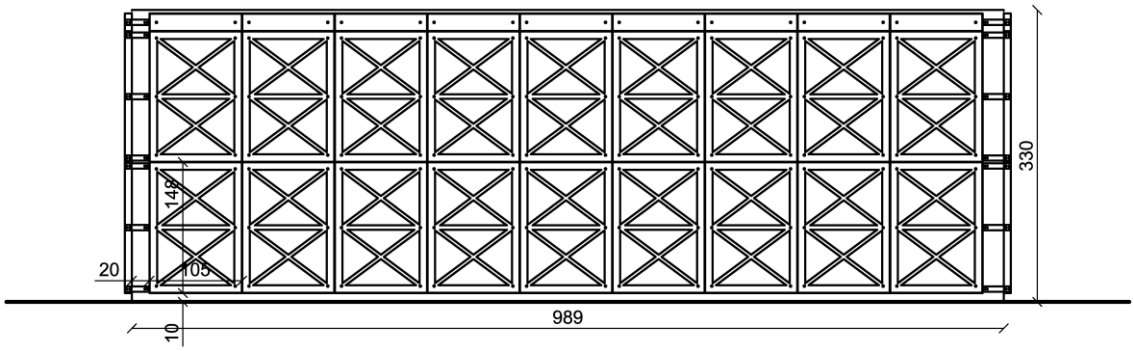

Figure 5.16 Reinforcement solution for a single-storey solid wall (measurements in [cm]).

5.3.1 Simple overturning

In the calculation, a maximum value of F_{ro}, force that can be withstood by the single connection between the modular reinforcement systems of the wall under examination and the bracing walls is assumed to be 32.4 kN, based on the considerations given in Appendix A in § A.1.

5.3.1.1 Simple overturning of a single-storey solid wall

With the parameter values given in Table 5.4, the multiplier α_0 of activation of the kinematics associated with the overturning of the wall with respect to the base can be evaluated, respectively in the pre-intervention condition and in the reinforced configuration of the wall, by means of the following expressions, obtained by adapting (24) and (26) to the specific case:

$$\alpha_0 = \frac{(W + P_S)\frac{s}{2}}{W\frac{h}{2} + P_S h} = \frac{23.5}{379.3} = 0.062 \tag{51}$$

$$\alpha_{0,r} = \frac{(W + P_S)\frac{s}{2} + \Delta M_{S,r}}{W\frac{h}{2} + P_S h} = \frac{842.6}{379.3} = 2.221 \tag{52}$$

being:

$$\Delta M_{S,r} = 2F_{ro}\sum_{j=1}^{n_{ro}} h_{rj} = 2 \cdot 32.4 \cdot 12.64 = 819.1\ [kNm] \tag{53}$$

Table 5.4. Calculation parameter values

W [kN]	P_S [kN]	s [m]	h [m]
146.9	41.5	0.25	3.30

It should be noted that, on the basis of the assumptions adopted in the definition of the reinforcement scheme of the blind wall considered, the contribution of the reinforcement is obtained by considering the summation that appears as a numerator in (53) extended to the first 7 levels of reinforcement shown in Table 5.2.

5.3.1.2 Simple overturning of the wall under verification

In the evaluation of the local mechanism of simple overturning of the two-storey wall subject to verification, two possible kinematics (Figure 5.17) are considered:

- The first involves the overturning of the entire wall in relation to the base;
- The second involves the overturning of only the wall portion at the second level of the wall.

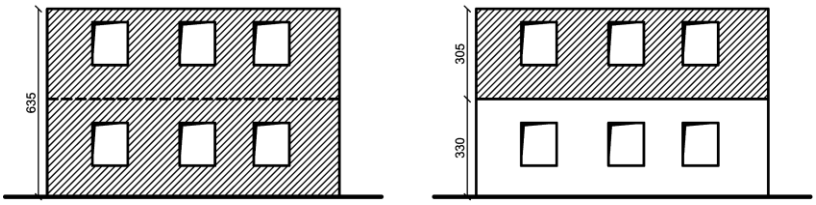

Figure 5.17 Simple overturning mechanisms considered: (a) entire façade; (b) second level (measurements in [cm]).

The self-weight W_i and the y_{Gi} centre of gravity of each wall level, in the presence of openings distributed with sufficient regularity, can be evaluated using the following expressions, by breaking down the geometry into three strips (spandrel, intermediate and transom), of known height h_{ij} and total length L_{ij} (net of openings, in the case of the intermediate strip), as illustrated in Figure 5.18:

$$W_i = \left(\sum_{j=1}^{3} L_{ij} h_{ij}\right) s_i \gamma_i \tag{54}$$

$$y_{Gi} = \frac{\sum_{j=1}^{3} L_{ij} h_{ij} \left(\sum_{k}^{j-1} h_{ik} + \frac{h_{ij}}{2}\right)}{\sum_{j=1}^{3} L_{ij} h_{ij}} \tag{55}$$

with s_i and γ_i, respectively, wall thickness and specific weight of the masonry at the level considered.

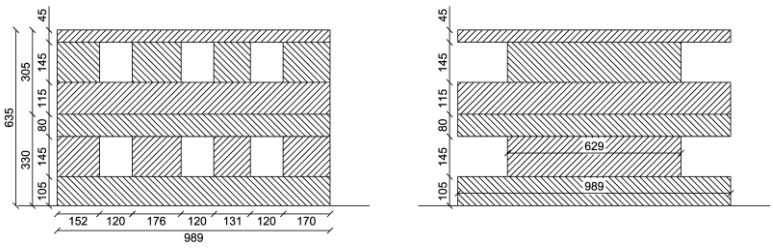

Figure 5.18 Identification of the geometry of the strips constituting each level of the wall under verification (measurements in [cm]).

The kinematic activation multiplier α_0 associated with the collapse modes considered in Figure 5.17 (identified as “2-1” and “2” respectively), can be evaluated in the pre-intervention condition and in the reinforced wall configuration, assuming the values of the calculation parameters given in Table 5.5, by means of the following expressions, obtained from (24) and (26):

$$\alpha_{0(2-1)} = \frac{(W_1 + W_2 + P_{S1} + P_{S2})\frac{s}{2}}{W_1 y_{G1} + W_2(h_1 + y_{G2}) + P_{S1} h_1 + P_{S2}(h_1 + h_2)} = \frac{39.3}{1108.3} = 0.035 \tag{56}$$

$$\alpha_{0,r(2-1)} = \frac{(W_1 + W_2 + P_{S1} + P_{S2})\frac{s}{2} + \Delta M_{S,r(2-1)}}{W_1 y_{G1} + W_2(h_1 + y_{G2}) + P_{S1}h_1 + P_{S2}(h_1 + h_2)} = \frac{3097.9}{1108.3} = 2.795 \quad (57)$$

$$\alpha_{0(2)} = \frac{(W_2 + P_{S2})\frac{s_2}{2}}{W_2 y_{G2} + P_{S2}h_2} = \frac{18.7}{276.8} = 0.068 \quad (58)$$

$$\alpha_{0,r(2)} = \frac{(W_2 + P_{S2})\frac{s_2}{2} + \Delta M_{S,r(2)}}{W_2 y_{G2} + P_{S2}h_2} = \frac{761.3}{276.8} = 2.751 \quad (59)$$

being:

$$\Delta M_{S,r(2-1)} = 2F_{ro} \sum_{j=1}^{n_{or(2-1)}} h_{rj} = 2 \cdot 32.4 \cdot 47.20 = 3058.6\ [kNm] \quad (60)$$

$$\Delta M_{S,r(2)} = 2F_{ro} \sum_{j=1}^{n_{or(2)}} (h_{rj} - h_1) = 2 \cdot 32.4 \cdot 11.46 = 742.6\ [kNm] \quad (61)$$

In the last two expressions, the summations are understood to refer, respectively, to all 14 connection levels of the wall, shown in Table 5.2 and only to the levels above h_1 (i.e. the 7 connection levels between 8 and 14).

Table 5.5. Calculation parameter values

Elevation	W_i [kN]	P_{Si} [kN]	s_i [m]	h_i [m]	y_{Gi} [m]
1	123.4	41.5	0.25	3.30	1.63
2	112.0	37.6	0.25	3.05	1.45

Knowing the activation multiplier α_0 of the mechanism, it is possible to assess the corresponding spectral acceleration a_0 of the oscillator equivalent to a single degree of freedom by means of the expression (4), once the participating mass e^* has been defined by means of (3) and assumed the value of the level of knowledge FC LC attained.

For the two kinematics considered in the evaluation of the local simple overturning mechanism of the wall under verification, the general expression (3) can be reformulated as follows, depending on the parameters defined above:

$$e^*_{(2-1)} = \frac{[W_1 y_{G1} + W_2(h_1 + y_{G2}) + P_{S1}h_1 + P_{S2}(h_1 + h_2)]^2}{(W_1 + W_2 + P_{S1} + P_{S2}) \cdot [W_1 y_{G1}^2 + W_2(h_1 + y_{G2})^2 + P_{S1}h_1^2 + P_{S2}(h_1 + h_2)^2]} \quad (62)$$

$$e^*_{(2)} = \frac{[W_2 y_{G2} + P_{S2}h_2]^2}{(W_2 + P_{S2}) \cdot [W_2 y_{G2}^2 + P_{S2}h_2^2]} \quad (63)$$

Table 5.6 reports the values of the activation multiplier α_0 of the mechanism, of the participating mass $e^*$and of the spectral acceleration a_0 of the oscillator equivalent to a single degree of freedom obtained for each kinematic mechanism considered, respectively in the pre-intervention condition and in the reinforced configuration of the wall.

Table 5.6. Local simple overturning mechanism: results

Kinematic mechanism	Condition	α_0 [-]	e^* [-]	a_0 [g]
2-1	pre-intervention	0.035	0.810	0.036
	post-intervention	2.795		2.874
2	pre-intervention	0.068	0.877	0.064
	post-intervention	2.751		2.613

5.3.2 Vertical bending

Based on the considerations given in Appendix A, the following are assumed in the calculations:

- a maximum value of F_{ro}, force that can be withstood by the single connection between the modular reinforcement systems of the wall under examination and the bracing walls is assumed to be 32.4 kN (see § A.1);
- a maximum value of F_{rv} vertical force that can be withstood by each individual continuous vertical reinforcement line arranged in the wall defined as:

$$F_{rv} = min\{\overline{B_p}; n_{a,min} \cdot V_a; n_{a,min} \cdot F_b\} \quad (64)$$

being $\overline{B_p}$ = 32.4 kN the puncture strength of the metal frame plate in correspondence with the bolted connection of the frame-to-frame connection, V_a = 5.4 kN the maximum force that can be withstood by the anchoring of the frame to the masonry resulting from experimental shear tests carried out in situ (obtained by adopting a safety coefficient $\gamma_{Mm} = 2.5$), F_b = 27.7 kN la the bearing strength of the frame element at the section weakened by the anchoring hole and $n_{a,min}$ the smallest number of anchors between the two rigid bodies involved in the kinematic mechanism (see § A.2).

It should be noted that, while the position of the intermediate cylindrical hinge should be made to vary parametrically along the height of the wall in order to identify the “critical” geometric configuration associated with the minimum activation multiplier for a rigorous verification of the wall with respect to the vertical bending mechanism, it is here arbitrarily assumed to be fixed.

5.3.2.1 Vertical bending of a single-storey solid wall

The activation multiplier α_0 of the mechanism in the pre-intervention condition and in the reinforced wall configuration is evaluated using the following expressions, derived from (30) and (32). The calculation is performed assuming the formation of the intermediate cylindrical hinge at mid-height of the wall (at 1.65 m from the base).

$$\alpha_0 = \frac{N}{D} = \frac{52.5}{121.2} = 0.433 \quad (65)$$

$$\alpha_{0,r} = \frac{N + N_{rv} + N_{ro}}{D} = \frac{557.9}{121.2} = 4.605 \quad (66)$$

with:

$$N = W_1 \frac{s}{2} + (W_2 + P_s)s\left(1 + \frac{1}{2}\frac{h_1}{h_2}\right) = 52.5\ [kNm] \quad (67)$$

$$N_{rv} = n_{rv} F_{rv} s\left(1 + \frac{h_1}{h_2}\right) = 145.8\ [kNm] \quad (68)$$

$$N_{ro} = 2F_{ro}\left[\sum_{j=1}^{\overline{n_{ro}}} h_{roj} + \sum_{j=\overline{n_{ro}}+1}^{n_{ro}} \left(h - h_{roj}\right)\frac{h_1}{h_2}\right] = 359.6\ [kNm] \quad (69)$$

$$D = (W_1 + W_2)\frac{h_1}{2} = 121.2\ [kNm] \tag{70}$$

where s = 0.25 m and h = 3.30 m are the thickness and height of the wall, respectively; P_S = 41.5 kN is the load transmitted by the floor and W_1 and W_2 and h_1 and h_2 represent the self-weight and height of the two rigid bodies participating in the kinematic motion, respectively. For the fixed position of the intermediate cylindrical hinge, W_1 = W_2 = 73.4 kN and h_1 = h_2 = 1.65 m.

Based on the geometry of the reinforcement system adopted, the assumption of the position of the intermediate hinge leads to a value of $n_{a,min}$ equal to 3 (as shown in Table 5.2) and thus to a value of the maximum force F_{rv} that can be withstood by each of the continuous lines of vertical reinforcement equal to 16.2 kN. There are n_{rv} = 18 continuous vertical reinforcement lines in the wall and n_{ro} = 7 levels of connection of the modular wall reinforcement system with those of the orthogonal walls, of which the first $\overline{n_{ro}}$ = 3 belong to rigid body 1 and the next $n_{ro} - \overline{n_{ro}}$ = 4 belong to rigid body 2.

5.3.2.2 Vertical bending of the wall under verification

In the evaluation of the local mechanism of vertical bending of the two-storey wall subject to verification, three possible kinematics (Figure 5.19) are considered:

- The first envisages that the kinematic motion involves the entire wall, in the hypothesis of the formation of the intermediate cylindrical hinge at the extrados of the intermediate floor (at 3.30 m from the base of the wall);
- The second envisages that the kinematic motion involves only the portion of masonry at the second level of the wall, in the hypothesis of the formation of the intermediate cylindrical hinge at the top of the spandrel strip (at 1.15 m from the extrados of the intermediate floor);
- The third envisages that the kinematic motion involves only the portion of masonry at the first level of the wall, in the hypothesis of the formation of the intermediate cylindrical hinge at the top of the spandrel strip (at 1.05 m from the base of the wall).

The three kinematics are hereafter identified as “1-2”, “2” and “1” respectively.

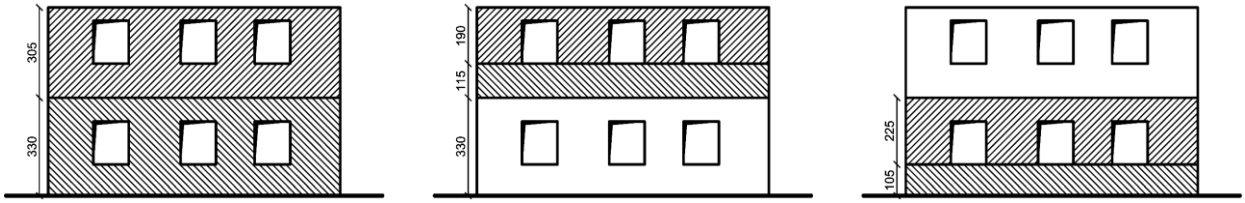

Figure 5.19 Vertical bending mechanisms considered: (a) entire façade; (b) second level; (c) first level (measurements in [cm]).

Table 5.7 contains the values of the self-weight W_i, height h_i and vertical arm y_{Gi} of the centre of gravity of the two rigid bodies involved in the collapse mechanism with respect to their respective pole, defined on the basis of geometric considerations entirely analogous to those used for the definition of the previous expressions (54) and (55). In fact, one must proceed to break down each of the two rigid bodies into one or more horizontal strips of constant width depending on the geometry of the portion of the wall considered (shown in Figure 5.19) and the position of the intermediate hinge assumed for each kinematic mechanism and then proceed to evaluate the corresponding weight and centre of gravity.

Table 5.7. Calculation parameter values relating to the geometry of the rigid bodies involved in the kinematics

	Kinematic mechanism								
	1-2			2			1		
Rigid body	W_i [kN]	h_i [m]	y_{Gi} [m]	W_i [kN]	h_i [m]	y_{Gi} [m]	W_i [kN]	h_i [m]	y_{Gi} [m]
1	123.4	3.30	1.63	51.2	1.15	0.58	46.7	1.05	0.52
2	112.0	3.05	1.60	60.8	1.90	0.86	76.7	2.25	1.00

Table 5.8 contains the data required to evaluate the contribution of the wall reinforcement, defined as a function of the position assumed for the intermediate cylindrical hinge: the number $n_{a,min}$ of the smallest of the anchors in the two rigid bodies; the value of the maximum force F_{rv} that can be withstood by each n_{rv} of the continuous lines of vertical reinforcement; the number n_{ro} of connection levels of the modular wall reinforcement system with those of the orthogonal walls; and the number $\overline{n_{ro}}$ of connections belonging to rigid body 1.

Table 5.8. Calculation parameter values relating to the contribution of the reinforcement

Kinematic mechanism	$n_{a,min}$ [-]	F_{rv} [kN]	n_{rv} [-]	n_{ro} [-]	$\overline{n_{ro}}$ [-]
1-2	7	32.4	12	14	7
2	2	10.8	12	7	2
1	2	10.8	12	7	2

The activation multiplier α_0 of the mechanism in the pre-intervention condition and in the reinforced wall configuration is evaluated using the expressions derived from (30) and (32) for each of the kinematics considered:

$$\alpha_0 = \frac{N}{D} \tag{71}$$

$$\alpha_{0,r} = \frac{N + N_{rv} + N_{ro}}{D} \tag{72}$$

Knowing the activation multiplier α_0 of the mechanism, it is possible to assess the corresponding spectral acceleration a_0 of the oscillator equivalent to a single degree of freedom by means of the expression (4), once the participating mass e^* has been defined by means of (3) and assumed the value of the level of knowledge FC LC attained.

The expression (3) can be reformulated as:

$$e^* = \frac{N^{*2}}{D_1^* \cdot D_2^*} \tag{73}$$

The terms at the numerator and denominator of (71), (72) and (73) are evaluated by means of the expressions in the following three sub-sections, suitably differentiated for each of the kinematics considered.

Table 5.9 summarises the results of the calculation for each of the kinematics considered in terms of the values of the activation multiplier α_0 of the mechanism, the participating mass $e^*$and the spectral acceleration a_0 of the oscillator equivalent to a single degree of freedom, respectively, in the pre-intervention condition and in the reinforced wall configuration.

Table 5.9. Local vertical bending mechanism: results

Kinematic mechanism	Condition	α_0 [-]	e^* [-]	a_0 [g]
1-2	pre-intervention	0.147	0.916	0.134
	post-intervention	3.371		3.068
2	pre-intervention	0.628	0.998	0.523
	post-intervention	5.094		4.255
1	pre-intervention	1.464	0.997	1.228
	post-intervention	5.734		4.794

5.3.2.2.1 Vertical bending of the entire wall

$$N = (W_1 + P_{S1})\frac{s}{2} + (W_2 + P_{S2})s\left(1 + \frac{1}{2}\frac{h_1}{h_2}\right) = 78.3\ [kNm] \tag{74}$$

$$N_{rv} = n_{rv}F_{rv}s\left(1 + \frac{h_1}{h_2}\right) = 202.5\ [kNm] \tag{75}$$

$$N_{ro} = 2F_{ro}\left[\sum_{j=1}^{\overline{n_{ro}}} h_{roj} + \sum_{j=\overline{n_{ro}}+1}^{n_{ro}} \left(h_{P1} + h_{P2} - h_{roj}\right)\frac{h_1}{h_2}\right] = 1511.2\ [kNm] \tag{76}$$

$$D = W_1 y_{G1} + W_2 y_{G2}\frac{h_1}{h_2} + P_{S1}h_{P1} = 531.5\ [kNm] \tag{77}$$

$$N^* = W_1 y_{G1} + W_2 y_{G2}\frac{h_1}{h_2} + P_{S1}h_{P1} = 531.5\ [kNm] \tag{78}$$

$$D_1^* = W_1 + W_2 + P_{S1} = 276.9\ [kN] \tag{79}$$

$$D_2^* = W_1 y_{G1}^2 + W_2\left(y_{G2}\frac{h_1}{h_2}\right)^2 + P_{S1}h_{P1}^2 = 1114\ [kN^2m^2] \tag{80}$$

In (76) the summation is understood to extend to all 14 levels of horizontal reinforcement arranged in the wall (see Table 5.2).

5.3.2.2.2 Vertical bending of the wall at the second level

$$N = W_1\frac{s}{2} + (W_2 + P_{S2})s\left(1 + \frac{1}{2}\frac{h_1}{h_2}\right) = 38.5\ [kNm] \tag{81}$$

$$N_{rv} = n_{rv}F_{rv}s\left(1 + \frac{h_1}{h_2}\right) = 52.1\ [kNm] \tag{82}$$

$$N_{ro} = 2F_{ro}\left[\sum_{j=1}^{\overline{n_{ro}}} h_{roj} + \sum_{j=\overline{n_{ro}}+1}^{n_{ro}} \left(h_{P1} + h_{P2} - h_{roj}\right)\frac{h_1}{h_2}\right] = 221.5\ [kNm] \tag{83}$$

$$D = W_1 y_{G1} + W_2 y_{G2}\frac{h_1}{h_2} = 61.2\ [kNm] \tag{84}$$

$$N^* = W_1 y_{G1} + W_2 y_{G2} \frac{h_1}{h_2} = 61.2\ [kNm] \tag{85}$$

$$D_1^* = W_1 + W_2 = 112.0\ [kN] \tag{86}$$

$$D_2^* = W_1 y_{G1}^2 + W_2 \left(y_{G2} \frac{h_1}{h_2} \right)^2 = 33.6\ [kN^2 m^2] \tag{87}$$

In (83) the summation is understood to extend to 7 levels of horizontal reinforcement arranged above the height of the first level of the wall (see Table 5.2).

5.3.2.2.3 Vertical bending of the wall at the first level

$$N = W_1 \frac{s}{2} + (W_2 + N + P_{S1}) s \left(1 + \frac{1}{2} \frac{h_1}{h_2} \right) = 88.4\ [kNm] \tag{88}$$

$$N_{rv} = n_{rv} F_{rv} s \left(1 + \frac{h_1}{h_2} \right) = 47.5\ [kNm] \tag{89}$$

$$N_{ro} = 2F_{ro} \left[\sum_{j=1}^{\overline{n_{ro}}} h_{roj} + \sum_{j=\overline{n_{ro}}+1}^{n_{ro}} \left(h_{P1} + h_{P2} - h_{roj} \right) \frac{h_1}{h_2} \right] = 210.3\ [kNm] \tag{90}$$

$$D = W_1 y_{G1} + W_2 y_{G2} \frac{h_1}{h_2} = 60.4\ [kNm] \tag{91}$$

$$N^* = W_1 y_{G1} + W_2 y_{G2} \frac{h_1}{h_2} = 60.4\ [kNm] \tag{92}$$

$$D_1^* = W_1 + W_2 = 123.4\ [kN] \tag{93}$$

$$D_2^* = W_1 y_{G1}^2 + W_2 \left(y_{G2} \frac{h_1}{h_2} \right)^2 = 29.6\ [kN^2 m^2] \tag{94}$$

In (90) the summation is understood to extend to 7 levels of horizontal reinforcement arranged in the wall, below the height of the first level (see Table 5.2).

5.3.3 Horizontal bending

In the evaluation of the local mechanism of horizontal bending of the two-storey wall subject to verification, two possible kinematics (Figure 5.20) are considered:

- The first envisages that the kinematic motion involves the masonry strip above the window of the second level of the wall;
- The second envisages that the kinematic motion involves the masonry strip between the openings of the two levels of the wall.

It should be noted that, while the position of the intermediate cylindrical hinge should be made to vary parametrically along the longitudinal development of the wall in order to identify the “critical” geometric configuration associated with the minimum activation multiplier for a rigorous verification of the wall with respect to the horizontal bending mechanism, it is arbitrarily assumed here to be fixed. In particular, in both cases considered (identified below, respectively, as “2” and “1-2”), it is assumed that the intermediate hinge activates at 4.48 m from the left edge of the wall, at the edge of the central window.

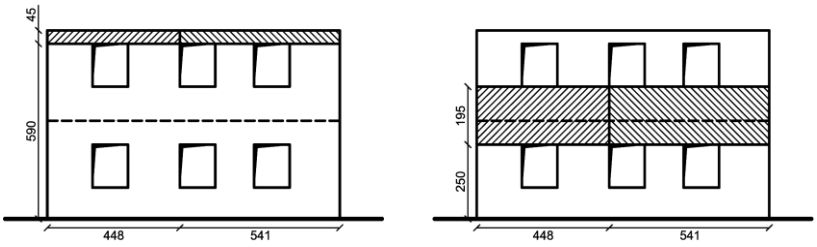

(a) (b)

Figure 5.20 Horizontal bending mechanisms considered: (a) wall strip above window on second level; (b) masonry strip between the two levels of wall openings (measurements in [cm]).

Table 5.10 contains the values of self-weight W_i, length L_i and arm x_{Gi} relative to the respective pole of the centre of gravity of the two rigid bodies involved in the collapse mechanism, defined as a function of the geometry of the portion of the wall considered (shown in Figure 5.20) and the position of the intermediate hinge assumed for each kinematic mechanism.

Table 5.10. Calculation parameter values relating to the geometry of the rigid bodies involved in the kinematics

	Kinematic mechanism					
	2			**1-2**		
Rigid body	W_i [kN]	L_i [m]	x_{Gi} [m]	W_i [kN]	L_i [m]	x_{Gi} [m]
1	8.97	4.48	2.24	39.3	4.48	2.24
2	10.83	5.41	2.71	47.5	5.41	2.71

In the evaluation of the activation multiplier α_0, a uniformly distributed p_V load at the head of the portion of the wall affected by the collapse mechanism of 3.8 kN/m and 4.2 kN/m, respectively, for kinematics 2 and 1-2 is also considered. With reference to this last kinematic motion, it is also necessary to consider the concentrated loads, transmitted at the head of the rigid bodies from the portion of wall above the masonry strip under verification, illustrated in Figure 5.21 and defined in Table 5.11, in terms of value $P_{V_{ij}}$ and distance d_{ij} of the point of application with respect to the respective pole. With reference to this last kinematic motion, it is also necessary to consider the concentrated loads, transmitted at the head of the rigid bodies from the portion of wall above the masonry strip under verification, illustrated in and defined in Figure 5.21, in terms of value and distance of the point of application with respect to the respective pole.

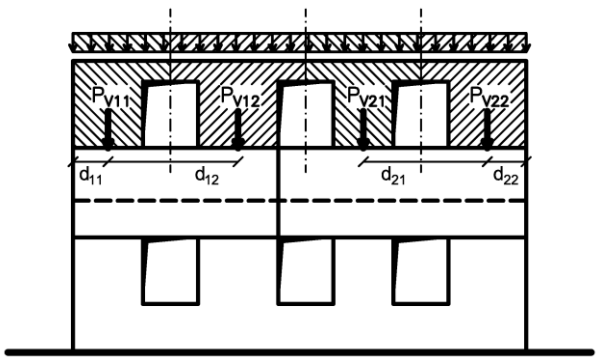

Figure 5.21 Identification of the loads transmitted by the overhead portion of the structure at the head of bodies 1 and 2 involved in kinematics 1-2 and of the horizontal arms with respect to their respective poles.

Table 5.11. Calculation parameter values relating to the loads transmitted from the overlying portion of the structure to the rigid bodies involved in the kinematics 1-2

$P_{V_{11}}$ [kN]	d_{11} [m]	$P_{V_{12}}$ [kN]	d_{12} [m]	$P_{V_{21}}$ [kN]	d_{21} [m]	$P_{V_{22}}$ [kN]	d_{22} [m]
22.2	0.76	28.7	3.60	23.1	3.56	24.4	0.85

For the evaluation of the maximum value of the reaction *H* to the thrust of the horizontal arch effect that can be borne by the bracing walls, the perimeter wall on the left side of the façade under verification is considered to be the weaker of the two bracing walls. The wall is defined by the parameters given in Table 5.12: the thickness s_{ci} of the wall, the height h_{ci} at which the load transmitted by the floor is applied, the façade area A_{ci}, the corresponding weight W_{ci} (defined considering a specific weight of the masonry of 18 kN/m^3) and the load P_{sci} transmitted by the floor at the different levels.

Table 5.12. Descriptive calculation parameter values of the bracing wall

Elevation	s_{ci} [m]	h_{ci} [m]	A_{ci} [m^2]	W_{ci} [kN]	P_{sci} [m]
1	0.25	3.30	14.2	63.9	-
2	0.25	3.05	13.0	58.3	13.1

The elevation h_H of the point of application of the thrust reaction H due to the horizontal arch effect on the bracing wall with respect to the base is evaluated using the expression:

$$h_H = y_b + (1-\theta)b \tag{95}$$

as a function of the height b and the intrados height y_b (relative to the base of the wall) of the masonry strip affected by the collapse mechanism, the parameter θ being assumed to be 0.5 in the case of a rectangular wall strip. Table 5.13 shows the values of the parameters mentioned for the two kinematics considered.

Table 5.13. Evaluation of the application height h_H of the force *H*

Kinematic mechanism	b [m]	y_b [m]	h_H [m]
2	0.45	5.90	6.12
1-2	1.95	2.50	3.48

The activation multiplier α_0 of the mechanism in the pre-intervention condition and in the reinforced wall configuration are evaluated using the following expressions, derived from (40) and (45).

$$\alpha_{0(2)} = \frac{H_{(2)} s \left(1 + \frac{L_1}{L_2}\right)}{W_1 x_{G1} + W_2 \frac{L_1}{L_2} x_{G2} + p_V L_1 (x_{G1} + x_{G2})} = \frac{1.3}{128.6} = 0.010 \tag{96}$$

$$\alpha_{0(1-2)} = \frac{H_{(1-2)} s \left(1 + \frac{L_1}{L_2}\right)}{W_1 x_{G1} + W_2 x_{G2} \frac{L_1}{L_2} + p_V L_1 (x_{G1} + x_{G2}) + \sum_i P_{Vi1} d_{i1} + \sum_i P_{Vi2} d_{i2} \frac{L_1}{L_2}} = \frac{2.2}{492.7} = 0.005 \tag{97}$$

$$\alpha_{0,r(2)} = \frac{H_{r(2)} s \left(1 + \frac{L_1}{L_2}\right)}{W_1 x_{G1} + W_2 x_{G2} \frac{L_1}{L_2} + p_V L_1 (x_{G1} + x_{G2})} = \frac{44.1}{128.6} = 0.343 \tag{98}$$

$$\alpha_{0,r(1-2)} = \frac{H_{r(1-2)} s \left(1 + \frac{L_1}{L_2}\right)}{W_1 x_{G1} + W_2 x_{G2} \frac{L_1}{L_2} + p_V L_1 (x_{G1} + x_{G2}) + \sum_i P_{Vi1} d_{i1} + \sum_i P_{Vi2} d_{i2} \frac{L_1}{L_2}} = \frac{77.6}{492.7} = 0.157 \tag{99}$$

where subscripts "2" and "1-2" denote the maximum values of the reaction to the thrust of the horizontal arch effect that can be withstood by the bracing walls in the pre-intervention condition and in the reinforced wall configuration obtained for the two kinematics considered.

These contributions for each generic j-th kinematic mechanism can be defined as:

$$H_{(j)} = \frac{\sum_i (W_{ci} + P_{sci}) \frac{s_{ci}}{2}}{h_{H(j)}} \tag{100}$$

$$H_{r(j)} = \frac{\sum_i (W_{ci} + P_{sci}) \frac{s_{ci}}{2} + M_{ro}}{h_{H(j)}} \tag{101}$$

Where the summation is understood to extend to all levels of the bracing wall considered. It should be noted that, all other parameters being equal (see Table 5.12) in the case of the two kinematics considered, the value of $h_{H,j}$ (according to Table 5.13) varies.

For both kinematics, the contribution of the reinforcement system M_{ro} is evaluated using the expression:

$$M_{ro} = F_{ro} \sum_i h_{roi} = 32.4 \cdot 17.69 = 573.2 \; [kNm] \tag{102}$$

in which the summation is understood to extend to the 7 continuous horizontal reinforcement levels arranged in the wall (identified with "*" in Table 5.2) and the maximum force F_{ro} that can be withstood from each reinforcement level is defined, based on the considerations in Appendix A in § A.3, as:

$$F_{ro} = min\{\overline{B_p}; n_{a,min} \cdot V_a; n_{a,min} \cdot F_b\} \tag{103}$$

being $\overline{B_p}$ = 32.4 kN the puncture strength of the metal frame plate in correspondence with the bolted connection of the frame-to-frame connection, V_a = 5.4 kN the maximum force that can be withstood by the anchoring of the frame to the masonry resulting from experimental shear tests carried out in situ (obtained by adopting a safety coefficient $\gamma_{Mm} = 2.5$), F_b = 27.7 kN the bearing strength of the frame element at the section weakened by the anchoring hole and $n_{a,min}$ the smallest number of anchors between the two rigid bodies involved in the kinematic mechanism. Based on the geometry of the reinforcement system adopted, the position of the intermediate hinge (assumed to be identical for the two kinematics considered) leads to a value $n_{a,min}$ of10 (as shown in Table 5.3) and therefore to a value of F_{ro} 32.4 kN.

It then follows in (100) and (101) that, for the two mechanisms considered, the maximum value of the thrust reaction of the horizontal arch effect that can be borne by the bracing walls in the pre-intervention condition and in the reinforced wall configuration is equal to, respectively:

$$H_{(2)} = \frac{16.91}{6.12} = 2.7 \; [kN] \tag{104}$$

$$H_{(1-2)} = \frac{16.91}{3.48} = 4.9 \; [kN] \tag{105}$$

$$H_{r(2)} = \frac{590.1}{6.12} = 96.4\ [kN] \tag{106}$$

$$H_{r(1-2)} = \frac{590.1}{3.48} = 169.8\ [kN] \tag{107}$$

Knowing the activation multiplier α_0 of the mechanism, it is possible to assess the corresponding spectral acceleration a_0 of the oscillator equivalent to a single degree of freedom by means of the expression (4), once the participating mass e^* has been defined by means of (3) and assumed the value of the level of knowledge FC LC attained.

The expression (3) can be reformulated as:

$$e^* = \frac{N^{*2}}{D_1^* \cdot D_2^*} \tag{108}$$

The terms in the numerator and denominator of (108) for the horizontal bending mechanism, take on the following expressions in the most general form:

$$N^* = W_1 x_{G1} + W_2 x_{G2} \frac{L_1}{L_2} + p_V L_1 x_{G1} + p_V L_2 x_{G2} \frac{L_1}{L_2} + \Sigma_i P_{Vi1} d_{i1} + \Sigma_i P_{Vi2} d_{i2} \frac{L_1}{L_2} \tag{109}$$

$$D_1^* = W_1 + W_2 + p_V L_1 + p_V L_2 + \Sigma_i P_{Vi1} + \Sigma_i P_{Vi2} \tag{110}$$

$$D_2^* = W_1 x_{G1}^2 + W_2 \left(x_{G2} \frac{L_1}{L_2}\right)^2 + p_V L_1 x_{G1}^2 + p_V L_2 \left(x_{G2} \frac{L_1}{L_2}\right)^2 + \Sigma_i P_{Vi1} d_{i1}^2 + \Sigma_i P_{Vi2} \left(d_{i2} \frac{L_1}{L_2}\right)^2 \tag{111}$$

depending on the parameters defined above. With particular reference to kinematic motion 2, the terms associated with concentrated loads P_{Vi1} and P_{Vi1} and non-concentrated loads must be considered in the calculation.

Table 5.14 reports the values of the activation multiplier α_0 of the mechanism, of the participating mass $e^*$and of the spectral acceleration a_0 of the oscillator equivalent to a single degree of freedom obtained for each kinematic mechanism considered, respectively in the pre-intervention condition and in the reinforced configuration of the wall.

Table 5.14. Local horizontal bending mechanism: results

Kinematic mechanism	Condition	$\boldsymbol{\alpha_0}$ [-]	$\boldsymbol{e^*}$ [-]	$\boldsymbol{a_0}$ [g]
2	pre-intervention	0.010	1.000	0.008
	post-intervention	0.343		0.286
1-2	pre-intervention	0.005	0.863	0.004
	post-intervention	0.157		0.152

5.3.4 Verification of local mechanisms

The verification is carried out as described previously in §§ 5.1.3 and 5.1.4, determining for each collapse mode (kinematism) envisaged for the local mechanisms considered PGA the capacity for the damage and life-preserving limit states $PGA^C_{L,SLD}$ and $PGA^C_{L,SLV}$, corresponding to the return periods $T^C_{RL,SLD}$ and $T^C_{RL,SLV}$.

The calculation is differentiated for kinematics developing around a hinge activated at the base of the construction and kinematics developing at an elevation. In order to verify the latter, it is necessary in particular to define the fundamental period T_1 of the building, which is estimated in approximate form as a function of height as:

$$T_1 = 0.05 \cdot H^{3/4} = 0.05 \cdot 6.35^{3/4} = 0.200\ s \tag{112}$$

The PGA of capacity are then compared with the corresponding PGA of demand which, for the reference site, are equal to $PGA^D_{SLD} = 0.061\ g$ and $PGA^D_{SLV} = 0.180\ g$, in order to define the safety indices of the local mechanisms at the two limit states, $\zeta_{EL,SLD}$ and $\zeta_{EL,SLV}$.

5.3.4.1 Verification at DLS

For kinematics developing around an activated hinge at the base of the construction, the following is assumed at DLS:

$$PGA^C_{L,SLD} = a_0 \tag{113}$$

For the evaluation of $T^C_{RL,SLD}$ you can use, for example, the spreadsheet “Spectra-NTC ver.1.0.3.xls”. After selecting the reference site in the “PHASE 1” sheet, the subsoil category, the topographic category and the damping value ξ in the “STEP 3” sheet, it is possible to modify the spectrum at the considered limit state until a value is obtained at the anchor point that satisfies the condition:

$$a_g S = a_0 \tag{114}$$

by varying the value of the nominal life V_N of the building by trial and error in the “PHASE 2” sheet. The return period value given in the same “PHASE 2” sheet for the limit state considered corresponds to the capacity return period sought.

The following Figures illustrate the entire procedure, applied to obtain a value of $a_g S$ 0.134 g: the return period $T^C_{RL.SLD}$ is 244 years.

Figure 5.22 Selection of the reference site (in red).

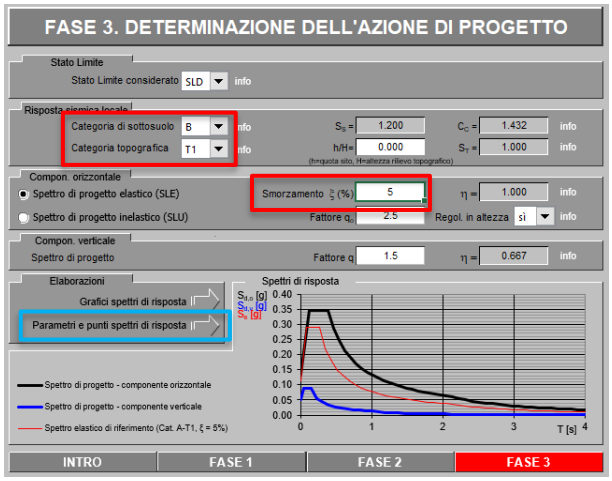

Figure 5.23 Assignment of subsoil and topographic categories and damping (in red).

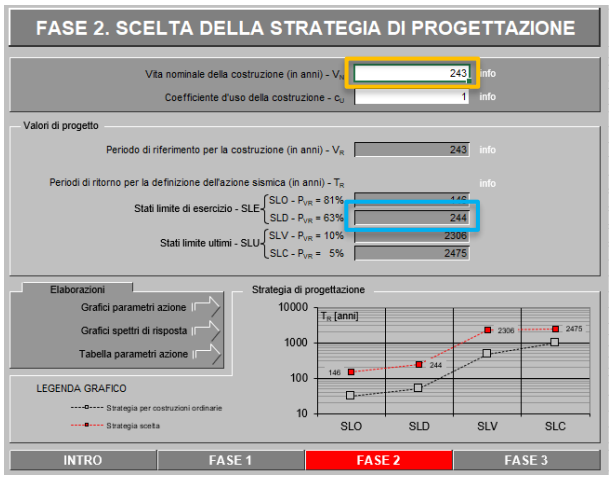

Figure 5.24 Variation of the nominal life of the structure (in orange) and definition of the capacity return period (in blue).

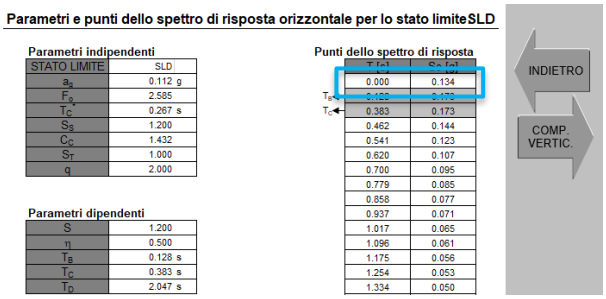

Figure 5.25 Checking the a_gS value for the considered return period (in blue).

For kinematics developing at an elevation, the $PGA^{C}_{L,SLD}$ is instead defined as the value of the anchor point of the elastic spectrum corresponding to a return period $T^{C}_{RL,SLD}$ for which the spectral ordinate $S_{e,SLD}(T_1,\xi)$ satisfies the following condition:

$$S_{e,SLD}(T_1,\xi) = \frac{a_0}{|\gamma_1 \psi_1(z)|\sqrt{1+0.0004\xi^2}} \tag{115}$$

being:

$$\gamma_1 = \frac{3n}{2n+1} = 1.2 \tag{116}$$

$$\psi_1(z) = \frac{z}{H} \tag{117}$$

In the previous expressions, n = 2 is the number of storeys of the building, H = 6.35 m is the total height and z is the centre of gravity with respect to the foundation of the constraint lines between the blocks affected by the kinematics and the rest of the structure (defined case by case as indicated below).

In this case, it is still possible to use the spreadsheet "Spectra-NTC ver.1.0.3.xls": by varying the nominal life of the building, it is possible to identify the spectral ordinate corresponding to the fundamental period T_1 of the building from the sheet shown in Figure 5.25 and thus identify the value of the spectrum at the anchoring point, corresponding to $PGA^C_{L,SLD}$ and the value of the return period $T^C_{RL,SLD}$.

In particular situations, the value of the activation multiplier α_0 of the mechanism may correspond to a very low or very high value of a_0 or $S_{e,SLD}(T_1, \xi)$ (in the case of kinematics developing at an elevation), such that it is even lower than that corresponding to 30 years or higher than that corresponding to 2475 years. In these cases, it is necessary to obtain from the spreadsheet "Spectra-NTC ver.1.0.3.xls" the values of the seismic parameters corresponding to the exceeded limit and to define the spectrum as a function of these values, varying the value of a_g until, depending on the type of kinematics considered, (114) or (115).

Once $PGA^C_{L,SLD}$ has been defined the safety index can be evaluated.

$$\zeta_{EL,SLD} = \frac{PGA^C_{L,SLD}}{PGA^D_{SLD}} \tag{118}$$

5.3.4.2 Simplified verification at LSLS with behaviour factor

Verification at LSLS is carried out by adopting two different values of the behaviour coefficient q: in particular, in addition to the value q = 2 proposed by Circular 7/2019 for simplified verification q = 1 is considered in order to guarantee the inhibition of the kinematic motion.

Defined for each value of q the corresponding $PGA^C_{L,SLV(q)}$:

$$PGA^C_{L,SLV(q)} = q \cdot PGA^C_{L,SLD} \tag{119}$$

the security index is immediately assessed:

$$\zeta_{EL,SLV(q)} = \frac{PGA^C_{L,SLV(q)}}{PGA^D_{SLV}} \tag{120}$$

The capacity return period $T^C_{RL,SLV(q)}$ can then be evaluated using the spreadsheet "Spectra-NTC ver.1.0.3.xls" according to the procedure described above.

The verification results for each local mechanism considered are given below. "NR" and "R" identify the pre-intervention condition (unreinforced) and the reinforced wall configuration, respectively.

5.3.4.3 Simple overturning

5.3.4.3.1 Overturning of the entire wall in relation to the base

Kinematics 2-1 is developed around a hinge that is activated at the base of the wall.

Table 5.15. Verification at DLS

Condition	a_0 [g]	$T^C_{RL,SLD}$ [years]	$PGA^C_{L,SLD}$ [g]	$\zeta_{EL,SLD}$ [-]
NR	0.036	<30	0.036	0.60
R	2,874	>2475	2.874	47.1

Table 5.16. Simplified verification at LSLS with behaviour factor

Condition	$PGA^C_{L,SLV(q=2)}$ [g]	$T^C_{RL,SLV(q=2)}$ [years]	$\zeta_{EL,SLV(q=2)}$ [-]	$PGA^C_{L,SLV(q=1)}$ [g]	$T^C_{RL,SLV(q=1)}$ [years]	$\zeta_{EL,SLV(q=2)}$ [-]
NR	0.073	72	0.40	0.036	<30	0.20
R	5.749	>2475	31.9	2.874	>2475	15.95

The unreinforced wall is not verified at either DLS or LSLS.

Reinforcement intervention using the Resisto 5.9 system produces a significant increase in the safety index at both limit states: the reinforced part is in fact amply verified.

5.3.4.3.2 Overturning of the wall at the second level

Kinematic mechanism 2 is developed at an elevation. The centre of gravity with respect to the foundation of the constraint lines between the blocks affected by the kinematics and the rest of the structure is assumed to be equal to the extrados height of the intermediate floor (height of the first level of the wall):

$$z = h_{P1} \tag{121}$$

It is therefore z = 3.30 m; the value of the component of the first modal form is therefore equal to $\psi_1(z)$ = 0.520.

Table 5.17. Verification at DLS

Condition	a_0 [g]	$S_{e,SLD}(T_1,\xi)$ [g]	$T^C_{RL,SLD}$ [years]	a_g * [g]	$PGA^C_{L,SLD}$ [g]	$\zeta_{EL,SLD}$ [-]
NR	0.064	0.102	<30	0.033	0.040	0.65
R	2.613	4.167	>2475	1.531	1.710	28.04

Note: * for $T^C_{RL,SLD} < 30$ or $T^C_{RL,SLD} > 2475$, a_g is the value of the reference ground acceleration on type A soil leading to a spectral ordinate for T_1 equal to the value $S_{e,SLD}(T_1,\xi)$ corresponding to a_0

Table 5.18. Simplified verification at LSLS with behaviour factor

Condition	$PGA^C_{L,SLV(q=2)}$ [g]	$T^C_{RL,SLV(q=2)}$ [years]	$\zeta_{EL,SLV(q=2)}$ [-]	$PGA^C_{L,SLV(q=1)}$ [g]	$T^C_{RL,SLV(q=1)}$ [years]	$\zeta_{EL,SLV(q=2)}$ [-]
NR	0.080	85	0.44	0.040	<30	0.22
R	3.421	>2475	18.98	1.710	>2475	9.49

The unreinforced wall is not verified at either DLS or LSLS.

Reinforcement intervention using the Resisto 5.9 system produces a significant increase in the safety index at both limit states: the reinforced part is in fact amply verified.

5.3.4.4 Vertical bending

5.3.4.4.1 Vertical bending of the entire wall

1-2 kinematics is developed around a hinge that is activated at the base of the wall.

Table 5.19. Verification at DLS

Condition	a_0 [g]	$T^C_{RL,SLD}$ [years]	$PGA^C_{L,SLD}$ [g]	$\zeta_{EL,SLD}$ [-]
NR	0.134	244	0.134	2.20
R	3.068	>2475	3.068	50.29

Table 5.20. Simplified verification at LSLS with behaviour factor

Condition	$PGA^C_{L,SLV(q=2)}$ [g]	$T^C_{RL,SLV(q=2)}$ [years]	$\zeta_{EL,SLV(q=2)}$ [-]	$PGA^C_{L,SLV(q=1)}$ [g]	$T^C_{RL,SLV(q=1)}$ [years]	$\zeta_{EL,SLV(q=2)}$ [-]
NR	0.268	1343	1.49	0.134	244	0.74
R	6.136	>2475	34.04	3.068	>2475	17.02

The unreinforced wall is verified at DLS and LSLS assuming a value of the behaviour coefficient q = 2, but not for q = 1.

Reinforcement intervention using the Resisto 5.9 system produces a significant improvement in the performance of the wall with respect to this kinematic mechanism, which is reflected in significant increases in the safety indices for all limit states considered.

5.3.4.4.2 Vertical bending of the wall at the second level

Kinematic mechanism 2 is developed at an elevation. The centre of gravity with respect to the foundation of the constraint lines between the blocks affected by the kinematics and the rest of the structure is assumed to be equal to the extrados height of the intermediate floor (height of the first level of the wall):

$$z = h_{P1} \tag{122}$$

It is therefore z = 3.30 m; the value of the component of the first modal form is therefore equal to $\psi_1(z)$ = 0.520.

Table 5.21. Verification at DLS

Condition	a_0 [g]	$S_{e,SLD}(T_1,\xi)$ [g]	$T^C_{RL,SLD}$ [years]	a_g * [g]	$PGA^C_{L,SLD}$ [g]	$\zeta_{EL,SLD}$ [-]
NR	0.526	0.838	>2475	0.308	0.344	5.64
R	4.255	6.784	>2475	2.492	2.785	45.65

Note: * for $T^C_{RL,SLD} < 30$ or $T^C_{RL,SLD} > 2475$, a_g is the value of the reference ground acceleration on type A soil leading to a spectral ordinate for T_1 equal to the value $S_{e,SLD}(T_1,\xi)$ corresponding to a_0

Table 5.22. Simplified verification at LSLS with behaviour factor

Condition	$PGA^{C}_{L,SLV(q=2)}$ [g]	$T^{C}_{RL,SLV(q=2)}$ [years]	$\zeta_{EL,SLV(q=2)}$ [-]	$PGA^{C}_{L,SLV(q=1)}$ [g]	$T^{C}_{RL,SLV(q=1)}$ [years]	$\zeta_{EL,SLV(q=2)}$ [-]
NR	0.688	>2475	3.82	0.344	>2475	1.91
R	5.570	>2475	30.90	2.785	>2475	15.45

The unreinforced wall is verified with respect to this kinematic mechanism at both limit states considered.

Reinforcement intervention using the Resisto 5.9 system produces an important increase in the performance of the wall, corresponding to a significant increase in the safety index.

5.3.4.4.3 Vertical bending of the wall at the first level

Kinematics 1 is developed around a hinge that is activated at the base of the wall.

Table 5.23. Verification at DLS

Condition	a_0 [g]	$T^{C}_{RL,SLD}$ [years]	$PGA^{C}_{L,SLD}$ [g]	$\zeta_{EL,SLD}$ [-]
NR	1.228	>2475	1.228	20.13
R	4.794	>2475	4.794	78.58

Table 5.24. Simplified verification at LSLS with behaviour factor

Condition	$PGA^{C}_{L,SLV(q=2)}$ [g]	$T^{C}_{RL,SLV(q=2)}$ [years]	$\zeta_{EL,SLV(q=2)}$ [-]	$PGA^{C}_{L,SLV(q=1)}$ [g]	$T^{C}_{RL,SLV(q=1)}$ [years]	$\zeta_{EL,SLV(q=2)}$ [-]
NR	2.456	>2475	13.62	1.228	>2475	6.81
R	9.588	>2475	53.19	4.794	>2475	26.60

The unreinforced wall is extensively verified at DLS and LSLS considering a behaviour coefficient value of both q = 2 and q = 1.

Reinforcement intervention using the Resisto 5.9 system produces a significant increase in the performance of the wall with respect to this kinematic mechanism, which is reflected in very high safety index values.

5.3.4.5 Horizontal bending

5.3.4.5.1 Horizontal bending of masonry strip above the window on the second wall level

Kinematic mechanism 2 is developed at an elevation. It is assumed that the centre of gravity with respect to the foundation of the constraint lines between the blocks affected by the kinematics and the rest of the structure is equal to:

$$z = h_H \tag{123}$$

It is therefore (see Table 5.13) z = 6.12 m; the value of the component of the first modal form is therefore equal to $\psi_1(z)$ = 0.965.

Table 5.25. Verification at DLS

Condition	a_0 [g]	$S_{e,SLD}(T_1,\xi)$ [g]	$T^C_{RL,SLD}$ [years]	a_g * [g]	$PGA^C_{L,SLD}$ [g]	$\zeta_{EL,SLD}$ [-]
NR	0.008	0.007	<30	0.002	0.003	0.04
R	0.286	0.245	114	-	0.093	1.52

Note: * for $T^C_{RL,SLD} < 30$ or $T^C_{RL,SLD} > 2475$, a_g is the value of the reference ground acceleration on type A soil leading to a spectral ordinate for T_1 equal to the value $S_{e,SLD}(T_1,\xi)$ corresponding to a_0

Table 5.26. Simplified verification at LSLS with behaviour factor

Condition	$PGA^C_{L,SLV(q=2)}$ [g]	$T^C_{RL,SLV(q=2)}$ [years]	$\zeta_{EL,SLV(q=2)}$ [-]	$PGA^C_{L,SLV(q=1)}$ [g]	$T^C_{RL,SLV(q=1)}$ [years]	$\zeta_{EL,SLV(q=2)}$ [-]
NR	0.005	<30	0.03	0.003	<30	0.02
R	0.186	510	1.03	0.093	114	0.51

The unreinforced wall is particularly exposed to this collapse kinematic mechanism, which is associated with very low values of the safety index at both limit states.

Reinforcement intervention using the Resisto 5.9 system produces a significant improvement in the performance of the wall, which is in fact verified at both DLS and LSLS, if a value of the behaviour coefficient q = 2 is assumed. Although the reinforced wall is thus verified according to the standard, adopting q =1 shows that, despite a more than appreciable increase in the safety index value compared to the pre-intervention condition, the activation of the mechanism is not inhibited even in the reinforced configuration.

5.3.4.5.2 Horizontal deflection of the masonry strip between the openings of the two wall levels

Kinematic mechanism 1-2 is developed at an elevation. It is assumed that the centre of gravity with respect to the foundation of the constraint lines between the blocks affected by the kinematics and the rest of the structure is equal to:

$$z = h_H \tag{124}$$

It is therefore (see Table 5.13) z = 3.48 m; the value of the component of the first modal form is therefore equal to $\psi_1(z)$ = 0.548.

Table 5.27. Verification at DLS

Condition	a_0 [g]	$S_{e,SLD}(T_1,\xi)$ [g]	$T^C_{RL,SLD}$ [years]	a_g * [g]	$PGA^C_{L,SLD}$ [g]	$\zeta_{EL,SLD}$ [-]
NR	0.004	0.007	<30	0.002	0.003	0.04
R	0.152	0.230	108	-	0.091	1.49

Note: * for $T^C_{RL,SLD} < 30$ or $T^C_{RL,SLD} > 2475$, a_g is the value of the reference ground acceleration on type A soil leading to a spectral ordinate for T_1 equal to the value $S_{e,SLD}(T_1,\xi)$ corresponding to a_0

Table 5.28. Simplified verification at LSLS with behaviour factor

Condition	$PGA^{C}_{L,SLV(q=2)}$ [g]	$T^{C}_{RL,SLV(q=2)}$ [years]	$\zeta_{EL,SLV(q=2)}$ [-]	$PGA^{C}_{L,SLV(q=1)}$ [g]	$T^{C}_{RL,SLV(q=1)}$ [years]	$\zeta_{EL,SLV(q=2)}$ [-]
NR	0.005	<30	0.03	0.003	<30	0.01
R	0.181	481	1.01	0.091	108	0.50

The unreinforced wall is particularly exposed to this collapse kinematic mechanism, which is associated with very low values of the safety index at both limit states.

Reinforcement intervention using the Resisto 5.9 system produces a significant improvement in the performance of the wall, which is in fact verified at both DLS and LSLS, if a value of the behaviour coefficient q = 2 is assumed. Although the reinforced wall is thus verified according to the standard, adopting q =1 shows that, despite a more than appreciable increase in the safety index value compared to the pre-intervention condition, the activation of the mechanism is not inhibited even in the reinforced configuration.

6 GLOBAL SEISMIC RESPONSE

6.1 Foreword

Verification of the global seismic response of existing masonry buildings can be performed using the methods of linear elastic or non-linear analysis on three-dimensional equivalent frame or finite element building models, as indicated in § C8.7.1.3 of Circular 7/2019 of NTC 2018. In particular, one of the following types of structural analysis can be adopted:

1) Static linear elastic analysis with behaviour factor *q*;
2) Dynamic linear elastic analysis (multimodal with response spectrum) with behaviour factor *q*;
3) Static non-linear analysis (*pushover*);
4) Dynamic non-linear analysis (*time-history*).

In professional practice, dynamic non-linear analysis is not normally used.

6.2 Criterion proposed for the analysis and verification of buildings reinforced with the Resisto 5.9 system

Based on the results of the numerical-experimental campaign conducted at the EUCENTRE Foundation in Pavia and the interpretation of the results obtained (Manzini et al., 2021; Manzini et al., 2022; Damiani et al, 2022), the improvement of the seismic performance in the masonry wall plane to be used in the global analysis of masonry buildings reinforced with the Resisto 5.9 system can be summarised as follows, depending on whether the reinforcement system is “connected” or “unconnected” to the reinforced concrete edge elements (foundation and floor kerb).

Generally speaking, the experimental tests and numerical analyses carried out so far at the EUCENTRE Foundation on different types of load-bearing masonry (solid brick and lime mortar masonry and “double UNI” block and bastard mortar masonry) have shown that the Resisto 5.9 system significantly improves the performance of reinforced masonry panels, especially in terms of ultimate deformation capacity but also in terms of deformation capacity at DLS, both for the unconnected and connected situation.

With regards to strength, an increase in shear strength was noted in the unconnected solution, while the increase in flexural strength was negligible. On the other hand, with regards to the connected solution, an increase in both shear strength and strength to buckling was manifested.

In all cases, the increase in the stiffness of the masonry panels was negligible and, therefore, the stiffness parameters in the numerical modelling can be kept equal to those of the unreinforced masonry.

With regard to the analyses to be performed, in the case of static non-linear analysis (*pushover*), it is possible to adopt limits of deformation capacity for the individual masonry elements of the reinforced walls in the plane at the CPLS and at the DLS suitably amplified with respect to the values fixed in § C8.7.1.3.1.1. of Circular 7/2019 of NTC 2018 for unreinforced masonry, directly obtaining the improvement of the seismic performance with respect to the unreinforced situation. Furthermore, it is also possible to increase the strength of the masonry walls in cases where this situation is configured (for example, in the case of shear strength of unconnected masonry or in the case of shear strength and strength to buckling for connected masonry).

The execution of linear elastic analyses of a static or dynamic type is possible for the evaluation of the seismic improvement provided by the reinforcement system, only in cases where an increase in strength is configured, maintaining the value of the behaviour factor *q* equal to that imposed by the standards. In this case, the verifications envisage the comparison at DLS between the inter-storey displacement demand and the amplified deformation limits for the walls reinforced as specified above and the comparison at LSLS between the stresses in the masonry elements and the shear strength and buckling strength, appropriately increased to take into account the effect of the reinforcement.

The evaluation of the seismic performance of buildings reinforced with the Resisto 5.9 system is much more effective in the case of adopting non-linear static analyses (*pushover*) compared to the use of linear elastic analyses (regardless of whether they are carried out using equivalent frame or linear "finite element" modelling).

In the following, the criteria for evaluation of improvement in seismic performance in the plane of masonry walls reinforced with the Resisto 5.9 system, in terms of increase in both deformation capacity and strength, are given.

6.2.1 Increased deformation capacity in the plane of reinforced walls

Based on the results obtained so far during the experimental campaign and numerical research carried out, **the following deformation capacity increment factors are proposed in the presence of reinforcement with the Resisto 5.9 system** compared to the values used for the corresponding unreinforced masonry, defined according to the prescriptions of NTC 2018 and Circular 7/2019 referring to ordinary masonry:

Table 6.1. Increased deformation capacity of walls reinforced with Resisto 5.9

Limit State	Damage type	Masonry type	Connection type	Increment factor
DLS	(all cases)			**1.50**
CPLS	Buckling	B/D	NC/C	**1.00**
	Shear	B	NC/C	**1.50**
		D	NC	**1.50**
			C	**1.25**

Notes: B solid bricks; D "double UNI" type blocks, NC reinforcement not connected to r.c. edge elements; C reinforcement not connected to r.c. edge elements

6.2.2 Increased strength on the plane of reinforced walls

6.2.2.1 Buckling strength

On the basis of the results of the experiments and numerical research, it is considered that the in-plane bucking strength of walls reinforced with the Resisto 5.9 system by means of a solution connected to the r.c. edge elements can be increased, compared to that of the same unreinforced masonry, by a value of $\Delta \boldsymbol{M_{u,r}}$, as shown in the expression (125):

$$M_{u,r} = M_u + \Delta \boldsymbol{M_{u,r}} = \left(l^2 t \frac{\sigma_0}{2}\right)\left(1 - \frac{\sigma_0}{0.85 f_d}\right) + \Delta \boldsymbol{M_{u,r}} \qquad (125)$$

where M_u is the resistant moment of unreinforced masonry walls (as per NTC 2018, § 7.8.2.2.1.), l and t are the length and thickness of the walls, σ_0 is the average vertical tension and f_d is the compressive strength of the design masonry. The value of the increase in the bucking strength $\Delta \boldsymbol{M_{u,r}}$, which should strictly be defined as a function of the evolution of the tension state of the metallic elements (similarly, for example, to the case of reinforced masonry walls) can be evaluated in a simplified manner by means of the following expression:

$$\Delta \boldsymbol{M_{u,r}} = \overline{F_{rv}} \cdot i \qquad (126)$$

where *i* is the spacing between the two outermost vertical posts of the steel frame (taken in relation to the vertical line of the anchors in the masonry) and $\overline{F_{rv}}$ is the vertical tensile force in these elements.

In this simplified formulation, the value of the vertical tensile force $\overline{F_{rv}}$ acting in the metal elements is assumed to be equal to the maximum tensile force that can be withstood by the system, based on its characteristics, and is therefore evaluated as the lesser of:

- The tensile strength of the vertical member;

- The tensile strength of the bolted connection between the frame modules, to be assessed according to the number of bolts, the tensile strength of the individual bolt and the puncture strength of the plate;
- The strength in the vertical direction of the connections to the edge elements (foundation and kerb).
- the strength in the vertical direction of the anchoring system between the reinforcement and masonry.

The maximum vertical force that can be withstood by each anchoring is assumed to be the lesser of:

- The shear strength of the anchoring (to be determined by appropriate in situ tests or from the epoxy resin manufacturer's data sheets);
- The bearing strength of the member at the section weakened by the hole for the anchoring bar section.

It should be noted that the vertical strength of the connection to the edge elements must be evaluated according to the details of the solution adopted on a case by case basis (based on the structural characteristics of the individual reinforced building). In particular, it must be assessed considering the tensile strength and/or puncture strength of the plates, the shear and/or tensile strength of the bolted connections, the shear and/or tensile strength of the welds, the shear or tensile strength (depending on the solution adopted) of the anchorages to the reinforced concrete elements.

We would like to reiterate that the increase in the strength to buckling $\Delta M_{u,r}$ can only be assumed in the case of a reinforcement solution connected to the reinforced concrete edge elements. In the case of an unconnected solution, one must instead assume $\Delta M_{u,r} = 0$.

6.2.2.2 Shear strength

The in-plane shear strength of walls reinforced with Resisto 5.9 can be increased, compared to that of unreinforced masonry, by a value equal to as $\Delta V_{t,r}$ shown in the following expression:

$$V_{t,r} = V_t + \Delta V_{t,r} \tag{127}$$

in which V_t is the shear strength of an unreinforced masonry wall calculated using the expressions of NTC 2018 and Circular 7/2019 and $\Delta V_{t,r}$ is the amplification of the shear strength provided by the reinforcement, which can be calculated according to the expression (128):

$$\Delta V_{t,r} = \frac{\Delta M_{u,r}}{h_0} + \frac{\Delta M_{t,r}}{h_0} \tag{128}$$

where $\Delta M_{u,r}$ is the increase in strength offered by the connection to the reinforced concrete edge elements (in this regard, see the description given above regarding the increase in buckling strength), $\Delta M_{t,r}$ is the increase in strength offered by the connection to the masonry, while h_0 is the distance from the inflection point to the verification sections (which varies according to the panel's constraint conditions).

The value of the increase in strength $\Delta M_{t,r}$ can be evaluated in a simplified manner, similarly to what has been proposed for the increase due to the connection to the reinforced concrete elements, by means of the following expression:

$$\Delta M_{t,r} = \overline{F_{rt}} \cdot i \tag{129}$$

where *i* is still the spacing between the two outermost vertical posts of the steel frame (taken in relation to the vertical line of the anchors in the masonry) and $\overline{F_{rt}}$ is the vertical tensile force in these elements.

The value of the vertical tensile force $\overline{F_{rt}}$ acting in the metal elements is assumed to be equal to the maximum tensile force that can be withstood by the system, based on its characteristics, and is therefore evaluated as the lesser of:

- The tensile strength of the vertical member;

- The tensile strength of the bolted connection between the frame modules, to be assessed according to the number of bolts, the tensile strength of the individual bolt and the puncture strength of the plate;
- the strength in the vertical direction of the anchoring system between the reinforcement and masonry.

The maximum vertical force that can be withstood by each anchoring is assumed to be the lesser of:

- The shear strength of the anchoring (to be determined by appropriate in situ tests or from the epoxy resin manufacturer's data sheets);
- The bearing strength of the member at the section weakened by the hole for the anchoring bar section.

In the event that the reinforcement solution adopted does not provide for connection to the reinforced concrete edge elements, the relative contribution of increased strength $\frac{\Delta M_{u,r}}{h_0}$ must obviously be ignored.

6.3 Structural analysis: static non-linear analysis (*pushover*)

In the case of non-linear static analysis, it is possible to adopt limits of deformation capacity for reinforced walls in the plane at the CPLS and the DLS suitably amplified with respect to the values fixed for unreinforced masonry in § C8.7.1.3.1.1. of Circular 7/2019 of NTC 2018. In particular, the values of the deformation limits that can be cautiously adopted for reinforced walls are given in § 6.2.1 for the DLS and for the CPLS (in relation to both buckling and shear behaviour).

In addition, it is also possible to increase the strength of the masonry walls in those cases in which this situation is apparent on the basis of the results of the experimental tests and numerical analyses carried out to date. In particular, the shear strength alone may be increased in the case of a reinforced solution not connected to the reinforced concrete edge elements and the shear strength and buckling strength of masonry of any type (brick or "double UNI" block) reinforced with a solution connected to the reinforced concrete edge elements. The increase in strength to be adopted in the calculation can be evaluated as shown in § 6.2.2.

For the modelling, analysis and safety check criteria, the provisions for unreinforced load-bearing masonry in the national technical regulations (NTC 2018 and Circular 7/2019) apply, without any changes. Below, the main aspects related to non-linear static analysis and global verification of existing load-bearing masonry buildings are summarised.

6.3.1 Definition of numerical model

6.3.1.1 Geometrical modelling

As prescribed in § 7.2.6 of NTC 2018, the model of the structure to be adopted for analysis must be three-dimensional and adequately represent the actual spatial distributions of mass, stiffness and strength.

In the professional sphere, non-linear static analysis normally involves macro-element modelling of buildings in which the load-bearing structure, consisting of vertical elements (e.g. masonry panels) and horizontal elements (e.g. coupling beams, concrete kerbs and reinforced concrete beams), is schematized into an equivalent frame, consisting of one-dimensional elements, as represented for example in Figure 6.1. Numerous commercial software packages are currently available on the market that allow pushover analyses of existing masonry buildings, such as Pro_SAM (2Si), Tremuri (Sta Data), 3D Macro (CSI Italia), among others.

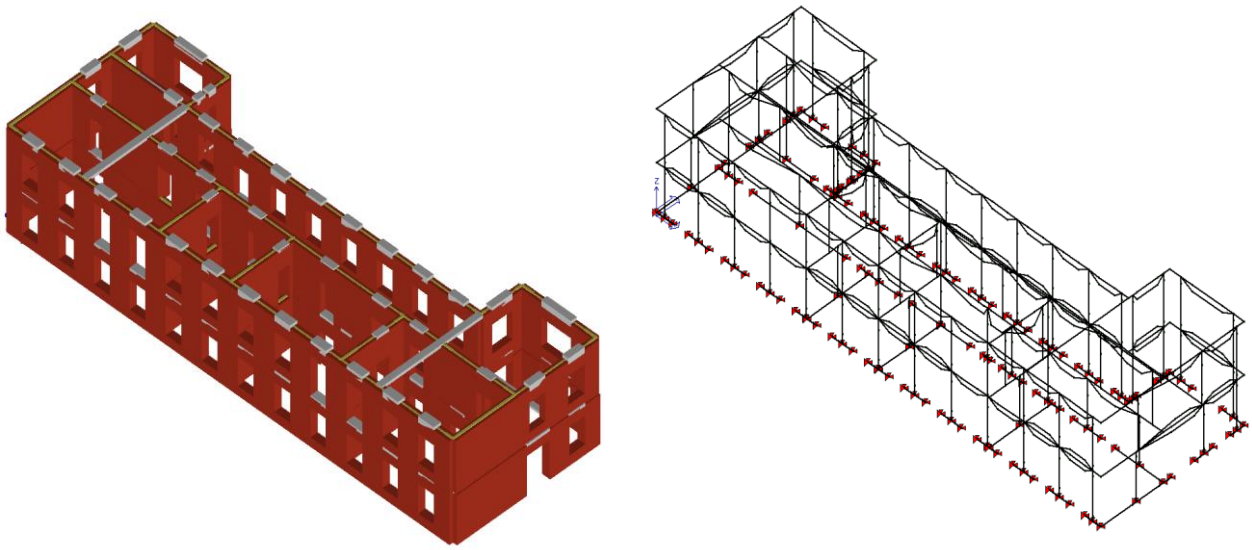

Figure 6.1 Example of equivalent frame modelling of a load-bearing masonry building.

Each masonry element, whether vertically or horizontally developed, is represented as a one-dimensional element by its own main barycentric axis and is bounded by nodes, usually positioned at its intersections with the barycentric axes of the elements to which the element is connected. In this regard, consider the following Figure 6.2 a), in which a single-storey masonry wall with reinforced concrete kerb is schematically represented. As illustrated in Figure 6.2 b) the masonry panels are represented with a frame element in which the lower node is positioned at the level of the foundation ledge and the upper node is positioned at the level of the barycentric axis of the kerb. The horizontal elements, such as the masonry lintel and the reinforced concrete kerb, are represented with frame elements with a horizontal axis, the deformable part of which is assumed to correspond approximately to the free span of the opening, delimited by the line of the vertical elements. Figure 6.2 c) shows the four structural elements constituting the wall-equivalent frame separately so that the deformable portion and the rigid portions are displayed. Finally, Figure 6.2 d) shows the four-node equivalent frame model with the four elements assembled. With reference to the definition of the deformable length, the introduction of infinitely rigid arms ("rigid offsets") of appropriate dimensions at the ends of the elements, as shown in Figure 6.2 e), allows the reduced deformability of the masonry fields delimited by the openings in the wall ("node" zones or structural nodes) to be modelled.

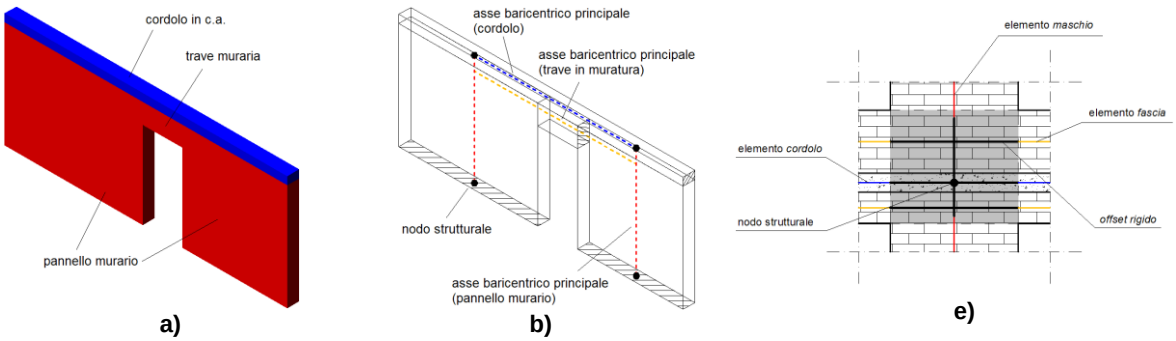

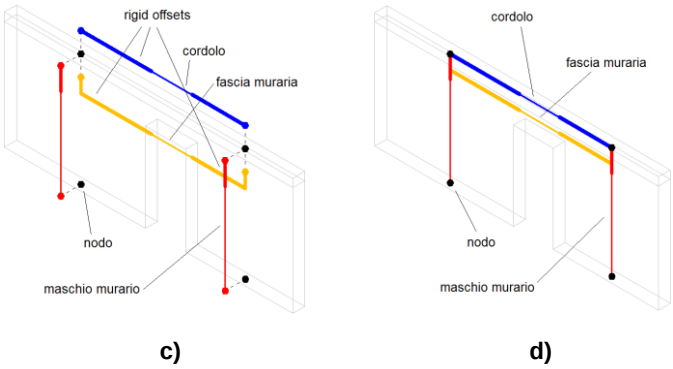

Figure 6.2 Identification of the structural elements of a masonry wall with masonry strip and reinforced concrete kerb; e) schematization of structural node.

Complex section walls (or flanged walls, typically L, T, C or H-shaped) are normally decomposed in equivalent frame models into several mutually incident rectangular-section pier elements. In order to model the cooperation of the masonry panels into which a complex wall decomposes, a rigid connection, consisting of infinitely rigid shear and bending arms, is typically inserted at the plan intersection between two masonry panels, at the barycentric plane of the floor above. The connection by means of rigid offsets (at floor level) ensures the compatibility of the vertical displacements of the walls at the intersection, in the event of perfect coupling between the panels in the area of intersection. Where the bonding between the masonry blocks is not effective and there is no reinforced concrete floor kerb, it is possible to disregard this effect, by not including the rigid offsets in the structural model; in the case of partial coupling between the core and the flange, it is possible to use horizontal elements of suitably calibrated stiffness instead of the rigid offsets.

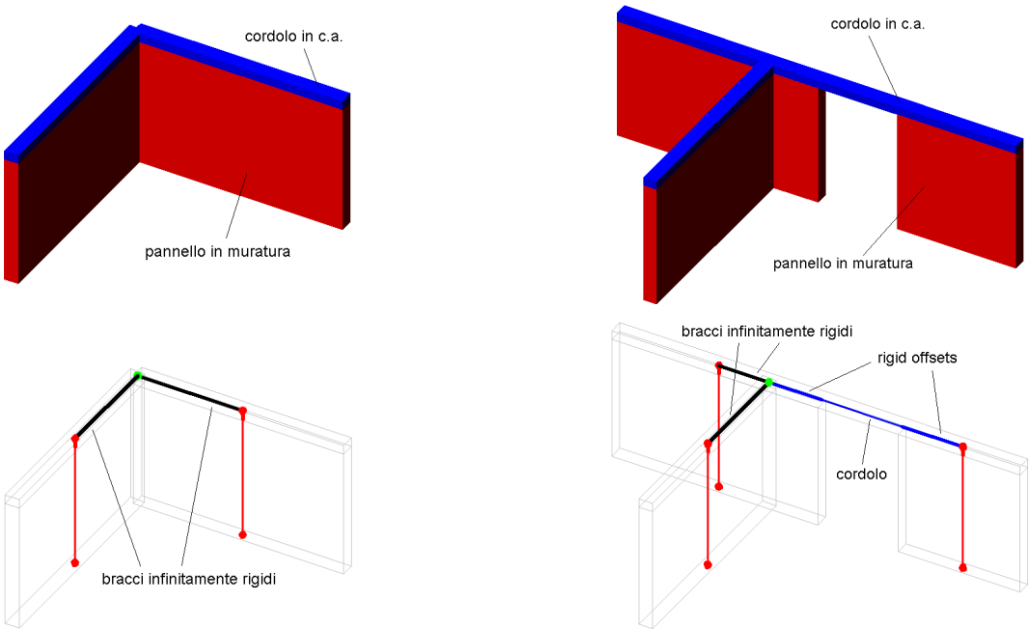

Figure 6.3 Modelling the intersection of masonry panels with rigid offsets: a) T-shaped intersection; b) L-shaped intersection.

6.3.1.2 Floors and roofing

A critical aspect to which the designer must pay particular attention when defining the numerical model is the correct assessment of the stiffness of floors and roofing, since the distribution of storey loads between masonry elements is strictly dependent on it.

Again in § 7.2.6, the NTC 2018 specify that, unless specifically assessed and provided that the openings present do not significantly reduce the stiffness, the horizontal structures can be considered infinitely rigid in their own average plane, provided they are made of reinforced concrete, or of brick-cement with a reinforced concrete slab at least 40 mm thick, or in a mixed structure with a reinforced concrete slab at least 50 mm thick connected to the steel or timber structural elements by suitably sized shear connectors.

In § C7.2.6, Circular 7/2019 also states that in order to effectively fulfil the function of a rigid diaphragm for the purpose of distributing horizontal forces between the vertical members supporting them, the horizontal structures must be effectively connected to the members themselves.

In cases where the floor and/or roofs cannot be considered infinitely rigid in their mid-plane (for example, in the case of wooden floors with simple planking or with “shaved” hollow-core concrete floors, i.e. without a collaborating concrete cap or stiffening elements), they can be modelled using plane finite elements with isotropic or orthotropic “membrane” behaviour, assigning appropriate elastic properties to these elements based on the stiffness in the plane of the horizontal structures and/or roof pitches to be modelled.

6.3.2 Structural elements

6.3.2.1 Stiffness

§ 7.2.6 in the NTC 2018 prescribes that the cracking of resistant sections must be appropriately taken into account when assessing the stiffness of structural elements. If no specific analysis is carried out, the flexural and shear stiffness of masonry, reinforced concrete and steel-concrete elements may be reduced by up to 50% of the stiffness of the corresponding non-cracked elements, depending on the limit state considered and the influence of the permanent axial stress.

With reference to load-bearing masonry constructions, § 7.8.1.5.2 below reiterates that the stiffnesses of masonry elements must be calculated considering both the flexural and shear contributions (thus adopting a Timoshenko formulation), preferably adopting reduced values to take account of the partialization of the sections following cracking. It is also stipulated that, in the absence of more accurate evaluations in the specific case of masonry elements, the cracked stiffnesses may be assumed to be half of the non-cracked stiffnesses.

As anticipated, the elastic stiffnesses of reinforced walls can be kept identical to those of unreinforced walls.

6.3.2.2 Constitutive binders

§ 7.8.1.5.4 of NTC 2018 states that, in the case of static non-linear analysis, perfectly plastic elastic bilinear constitutive binders can be assumed for masonry panels, with equivalent strength at the elastic limit and displacements at the elastic and ultimate limit corresponding to the flexural and shear response, until an ultimate deformation limit is reached (the value of which is defined differently, depending on the activated rupture criterion), beyond which the strength is nullified (as an example Figure 6.4 the buckling and shear constitutive bonds of the pier elements are shown). The last deformation is normally defined in terms of angular deformation (“chord rotation”) $\theta = \varphi + \gamma$, the sum flexural φ and shear deformation γ, as schematized in Figure 6.5.

Moreover, the strength criteria for unreinforced masonry elements are generally formulated in such a way that, when the vertical compression (tensile passage) is cancelled, the strength is cancelled (please refer to the requirements of §§ 7.8.2.2 of NTC 2018, with the additions of § C8.7.1.3.1.1 of Circular 7/2019 with regard to existing buildings).

As mentioned above, the strengths and CPLS deformation capacities of reinforced walls can be increased based on the information reported in paragraphs 6.2.2 and 6.2.1.

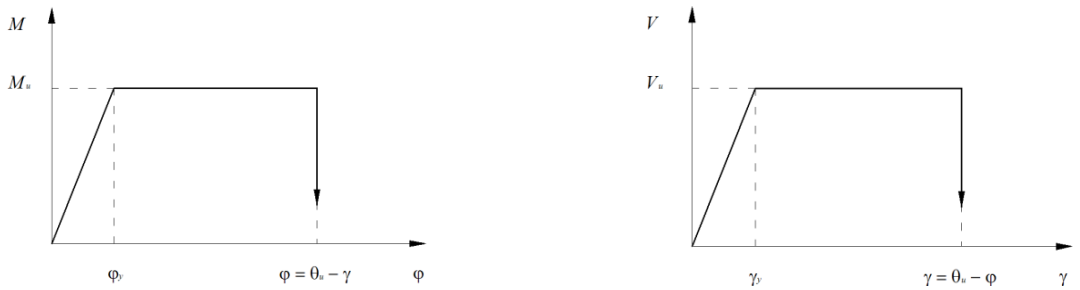

a) b)

Figure 6.4 Elasto-plastic behaviour of the masonry panel element: a) in bending; b) in shear.

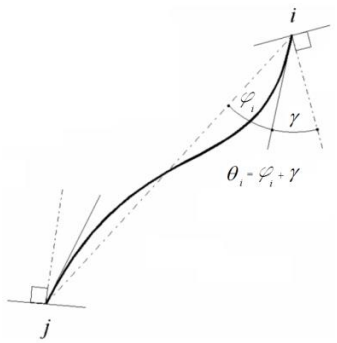

Figure 6.5 Definition of “chord rotation” θ.

6.3.2.3 Materials

Again with reference to existing constructions, § C8.5.4.1 of Circular 7/2019 specifies that, in the case in which the masonry in question can be traced back to the masonry types present in Tables C8.5.I and C8.5.II of the previous § C8.5.3.1, the average values of the mechanical parameters (strengths and elastic moduli of materials) to be used for the verifications can be defined according to different criteria, depending on the LC level of knowledge reached (LC1, LC2 or LC3), based on the corresponding minimum and maximum values of Table C8.5.I.

In the case of a non-linear analysis, according to § C8.7.1.3.1, the calculation values of the masonry strengths are then obtained by dividing the corresponding average values by the respective CF confidence factors (assuming a unit value for the partial material safety factor). The confidence factor value (which may be differentiated for different materials and/or specific structural elements) is defined according to the LC level of knowledge reached, as reported in § C8.5.4: CF = 1.35 for LC1; CF = 1.20 for LC2; CF = 1.00 for LC3. **This value is also to be applied for reinforced walls, obviously with reference only to the strength contribution of the unreinforced walls; the increase in strength offered by the reinforcement system, for which an LC3 is assumed and therefore CF = 1.00** (see previous § 6.2.2)**.**

6.3.3 Non-structural elements

§ 7.2.6 of the NTC 2018 prescribes that, in the definition of the model, non-structural elements that are not specifically designed as collaborating (such as infills and partitions) can only be represented in terms of mass; their contribution to the behaviour of the structural system in terms of stiffness and strength will only be considered if they have negative effects for safety purposes.

6.3.4 Definition of seismic action

Non-linear static analysis (§ 7.3.4.2 of NTC 2018) involves application of gravitational loads to the structural system and of horizontal forces proportional to the inertia forces having resultant (base shear) F_b for the considered direction of the seismic action at the horizontal building structures. These forces must be progressively scaled so that the horizontal displacement d_c of an appropriate control point coinciding with the centre of mass of the top level of the building (alternative control points, such as the ends of the plan of the top level, must also be considered when the coupling of translations and rotations is significant) grows monotonically, both in the positive and negative directions and until the local or global collapse conditions are reached. With particular reference to the analysis of existing masonry buildings characterised by diaphragms that cannot be considered as infinitely rigid, Circular 7/2019 at § C8.7.1.3.1 specifies the following:

- If the horizontal diaphragms are of negligible stiffness, or rather not able to guarantee a significant distribution of seismic actions among the various masonry walls, the global analysis of the seismic response may be carried out by analysing the individual walls, subjected to the actions of their competence on the basis of a subdivision by areas of influence;
- In the case of diaphragms of finite stiffness, since it is not possible to define the displacement of the centre of mass of the last level, the displacement d_c to be assumed for the capacity curve can be consistently assumed to be the average displacement between that of the different walls, weighted with the corresponding seismic masses.

Again according to § 7.3.4.2, at least two inertia force distributions must be considered in the analysis, one falling in the main distributions (Group 1) and the other in the secondary distributions (Group 2):

6.3.4.1 Group 1 - Main distributions

- If the fundamental mode of vibration in the direction considered has a mass participation of no less than 75 % (in § 7.8.1.5.4 below, limit reduced to 60% in the case of masonry constructions) one of the two following distributions applies:
  1) Distribution proportional to the static forces referred to in § 7.3.3.2, using the first distribution of Group 2 as the second distribution;
  2) Distribution corresponding to a pattern of accelerations proportional to the shape of the fundamental mode of vibration in the direction considered;
- In all cases, the following distribution may be used:
  3) Distribution corresponding to the development of plane forces acting on each horizontal structure calculated in a linear dynamic analysis, including in the direction considered a number of modes with a total mass participation of no less than 85%. The use of this distribution is mandatory if the fundamental period T_1 of the structure is greater than $1.3 \cdot T_C$.

6.3.4.2 Group 2 - Secondary distributions

1) Distribution of forces inferred from a uniform course of accelerations along the height of the construction;
2) Adaptive distribution, which changes as the displacement of the control point increases as a function of the plasticity of the structure;
3) Multimodal distribution, defined by considering at least six significant modes.

Finally, with specific reference to the global analysis of existing masonry buildings by means of non-linear static analysis, § C8.7.1.3.1 in Circular 7/2019 indicates that in this case it is possible to assign, as principal and secondary distributions, respectively, the first distribution of both Group 1 and Group 2, regardless of the percentage of participating mass in the first mode.

6.3.5 Definition of the set of analyses

§ 7.2.6 of the NTC 2018 prescribes that, in order to take into account the spatial variability of the seismic motion, as well as any uncertainties, an accidental eccentricity must be attributed to the

centre of mass with respect to its position as derived from the calculation, which for buildings only (and in the absence of more accurate determinations) in each direction cannot be considered less than 5% of the average size of the building, measured perpendicular to the direction of application of the seismic action and must be assumed constant in magnitude and direction on all horizontal structures.

In accordance with § 7.3.5 of NTC 2018, the analyses, regardless of the type, must be conducted taking into account the contemporaneity of three components of the seismic action, acting according to two main independent directions in the horizontal plane, E_x and E_y, and in the vertical plane, E_z. In particular, the most severe effects must be obtained by applying the expression $1.0 \cdot E_x + 0.3 \cdot E_y + 0.3 \cdot E_z$ and permuting the multiplicative coefficients circularly. The vertical component must only be considered in the cases referred to in § 7.2.2 above, from which masonry buildings may be considered excluded. For these, therefore, the previous expression is reduced to $1.0 \cdot E_x + 0.3 \cdot E_y$; the permutation of the coefficients leads to 4 combinations, which become 8 taking into account also the possible combinations of sign (positive and negative) of the two components. Taking into account the need to apply the translation of the centre of mass, the point of application of the seismic action, considering the accidental eccentricity in the two main directions with both positive and negative direction, a total of 32 different load cases should therefore be considered. As an exception to this requirement, § C7.3.5 in Circular 7/2019 indicates that, in the case of static non-linear analysis only, it is permitted to apply each of the two horizontal components separately (together with the vertical one where necessary). In the case of masonry buildings, this means that the number of load cases to be considered is reduced from 32 to 8 for each distribution considered.

6.3.6 Verification criteria

6.3.6.1 Foreword

§ 7.3.4.2 of NTC 2018 specifies that the diagram $F_b - d_c$ obtained from each analysis performed represents the capacity curve of the structure.

As indicated in § 7.8.1.6 below (and better specified in the corresponding § C7.8.1.6 of Circular 7/2019), safety checks on load-bearing masonry buildings consist in the case of non-linear static analysis in comparing the displacement capacity of the construction and the displacement demand at the different limit states.

6.3.6.2 System equivalent to a single degree of freedom

For the purpose of safety checks, it is first necessary to define a single-degree-of-freedom structural system that is equivalent to the real structural system, e.g. by means of the procedure indicated in § C7.3.4.2 of Circular 7/2019, according to which the force F^* and displacement d^* of the equivalent system are linked to the corresponding sizes F_b and d_c of the real system by relations:

$$F^* = \frac{F_b}{\Gamma} \tag{130}$$

$$d^* = \frac{d_c}{\Gamma} \tag{131}$$

in which Γ is the modal participation factor, defined as:

$$\Gamma = \frac{\varphi^T M \tau}{\varphi^T M \varphi} \tag{132}$$

the vector being τ the drag vector corresponding to the direction of the earthquake considered, φ the descriptive vector of the fundamental mode of vibration of the real system, normalised by placing $d_c = 1$ and M the mass matrix of the real system.

6.3.6.3 Bilinear curve equivalent to the capacity curve of the single-degree-of-freedom system

A bilinear curve is substituted for the equivalent system capacity curve thus defined, using techniques that are usually based on principles of energy equivalence (i.e. by which the areas subtended by the bilinear curve and the F*-d* curve are assumed to be equal). Of those proposed by Circular 7/2019, only Method A, which was also reported in Circular 617/2009, is cited here as an example.

According to this criterion, the equivalent bilinear curve is characterised by a first linear elastic section and a second section with a perfectly plastic course, as illustrated in Figure 6.6.

Given F_u the maximum strength of the real structural system and F_u^* the maximum strength of the equivalent system (defined using the previous (130)), the elastic section is identified by imposing its passage through the point $0.7 \cdot F_u^*$ (according to that prescribed for load-bearing masonry buildings in § 7.8.1.6 of NTC 2018 and as an exception to the general criterion given in § C7.3.4.2 of Circular 7/2019) of the capacity curve of the equivalent system, the plasticization force F_y^* is identified by imposing the equality of the areas subtended by the bilinear curve and the capacity curve for the maximum displacement d_u^*. .

In the case of existing load-bearing masonry buildings, the latter value (again, by way of derogation from the general indication for constructions given in § C7.3.4.2 of Circular 7/2019) must be assumed to be the lower of the displacement corresponding to a residual strength equal to $0.8 \cdot F_u^*$ and the displacement corresponding to reaching the limit threshold of angular deformation at CPLS in all vertical pier elements of any level in any wall considered significant for safety purposes (as described in § C8.7.1.3.1). This last check may be omitted in the analyses when the diaphragms are infinitely rigid or when a single wall analysis is performed.

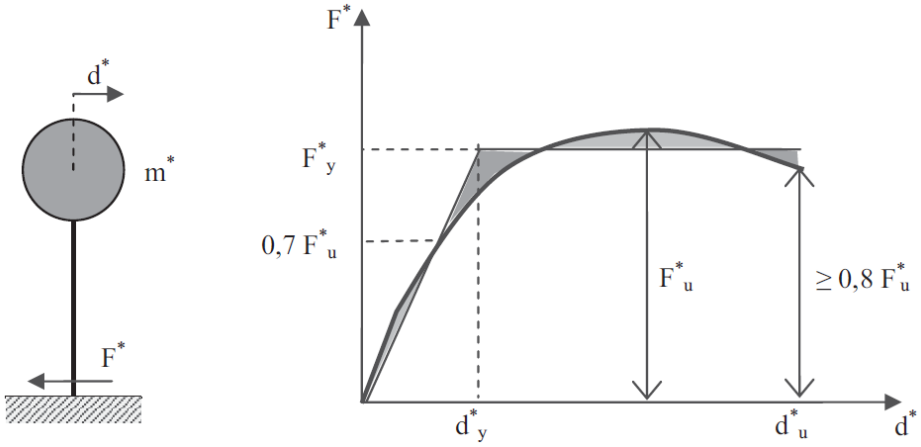

Figure 6.6 Equivalent bilinear system and diagram (as amended by Circular 7/2019)

The elastic period of the bilinear system is given by the expression:

$$T^* = 2\pi\sqrt{\frac{m^*}{k^*}} \tag{133}$$

where $m^* = \varphi^T M \tau$ and k^* is the stiffness of the elastic section of the bilinear.

6.3.6.4 Assessing displacement demand

In accordance with that indicated in § C8.7.1.3.1 of Circular 7/2019 with specific reference to existing buildings in load-bearing masonry, the displacement demand at the different limit states can be evaluated on the equivalent bilinear system by means of the expressions indicated in § C.7.3.4.2, referred to below.

In the case where the elastic period of the construction T^* is $T^* \geq T_C$ the displacement demand for the inelastic system is assumed to be equal to that of an elastic system of the same period, defined in accordance with the requirements of § 3.2.3.2.3 of NTC 2018 (Figure 6.7a):

$$d^*_{max} = d^*_{e,max} = S_{De}(T^*) \tag{134}$$

In the event that it is $T^* < T_C$ the displacement demand for the inelastic system is greater than that of an elastic system of the same period (Figure 6.7b) and is obtained from the latter using the expression:

$$d^*_{max} = \frac{d^*_{e,max}}{q^*}\left[1 + (q^* - 1)\frac{T_C}{T^*}\right] \geq d^*_{e,max} \tag{135}$$

being

$$q^* = \frac{S_e(T^*) \cdot m^*}{F^*_y} \tag{136}$$

the ratio between the force of the elastic response (with S_e defined as prescribed in § 3.2.3.2.1 of NTC 2018) and the yield strength of the equivalent system. In the event that it is $q^* \leq 1$ you must impose $d^*_{max} = d^*_{e,max}$.

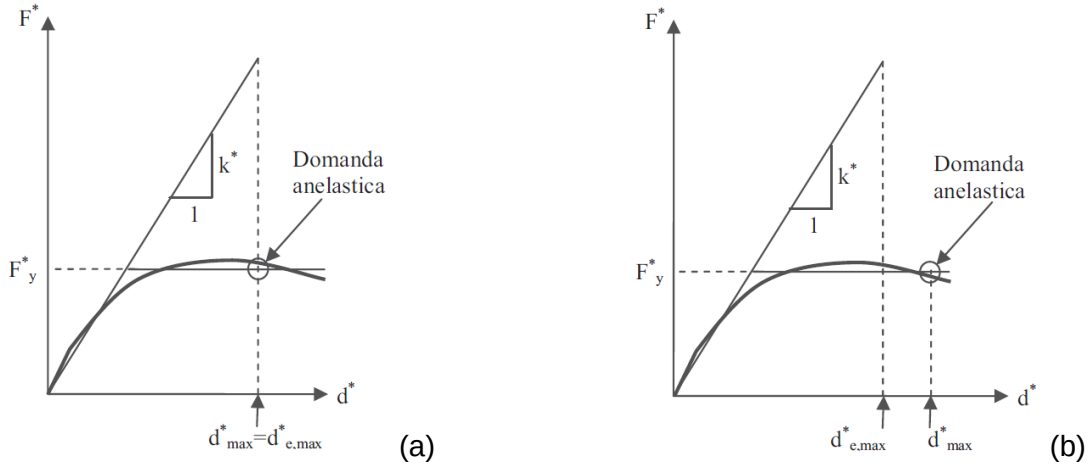

Figure 6.7 Reference displacement for $T^* \geq T_C$ (a) and for $T^* < T_C$ (b) (from Circular 7/2019)

In particular, the procedure described is valid both in the non-linear field (LSLS and CPLS) and in the equivalent linear field (OLS and DLS) and can be applied to evaluate the displacement demand as the value of the probability of exceedance P_{V_R} associated with the different limit states considered (and therefore the return period T_R and the corresponding values of the seismic reference parameters a_g , F_o and T^*_C which define the elastic response spectra in acceleration S_e and displacement S_{De}) vary.

6.3.6.5 Assessing displacement capacity

According to § C8.7.1.3.1 of Circular 7/2019, the displacement capacity for existing load-bearing masonry buildings relative to the different limit states must be evaluated on the force-displacement curve of the real system, at the following points:

CPLS: the smaller of the displacements corresponding to the following two conditions:

- residual base shear (after the peak is reached) equal to 80% of the maximum;
- reaching of the limit threshold of angular deformation at CPLS in all vertical pier elements of any level of any wall considered significant for safety purposes (this check may be omitted in the analyses when diaphragms are infinitely rigid or when the analysis of a single wall is performed).

LSLS: displacement corresponding to 3/4 of the displacement at CPLS;

DLS: the smaller of the displacements obtained from the following two conditions:

- reaching of the equivalent bilinear elastic limit, defined from the ultimate displacement at CPLS;
- reaching of the maximum shear strength in all vertical pier elements of any level of any wall considered significant for use of the building (and in any case not before the displacement for which a base shear equal to 3/4 of the maximum base shear is reached).

OLS: displacement corresponding to 2/3 of that at the DLS.

6.3.6.6 Safety checks

At each limit state considered, the capacity demand, defined as stated on the equivalent bilinear curve and then carried over to the capacity curve of the real system by inverting the previous (131) must not exceed the corresponding capacity.

Moreover, with particular reference to the verification at CPLS, Circular 7/2019 recommends (again in § C8.7.1.3.1) that the displacement capacity of the system at CPLS does not exceed the displacement corresponding to the value q*=4 for all types of masonry and that, similarly, the displacement capacity of the system at LSLS does not exceed the displacement corresponding to the value q*=3; this means that the conditions must also be verified:

$$q^*_{SLC} \leq 4 \tag{137}$$

$$q^*_{SLV} \leq 3 \tag{138}$$

Using superscripts C and D to identify the values of the parameters introduced below corresponding, respectively, to capacity and demand and subscript “G” to identify the values associated with the global response, as in the case of the analysis and verification of local mechanisms (see §§ 0 and 5.1.4 above), it will finally be possible to derive from the global analysis the capacity value of PGA, $PGA^C_{G,SLi}$, corresponding to reaching of the i-th limit state considered, which will be compared with the corresponding demand value PGA^D_{SLi}, evaluated for the associated exceedance probability $P_{V_{R,SLi}}$. Similarly, the return period of capacity $T^C_{RG,SLi}$ can be identified.

Finally, the safety index associated with the global response at each i-th limit state can be defined $\zeta_{EG,SLi}$ using the relationship:

$$\zeta_{EG,SLi} = \frac{PGA^C_{G,SLi}}{PGA^D_{SLi}} \tag{139}$$

6.4 Structural analysis: linear elastic analysis

In the linear analyses, for verification at LSLS, the buckling and shear stresses of each element, evaluated for a value of the seismic action reduced by behaviour factor *q*, must be lower than the respective strengths calculated for unreinforced masonry on the basis of the strength criteria of § C8.7.1.3.1.1 of Circular 7/2019 and for reinforced masonry on the basis of previous § 6.2.2.

6.4.1 Definition of numerical model

6.4.1.1 Geometrical modelling

As prescribed in § 7.2.6 of NTC 2018, the model of the structure to be adopted for analysis must be three-dimensional and adequately represent the actual spatial distributions of mass, stiffness and strength, as for non-linear static analysis.

Elastic and linear analyses can be conducted with equivalent structural frame models or with finite element models (FEM) of the “plate” type. Numerous commercial software packages are available on the market that allow elastic and linear analyses and the associated safety checks on masonry buildings, such as Pro-SAM (2Si), SISMICAD (Concrete), MasterSAP (AMV).

With regard to equivalent frame modelling, the same applies as for non-linear static analysis, to which reference is made.

In FEM modelling, masonry panels and strips are divided into elastic “plate” elements and can have either isotropic or orthotropic properties, depending on the characteristics of the masonry (Figure 6.8). In the case of FEM modelling, however, it is necessary to provide for the integration of stresses on the large sections of the elements since safety checks must be carried out according to regulations by comparing stresses (axial action, shear and moments) and strengths and not in terms of stresses.

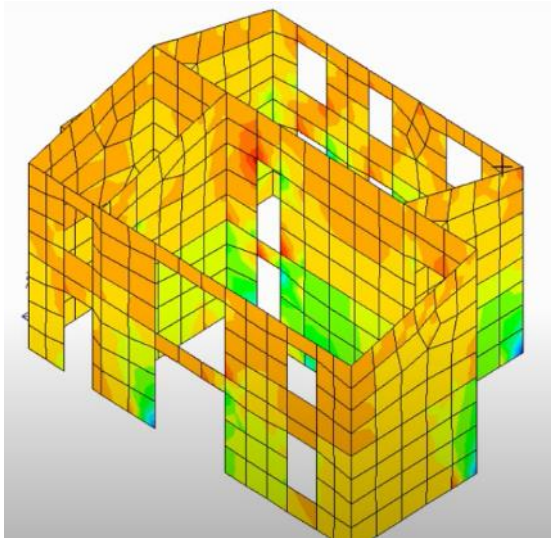

Figure 6.8 Finite element FEM model of a load-bearing masonry building.

6.4.1.2 Floors and roofing

With regard to the modelling of floors and roofs, the same applies as for the non-linear static analysis.

6.4.2 Structural elements

6.4.2.1 Stiffness

As in the case of non-linear static analysis, it should be noted that the elastic stiffnesses of masonry elements must be calculated considering both the flexural and shear contributions, using cracked stiffnesses equal to half of the non-cracked stiffnesses in the case of seismic action verifications.

As anticipated, the elastic stiffnesses of reinforced walls can be kept identical to those of unreinforced walls.

6.4.2.2 Strengths

The criteria for the evaluation of the strength of unreinforced walls (buckling and shear) refer to the prescriptions of §§ 7.8.2.2, with the additions of § C8.7.1.3.1 of Circular 7/2019 with regard to existing buildings. **The strengths of reinforced walls can be increased in relation to those of unreinforced walls based on the information reported in paragraphs 6.2.2.**

6.4.2.3 Materials

In the case of a linear analysis, according to § C8.7.1.3.1.1, the calculation values of the masonry strengths are obtained by dividing the average values by the respective confidence factors and the partial material safety factors γ_M (in seismic masonry verifications, γ_M = 2). The confidence factor

value (which may be differentiated for different materials and/or specific structural elements) is defined according to the LC level of knowledge reached, as reported in § C8.5.4: CF = 1.35 for LC1; CF = 1.20 for LC2; CF = 1.00 for LC3. **This value is also to be applied for reinforced walls, obviously with reference only to the strength contribution of the unreinforced walls; the increase in strength offered by the reinforcement system, for which an LC3 is assumed and therefore CF = 1.00** (see previous § 6.2.2)**.**

6.4.3 Non-structural elements

See the information reported with reference to the non-linear static analysis in the above § 6.3.3.

6.4.4 Definition of seismic action and behaviour factor q

In the case of seismic verifications, the permissible structural analyses are linear static analysis and dynamic modal analysis. In the case of masonry buildings, the linear static analysis is essentially always permitted, even in the case of irregular height constructions, also by virtue of the fact that the dynamic modal analysis does not provide any more reliable results than a simple static analysis, given the purely conventional nature of linear analyses applied to masonry buildings.

For the calculation of stresses on the masonry elements (axial action, bending and shear), the forces applied on the masonry buildings in an elastic analysis are derived from the spectral accelerations of the design, obtained by reducing the elastic response spectrum at LSLS by behaviour factor *q*. In accordance with § C8.5.5.1 of Circular 7/2019 of NTC 2018, the *q* values for existing load-bearing masonry buildings can be assumed to be equal to:

- q=2.0·α_u/α_1 for regular buildings in elevation, in the case of stone and/or solid brickwork;
- q=1.75·α_u/α_1 for regular buildings in elevation, in the case of artificial block masonry with a perforation percentage < 15% (semi-full, perforated elements).

being α_u and α_1 defined in § 7.8.1.3 of NTC 2018. In the absence of more precise assessments, a α_u/α_1 ratio of more than 1.50 (1.25 if the buildings are irregular in plan) cannot be assumed. If instead the value of α_u/α_1 is calculated by means of a non-linear static analysis, it cannot in any case be assumed to exceed 2.5.

In the case of non-regular buildings in elevation, the *q* values are reduced by 25%. The definition of regularity for an existing masonry building is that given in § 7.2.1 of the NTC.

Given the value of the spectral ordinate, the distribution of lateral forces in the case of static analysis to be applied to the different planes of the building for the stress evaluation will be equal to:

$$F_i = F_h \cdot z_i \cdot \frac{W_i}{z_j W_j} \tag{140}$$

in which $F_h = S_d(T_1) \cdot W\lambda/g$ is the total base shear, defined according to the ordinate $S_d(T_1)$ of the design spectrum at the main vibration period T_1, F_i is the force to be applied to the *i-th* mass, W_i and W_j and z_i and z_j are, respectively, the weights and heights in relation to the foundation plane of the *i-th* and *j-th* masses, W is the overall weight of the construction, λ is the coefficient equal to 0.85 if $T_1 < 2T_C$ and the construction has at least three horizontal structures and equal to 1.0 in all other cases and g is the acceleration of gravity.

Although the NTC 2018 provides for the evaluation of the principal period of vibration T_1 through a formulation that requires global modelling of the structure to calculate the lateral displacement of the building d ($T_1 = 2\sqrt{d}$), Circular 7/2019 re-presents the well-known approximate formulation as a function of building height H already present in the NTC2008, according to which the principal period for masonry buildings can be set equal to$T_1 = 0.05H^{3/4}$ (with H in metres).

6.4.5 Definition of the set of analyses

As presented in § 6.3.5, linear elastic analyses must be conducted taking into account the contemporaneity of the horizontal components of the seismic action (disregarding the vertical one), acting according to two main independent directions, E_x and E_y. In particular, the most severe effects

must be obtained by applying the expression $1.0 \cdot E_x + 0.3 \cdot E_y$ and permuting the multiplicative coefficients circularly. The permutation of the coefficients leads to 4 combinations, which become 8 taking into account also the possible combinations of sign (positive and negative) of the two components. Taking into account the need to apply the translation of the centre of mass, the point of application of the seismic action, taking into account the accidental eccentricity in the two main directions with both positive and negative direction, a total of 32 different load cases must therefore be considered, compared to the 16 considered in non-linear static analyses.

6.4.6 Verification criteria

In linear analyses, seismic verifications must be carried out at DLS in terms of displacement and at LSLS in terms of strength.

In particular, at DLS according to what is prescribed in § 7.3.6.1 of NTC 2018, the maximum inter-storey displacement is less than 0.002 times the inter-storey height *h* in the case of verification of unreinforced walls and, consequently (according to what is indicated in the previous § 6.2.1), equal to 1.5·0.002 = 0.003 times the inter-storey height in the case of reinforced walls. In existing buildings, DLS verification is only mandatory for use class IV constructions.

With regard instead to verification at LSLS, the buckling and shear stresses of each element must be lower than the respective strengths calculated for unreinforced masonry on the basis of the strength criteria of § C8.7.1.3.1.1 of Circular 7/2019 and for reinforced masonry on the basis of previous § 6.2.2.

Also in the case of linear analysis, it will be possible to derive the capacity value of PGA, $PGA^C_{G,SLi}$, corresponding to reaching of the i-th limit state considered, which will be compared with the corresponding demand value PGA^D_{SLi}, evaluated for the associated exceedance probability $P_{V_{R,SLi}}$. Similarly, the return period of capacity $T^C_{RG,SLi}$ can be identified.

Finally, the safety index associated with the global response at each *i*-th limit state can be defined, $\zeta_{EG,SLi}$, using the relationship:

$$\zeta_{EG,SLi} = \frac{PGA^C_{G,SLi}}{PGA^D_{SLi}} \tag{141}$$

6.5 Calculation example

Considered below, by way of example, is the verification under NTC 2018 of the global seismic response of an existing load-bearing masonry building, with reference to the current, unreinforced state and the design state, which involves reinforcing the perimeter walls using the Resisto 5.9 modular system.

In particular, it is assumed that the reinforcement intervention, carried out according to the details given in previous § 2, does not provide for connection of the metal modules to the edge elements (foundation and reinforced concrete floor kerbs) but only to the masonry.

6.5.1 Structural configuration

The case study considered is a two-storey, above ground residential building in load-bearing masonry, the structural configuration of which is schematized in Figure 6.9.

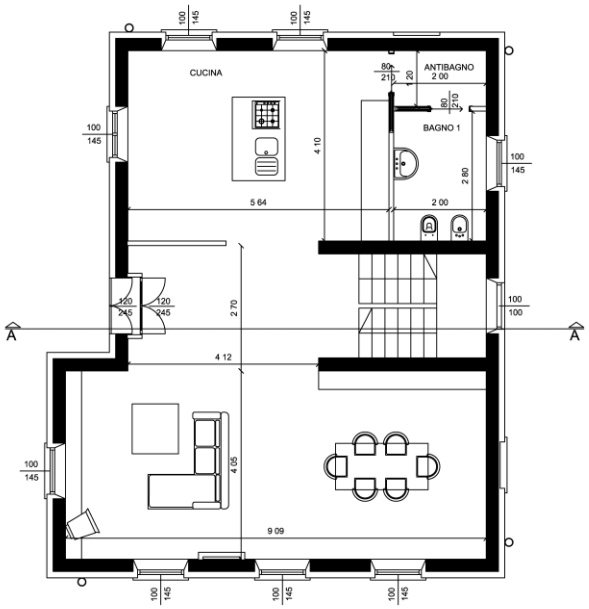

PIANO PRIMO

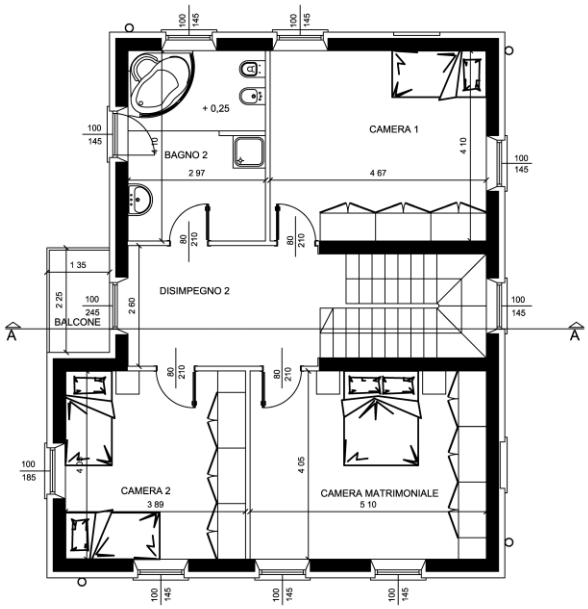

PIANO SECONDO

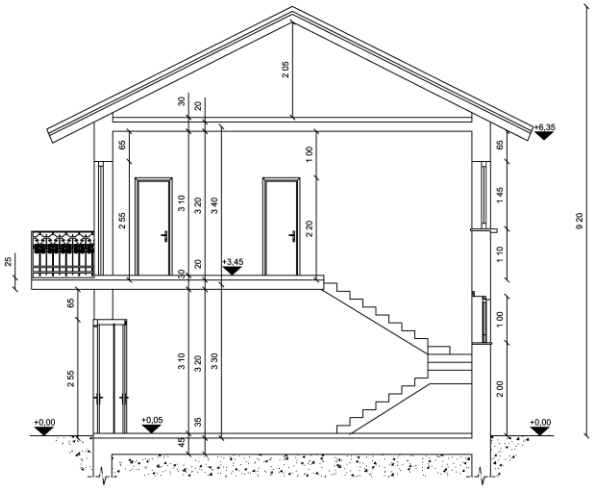

SEZIONE AA

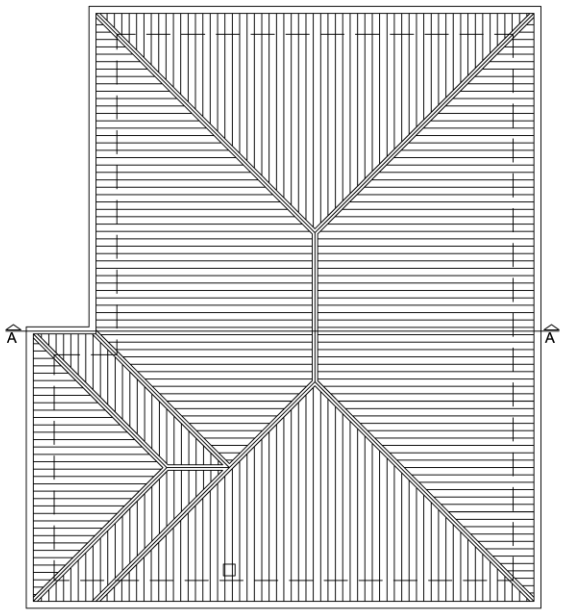

COPERTURA

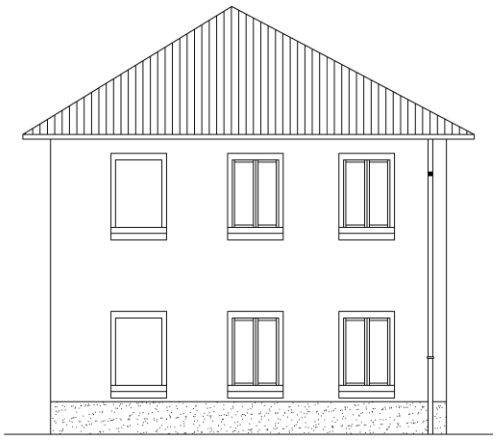

PROSPETTO NORD

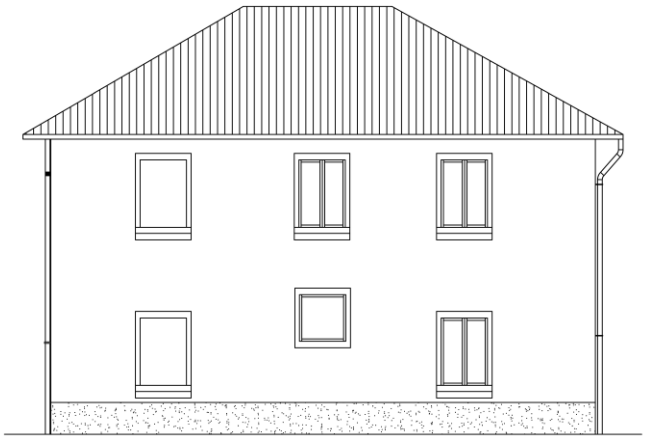

PROSPETTO EST

Figure 6.9 Structural configuration of the building subject to global seismic verification (dimensions in cm).

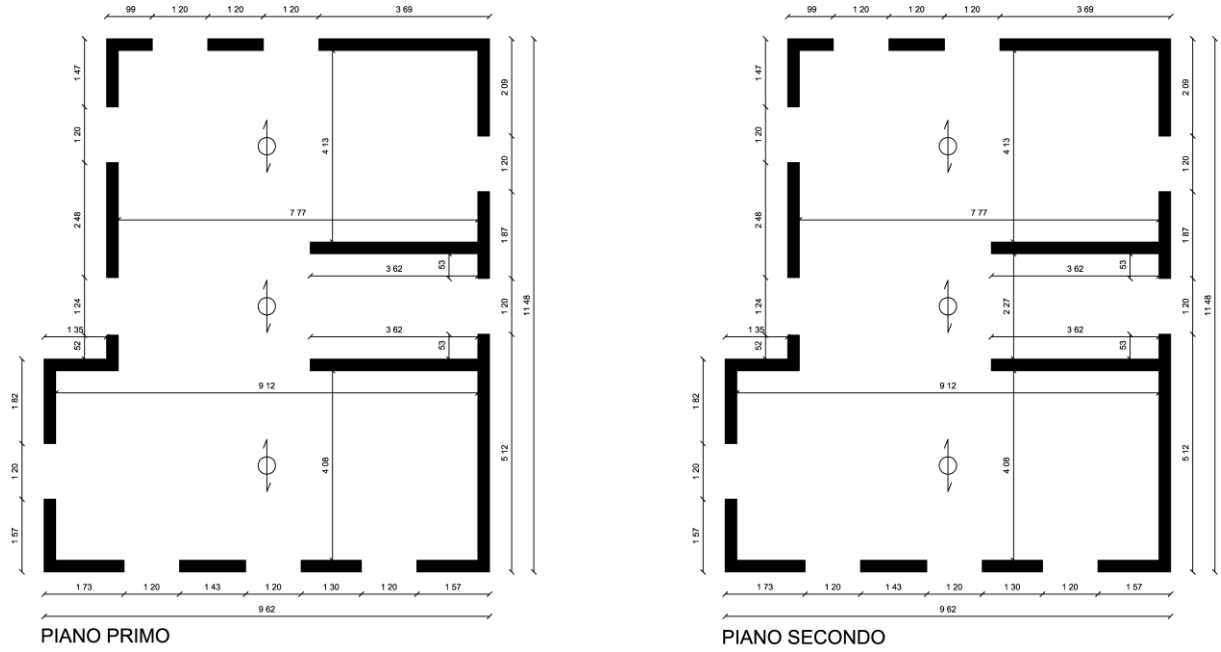

Figure 6.10 Dimensions (in cm) of the masonry panels (thickness of all walls 25 cm).

It is assumed that the building is located in the Municipality of Moglia (MN), in a site characterised by type B subsoil and topographical category T1. The seismic parameters relative to the site, assuming a nominal life of the building V_N of 50 years and a class of use C_u = 1, are given in Table 6.2. A damping of 5% is assumed in the definition of the elastic response spectrum.

Table 6.2. Seismic parameters for the reference site

LIMIT STATE	a_g [g]	F_o [-]	T_C^* [s]	S_S [-]	S_T [-]	C_C [-]	**S** [-]	T_B [s]	T_C [s]	T_D [s]
OLS	0.036	2.584	0.233	1.200	1.000	1.472	1.200	0.114	0.343	1.744
DLS	0.044	2.567	0.267	1.200	1.000	1.432	1.200	0.128	0.383	1.774
LSLS	0.122	2.580	0.277	1.200	1.000	1.422	1.200	0.131	0.394	2.088
CPLS	0.165	2.558	0.279	1.200	1.000	1.420	1.200	0.132	0.396	2.258

The load-bearing structure of the building is made of solid bricks and lime mortar with a full-header bond and is characterised by a thickness of 25 cm at both the perimeter walls and the internal walls (stairwell).

The net inter-floor height at both levels is 320 cm.

The intermediate and attic floors, which are warped in all three bays in a north-south direction, are 16 cm thick hollow-core concrete with a 4 cm reinforced concrete slab. For the purposes of the analyses, the horizontal structures were assumed to be infinitely rigid in their own plane in the numerical model.

The floors are effectively connected to the masonry. In particular, at the intersections between the floors and walls on each floor, there is a 20 cm high continuous reinforced concrete kerb reinforced with 2+2Ø14 beams and Ø6 brackets with 2 arms with a 25 cm pitch (in compliance with the minimum reinforcement requirements of the kerbs prescribed in § 1.3.1.1 of DM87). The width of the kerbs is equal to the thickness of the walls below. On both floors, there are also two emerging reinforced concrete beams with a 25x40 cm^2 cross-section which connect the internal walls of the stairwell to the west wall of the building, reinforced with 4+4 Ø14 beams and Ø6 brackets with 4 arms with a 10 cm pitch. All reinforced concrete elements are made of class C20/25 concrete and FeB44k reinforcing steel.

On the first floor at the entrance of the building (west façade) there is a balcony, created by means of a 15 cm thick cast-in-place reinforced concrete slab.

The building has a lightweight, pitched non-pushing roof (average slope 23°) with an eave projecting 80 cm along the entire perimeter, characterised by a load-bearing structure in brickwork and hollow clay planks and a roof covering of brick tiles.

The roof and balcony are considered exclusively in terms of mass increases and loads bearing on the masonry of the second and first levels of the building and are not explicitly included in the numerical model.

6.5.2 Materials

A type LC2 knowledge of the building is assumed; therefore a CF confidence factor value of 1.20 is adopted.

The masonry properties are assumed based on the indications of § C8.5.4.1 of Circular 7/2019 according to the level of knowledge reached. In particular, the average values of the strength and elastic moduli ranges given in Table C.8.5.I of § C8.5.3.1 are adopted, with reference to solid brick and lime mortar masonry. A shear strength limit is also assumed for breaking bricks $f_{v,lim}$ equal to 1.41 MPa, estimated using equation [C8.7.1.14] of Circular 7/2019 assuming an average compressive strength f_b of the bricks (size 250x120x50 mm^3) equal to 20 MPa (the corresponding normalised value of compressive strength, necessary for the calculation of $f_{v,lim}$, is assessed according to the procedure in Annex A of standard UNI EN 772-1 assuming air conditioning of the bricks. Furthermore, in the absence of more accurate assessments, the average tensile strength of the bricks is assumed to be 1/10 of the corresponding compressive strength. The design values of the mechanical parameters adopted in the calculation are obtained by dividing the average values, given in the following Table 6.3, by the CF confidence factor.

Table 6.3. Mechanical properties of the masonry

f [MPa]	τ_0 [MPa]	f_{v0} [MPa]	f_b [MPa]	f_{bt} [MPa]	$f_{v,lim}$ [MPa]	E [MPa]	G [MPa]	w [kN/m^3]
3.45	0.09	0.20	20.00	2.00	1.41	1500	500	18

Notes: f average compressive strength of masonry; τ_0 average shear strength of masonry in the absence of normal stresses (Eq. [C8.7.1.16] § C8.7.1.3); f_{v0} average shear strength of masonry in the absence of normal stresses (Eq. [C8.7.1.17] § C8.7.1.3) ; $f_{v,lim}$ shear strength limit of masonry for breaking bricks; f_b

average compressive strength of bricks; f_{bt} average tensile strength of bricks; E average value of normal modulus of elasticity of masonry; G average value of tangential modulus of elasticity of masonry; w average specific weight of masonry

Given the header bond of the masonry walls, the local coefficient of friction μ and the interlocking coefficient ϕ introduced in equation [C8.7.1.17] of Circular 7/2019 (see below) are 0.58 and 1.00, respectively.

The mechanical properties of the reinforced concrete elements (concrete class C20/25 and steel class FeB44k) are, finally, summarised in Table 6.4.

Table 6.4. The mechanical properties of the reinforced concrete elements

f_c [MPa]	E_c [MPa]	G_c [MPa]	w_c [kN/m^3]	f_{sy} [MPa]
28.75	30200	12584	25	452.63

Notes: f_c average compressive strength of concrete; E_c average value of normal modulus of elasticity of concrete; G_c average value of tangential modulus of elasticity of concrete; w_c average specific weight of concrete; f_{sy} average yield strength of steel

6.5.3 Loads

The characteristic values of the loads considered as acting on the structure, in addition to the self-weight of the masonry walls and reinforced concrete kerbs and beams, are shown below.

The evaluation of the loads is carried out in compliance with the prescriptions of §§ 2.5 and 3 of NTC 2018.

The loads acting on the attic floor and the roof are considered together (in this respect see the following § 6.5.4). It should be noted that the values given refer to the horizontal surface unit; the average slope of the roof pitches is 23°, while that of the flights of stairs is 30°.

Intermediate floor

Permanent structural load	g_1	2.85	[kN/m^2]
Permanent non-structural load	g_2	3.15	[kN/m^2]
Variable load (cat. B)	q	2.00	[kN/m^2]

Attic floor and roof

Permanent structural load	g_1	5.75	[kN/m^2]
Permanent non-structural load	g_2	1.95	[kN/m^2]
Variable load (snow at altitude ≤ 1000 m)	q	1.20	[kN/m^2]

Eave

Permanent structural load	g_1	1.90	[kN/m^2]
Permanent non-structural load	g_2	0.80	[kN/m^2]
Variable load (snow at altitude ≤ 1000 m)	q	1.20	[kN/m^2]

Balcony

Permanent structural load	g_1	3.75	[kN/m^2]
Permanent non-structural load	g_2	2.75	[kN/m^2]
Variable load (cat. C)	q	4.00	[kN/m^2]

Stairwell

Permanent structural load	g_1	3.60	[kN/m^2]
Permanent non-structural load	g_2	1.40	[kN/m^2]
Variable load (cat. C)	q	4.00	[kN/m^2]

For the purpose of the analyses, the (seismic) combination of loads, defined through the expression [2.5.5] of § 2.5.3 of NTC 2018, is considered:

$$E + G_1 + G_2 + \sum_i \psi_{2i} \cdot Q_i \quad (142)$$

in which E is the seismic action, G_1 is the resultant of the permanent structural loads, G_2 is the resultant of non-structural permanent loads, Q_i is the resultant of each i-th variable load, ψ_{2i} is the combination coefficient of the i-th variable action, the value of which is defined according to Table 2.5.I of § 2.5.2 of the NTC 2018 (in particular, in this specific case, since the site considered is at an altitude of 24 m. a.s.l., the snow load is not considered concurrent with the seismic action, resulting in the corresponding combination coefficient being null).

The effects of seismic action are assessed by taking into account the masses associated with the gravitational loads considered in the expression [2.5.7]:

$$G_1 + G_2 + \sum_i \psi_{2i} \cdot Q_i \quad (143)$$

6.5.4 Numerical model

Verification of the global seismic response of the building is carried out by means of static linear analysis on an equivalent three-dimensional frame model of the load-bearing structure (masonry walls and floor kerbs and reinforced concrete beams).

The numerical analyses are conducted with the PRO_SAM module of the commercial software PRO_SAP (2Si), which uses SAM II as its code solver (Manzini et al., 2019). Figure 6.11 shows the 3D model of the building (the horizontal structures have been excluded from the graphical representation to allow the structural configuration to be identified) and the equivalent frame model.

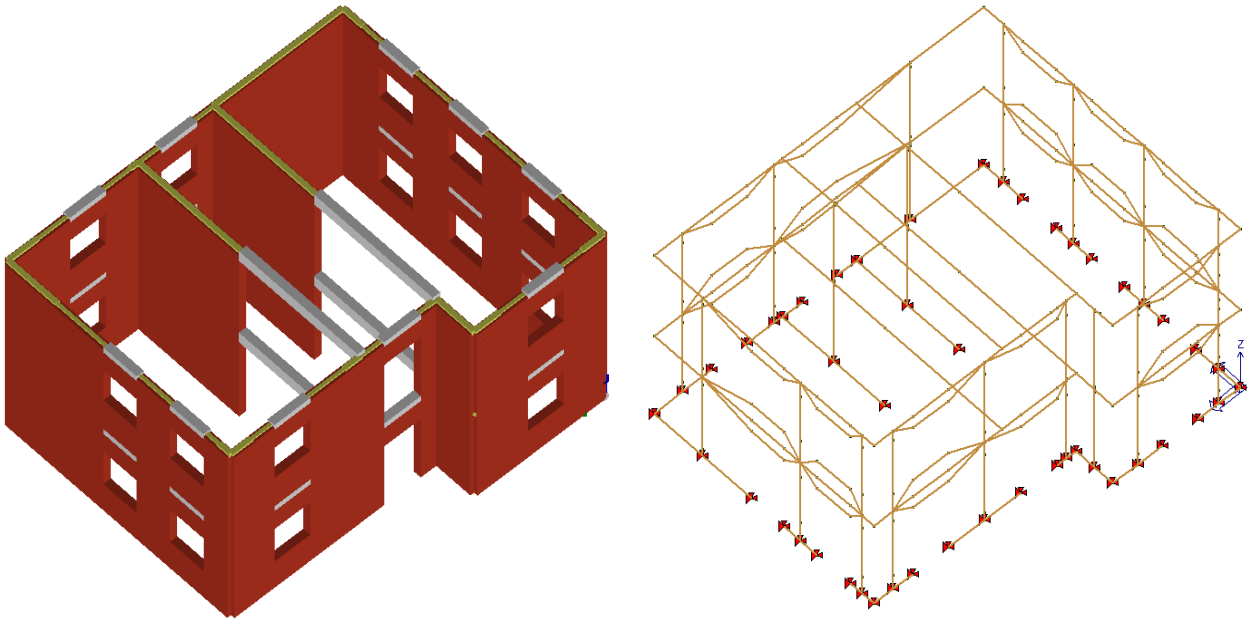

Figure 6.11 Three-dimensional model (left) and equivalent frame model (right) of the building.

For details regarding the equivalent frame modelling, analysis and verification criteria adopted, please refer to the previous § 6.3.

It should be noted here that the assumptions of infinite stiffness in the own plane of the horizontal structures and of perfect bonding in the area of intersection of the masonry walls are adopted on the basis of the structural characteristics of the building.

In addition, the deformable length of the pier elements is defined on the basis of Dolce's (1991) geometric criterion, while that of the masonry strips, kerbs and reinforced concrete beams is assumed to be equal to the span of the corresponding openings. In defining the geometric model, the floor masonry strips are interrupted at the first horizontal structure to take into account the presence of the continuous reinforced concrete kerb: a masonry strip above the window at the first level and a spandrel strip at the second level of the structure are therefore considered in the equivalent frame, separated from the floor kerb and adhering to it.

It should be emphasised that only the portion of the structure between the projection of the foundation level and the extrados of the attic floor is considered in the equivalent frame modelling, excluding the pitched roof and the overhangs. The roof and the balcony, which are therefore not explicitly included in the numerical model, are considered in the calculation exclusively in terms of the increase in mass and load on the load-bearing structure, respectively on the second and first levels of the building.

Finally, it should be noted that, in the definition in the numerical model of the distribution of gravitational loads:

- The contributions associated with the loads acting on the horizontal structures are considered as concentrated loads at the top end nodes of the vertical axis elements or as uniformly distributed loads on these elements in the presence of reinforced concrete beams;
- The contributions associated with the self-weight of the structural elements with a vertical axis at each level of the building are considered as concentrated loads at the upper and lower end nodes, with reference to the portions of each element included between the respective barycentre level of the floor and the inter-storey level;
- The contributions associated with the self-weight of the structural elements with a horizontal axis are considered as concentrated loads in the end nodes, subdividing each element at the centreline of the corresponding opening: in particular, while the weight of the reinforced concrete elements (kerbs and beams) is evaluated with reference to the entire length (from node to node), in the case of masonry strips, the weight of only the portion corresponding to the net span of the opening is considered since the end portions are already considered in the evaluation of the self-weight of the adjacent pier elements;
- The loads corresponding to the self-weight of the portion of load-bearing structure at the foot of the building (for a height equal to half of the first inter-storey) are considered to be directly discharged into the foundation and are therefore not considered for the purpose of defining the “seismic” weights;
- The masses, considered concentrated at the upper and lower end nodes of the vertical axis elements, are obtained by dividing the resultant of the load acting at each node (including the contributions transmitted by any reinforced concrete beams) by the value of the acceleration of gravity.

PRO_SAM performs these operations automatically by means of a preliminary analysis of the loaded model.

The building is analysed with reference to both the actual state (unreinforced condition) and the design state (reinforced condition). In this second configuration, the effect of the Resisto 5.9 system on the overall response is considered on the basis of the previous § 6.2.

In the evaluation of the stiffness of masonry and reinforced concrete elements, the effect of section partialization is taken into account by applying a 50% reduction in the geometric properties (moment of inertia and shear area) of the fully reacting sections. In the design state analysis, no variation is introduced in the stiffness of the reinforced masonry elements (bays and strips) with respect to the corresponding unreinforced elements in the configuration corresponding to the actual state.

The deformation limits of the reinforced masonry panels are assigned in the numerical model according to the indications given in § 6.2.1: in Table 6.5 summarises the deformation limits adopted in the analyses for the masonry elements under the two conditions considered.

Table 6.5. Deformation limits adopted for masonry elements in numerical analyses

Wall	**Unreinforced**		**Reinforced**	
DLS	0.2% H		(0.2·1.5)% H	
CPLS – buckling	1.0% H	$\nu \leq 0.2$	1.0% H	$\nu \leq 0.2$
	1.25% (1-ν) H	$\nu > 0.2$	1.25% (1- ν) H	$\nu > 0.2$
CPLS – shear	0.5% H		(0.5·1.5)% H	

Note: H effective height of the element

The formulation of equation [7.8.2] of the NTC 2018 is adopted for the evaluation of the compressive strength of the pier elements of the analysed building in the configuration corresponding to the actual state. The shear strength is instead evaluated as the lower of the strength values resulting from the formulations for creep and diagonal cracking of a regular-bond masonry, given respectively in equation [7.8.3] of NTC 2018 and in [C8.7.1.17] and [C8.7.1.18] of Circular 7/2019. With regard to masonry strips, the compressive strength is evaluated according to equation [7.8.5] of the NTC 2018 while the shear strength is evaluated in analogy to what has been done for pier elements, referring, however, to equation [7.8.4] of the NTC 2018 for creep behaviour. In the analysis of the building in the design state, the increases in strength provided by the reinforcement system illustrated in the previous § 6.2.2 are disregarded; it should be noted that this assumption is in any case to the benefit of safety.

For both pier elements and strips, elastic-perfectly plastic type constitutive bonds are assumed in buckling and shear without work hardening, with deformation limit (Figure 6.4).

6.5.5 Set of analyses

The analyses are conducted with reference to a Group 1 lateral force distribution proportional to the distribution of inertial forces and a Group 2 distribution proportional to the distribution of structural masses (respectively "G1stat" and "G2unif" below). The seismic actions are applied to the building separately in the two main directions, in both positive and negative directions, considering the effects of accidental eccentricity as prescribed by NTC 2018 in § 7.2.6, in the absence of more accurate determinations. Altogether, therefore, 16 different analyses are considered for each configuration (unreinforced and reinforced).

6.5.6 Results of the static non-linear analyses

This section reports the results of the global verifications made on the capacity curves with reference to the entire set of analyses carried out.

Figure 6.12 illustrates the capacity curves of the building in the actual state (in orange) and in the design state (in blue).

Table 6.6 and Table 6.7 summarise the descriptive parameters of the curves (please refer to the previous § 6.3.6 for the symbols used).

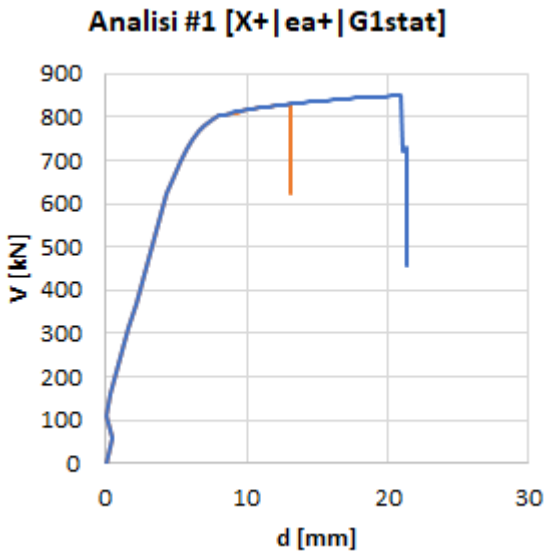

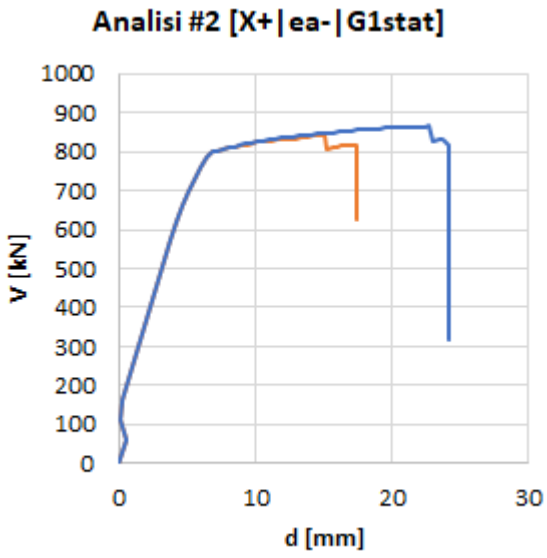

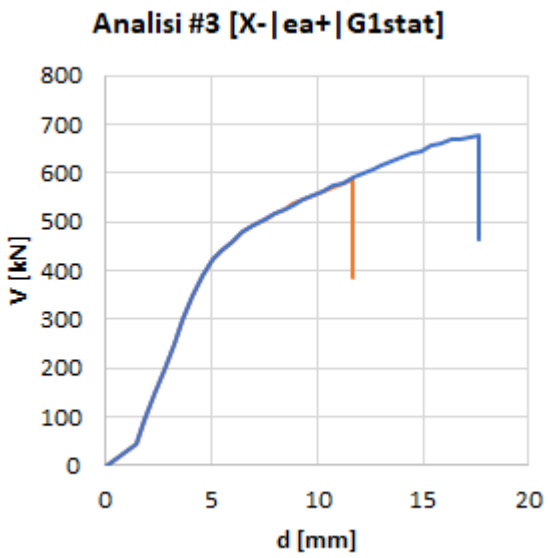

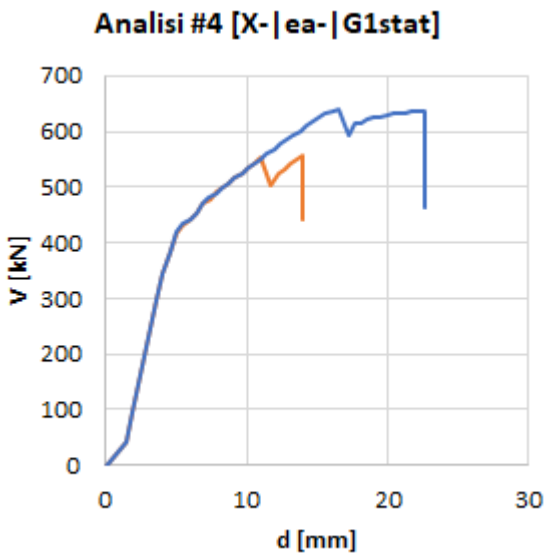

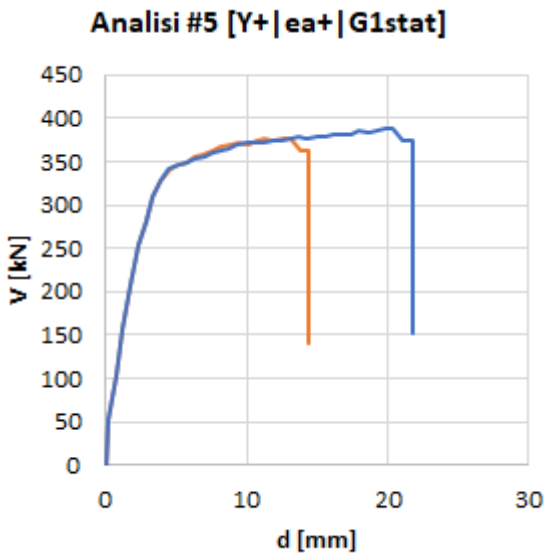

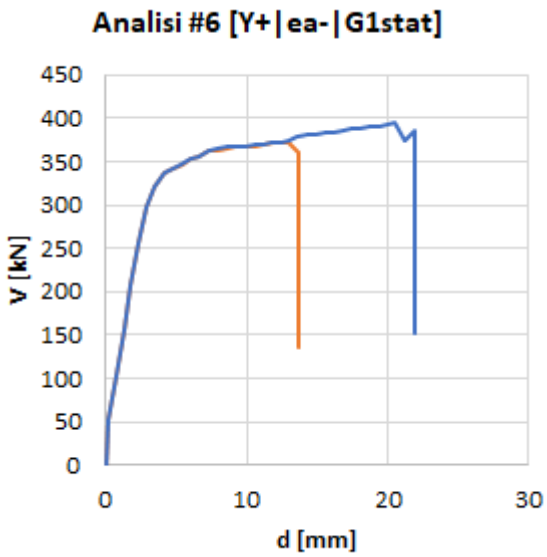

Analisi #7 [Y-|ea+|G1stat]

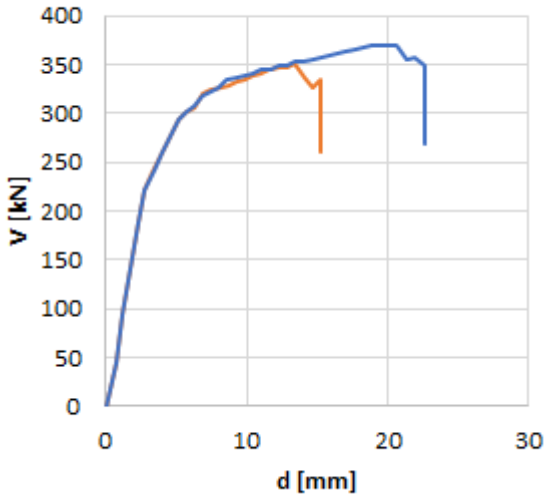

Analisi #8 [Y-|ea-|G1stat]

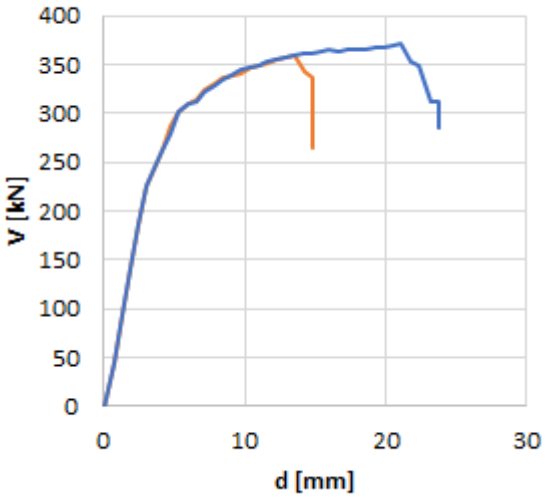

Analisi #9 [X+|ea+|G2unif]

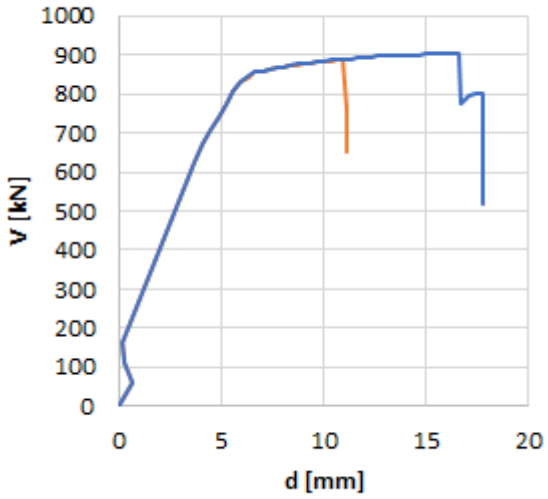

Analisi #10 [X+|ea-|G2unif]

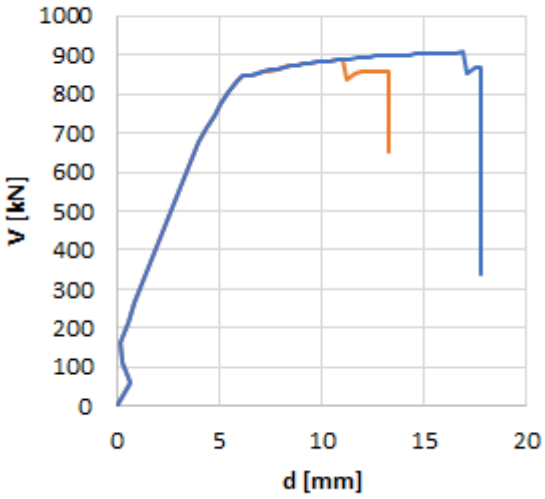

Analisi #11 [X-|ea+|G2unif]

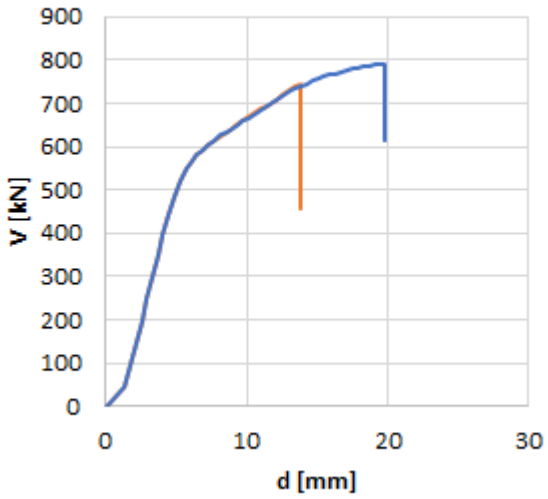

Analisi #12 [X-|ea-|G2unif]

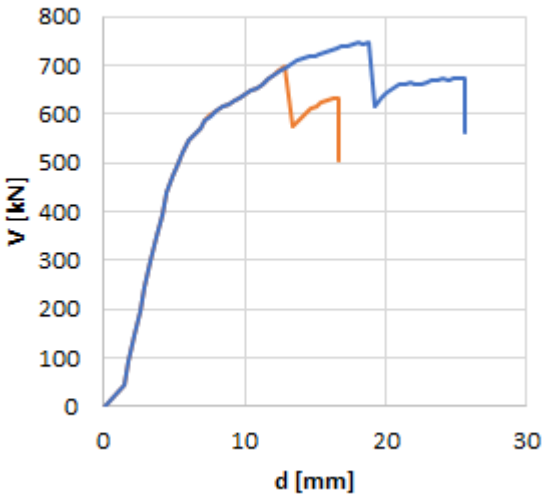

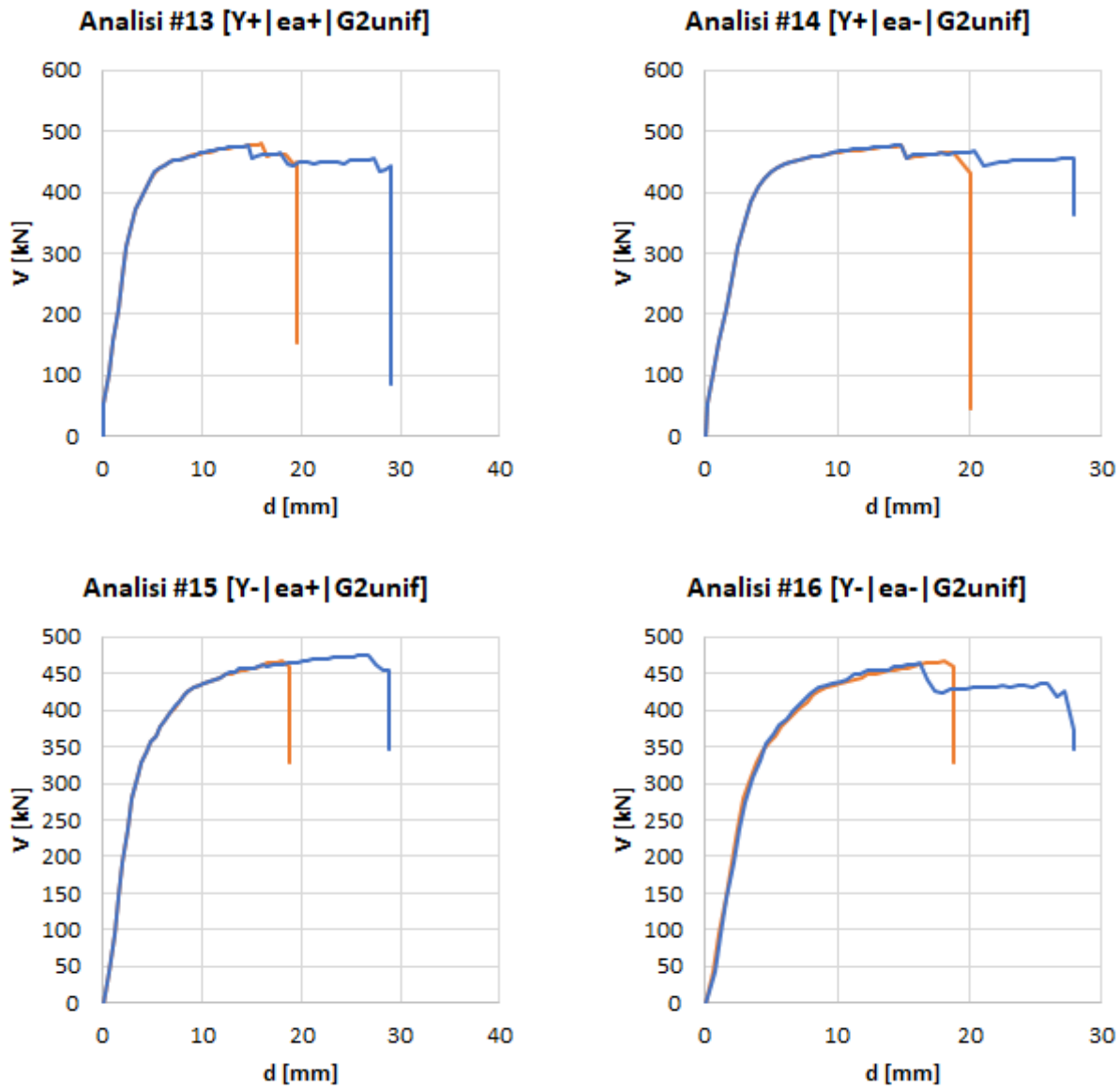

Figure 6.12 Global capacity curves of the building in the actual state (in orange) and design state (in blue).

Table 6.6. Parameters of global capacity curves of the building in the actual state

Analyses	State	Description			m*·g [kN]	K* [kN/m]	T* [sec]	Γ [-]	d_y [mm]	F_y [kN]	d_u [mm]	F_u [kN]	α_u/α_1 [-]
1	ok	X+	ea+	G1stat	1870.3	145300	0.2	1.2	5.7	821.2	13.2	831.1	12.8
2	ok	X+	ea-	G1stat	1870.3	148700	0.2	1.2	5.6	829.7	17.4	843.7	13.0
3	ko	X-	ea+	G1stat	1870.3	84310	0.3	1.2	5.9	501.5	11.7	589.1	12.2
4	ko	X-	ea-	G1stat	1870.3	84380	0.3	1.2	5.8	489.3	14.0	558.6	11.7
5	ok	Y+	ea+	G1stat	1870.3	106900	0.3	1.2	3.4	363.7	14.5	377.0	6.4
6	ko	Y+	ea-	G1stat	1870.3	107700	0.3	1.2	3.4	361.1	13.7	373.1	6.4
7	ko	Y-	ea+	G1stat	1870.3	69840	0.3	1.2	4.7	330.7	15.3	350.5	7.2
8	ko	Y-	ea-	G1stat	1870.3	65730	0.3	1.2	5.2	339.8	14.9	360.3	7.3
9	ok	X+	ea+	G2unif	1870.3	169100	0.2	1.2	5.2	883.9	11.1	889.0	13.4
10	ok	X+	ea-	G2unif	1870.3	174400	0.2	1.2	5.0	875.3	13.3	888.7	13.4
11	ko	X-	ea+	G2unif	1870.3	98310	0.3	1.2	6.5	637.2	13.8	742.5	15.7
12	ok	X-	ea-	G2unif	1870.3	95620	0.3	1.2	6.4	607.2	16.6	700.2	14.9
13	ok	Y+	ea+	G2unif	1870.3	123300	0.2	1.2	3.7	459.3	19.7	480.0	8.1
14	ok	Y+	ea-	G2unif	1870.3	121000	0.2	1.2	3.8	459.8	20.1	477.4	8.1
15	ok	Y-	ea+	G2unif	1870.3	83970	0.3	1.2	5.2	438.0	18.8	466.5	9.6
16	ok	Y-	ea-	G2unif	1870.3	81320	0.3	1.2	5.4	441.1	19.1	464.8	9.5

Table 6.7. Parameters of global capacity curves of the building in the design state

Analyses	State	Description			m*·g [kN]	K* [kN/m]	T* [sec]	Γ [-]	d_y [mm]	F_y [kN]	d_u [mm]	F_u [kN]	α_u/α_1 [-]
1	ok	X+	ea+	G1stat	1870.3	144300	0.2	1.2	5.8	829.9	21.4	851.1	13.1
2	ok	X+	ea-	G1stat	1870.3	147400	0.2	1.2	5.7	846.2	24.1	866.7	13.3
3	ok	X-	ea+	G1stat	1870.3	74650	0.3	1.2	8.1	601.5	17.6	679.3	14.1
4	ok	X-	ea-	G1stat	1870.3	72320	0.3	1.2	8.2	591.1	22.6	640.2	13.4
5	ok	Y+	ea+	G1stat	1870.3	102900	0.3	1.2	3.6	372.6	21.7	388.8	6.6
6	ok	Y+	ea-	G1stat	1870.3	105100	0.3	1.2	3.6	373.8	21.9	394.9	6.7
7	ok	Y-	ea+	G1stat	1870.3	66340	0.3	1.2	5.3	349.8	22.7	370.7	7.6
8	ok	Y-	ea-	G1stat	1870.3	63610	0.3	1.2	5.5	351.3	23.7	371.1	7.5
9	ok	X+	ea+	G2unif	1870.3	168000	0.2	1.2	5.3	884.7	17.7	904.9	13.6
10	ok	X+	ea-	G2unif	1870.3	173300	0.2	1.2	5.1	891.0	17.7	906.7	13.7
11	ok	X-	ea+	G2unif	1870.3	95500	0.3	1.2	7.4	704.7	19.8	792.7	16.7
12	ok	X-	ea-	G2unif	1870.3	92640	0.3	1.2	7.2	667.0	25.6	747.6	15.9
13	ok	Y+	ea+	G2unif	1870.3	123700	0.2	1.2	3.7	454.2	29.0	477.3	8.1
14	ok	Y+	ea-	G2unif	1870.3	120900	0.2	1.2	3.8	459.2	27.9	478.7	8.1
15	ok	Y-	ea+	G2unif	1870.3	81650	0.3	1.2	5.5	452.4	28.8	475.0	9.8
16	ok	Y-	ea-	G2unif	1870.3	81360	0.3	1.2	5.3	432.8	27.9	465.6	9.5

The following Tables summarise the results of the verifications at the different limit states considered (OLS, DLS, LSLS and CPLS) in terms of comparison between demand (subscript D) and capacity (subscript C) values of displacement d, PGA and return period T_R. Furthermore, the values of the ratios between capacity and demand in terms of PGA and T_R ($a_{PGA,SLi}$ and $a_{TR,SLi}$, respectively) are reported; the minimum values over the entire set of analyses are highlighted in yellow, while the verification conditions that were met and not met are identified in green and red.

6.5.6.1 Verification at OLS

As can be seen from the comparison of the data in Table 6.8 and Table 6.9, the building is largely verified at OLS in its actual state ($\zeta_{EG,SLO}$ = $a_{PGA,OLS}$ = 1.697 > 1.000).

Table 6.8. Verifications at OLS in the actual state

Analyses	State	$d_{D,OLS}$ [mm]	$d_{C,OLS}$ [mm]	$PGA_{D,OLS}$ [g]	$PGA_{C,OLS}$ [g]	$a_{PGA,OLS}$ [-]	$TR_{D,OLS}$ [years]	$TR_{C,OLS}$ [years]	$a_{TR,OLS}$ [-]
1	ok	1.76	7.08	0.043	0.160	3.703	30.1	577.9	19.191
2	ok	1.72	6.81	0.043	0.159	3.675	30.1	567.5	18.847
3	ok	3.03	6.49	0.043	0.093	2.144	30.1	167.0	5.545
4	ok	3.03	5.96	0.043	0.087	2.014	30.1	146.6	4.868
5	ok	2.39	6.32	0.043	0.098	2.278	30.1	190.3	6.319
6	ok	2.37	6.65	0.043	0.102	2.372	30.1	207.9	6.903
7	ok	3.66	6.36	0.043	0.074	1.717	30.1	105.3	3.499
8	ok	3.88	6.60	0.043	0.073	1.697	30.1	102.9	3.417
9	ok	1.51	5.57	0.043	0.156	3.600	30.1	539.1	17.904
10	ok	1.46	6.14	0.043	0.167	3.858	30.1	636.8	21.148
11	ok	2.60	7.32	0.043	0.118	2.739	30.1	288.2	9.570
12	ok	2.67	6.81	0.043	0.109	2.522	30.1	238.3	7.915
13	ok	2.07	8.14	0.043	0.136	3.153	30.1	396.0	13.151
14	ok	2.11	8.61	0.043	0.141	3.261	30.1	427.6	14.202
15	ok	3.04	8.13	0.043	0.107	2.469	30.1	227.1	7.544
16	ok	3.14	8.06	0.043	0.104	2.400	30.1	212.9	7.069

Table 6.9. Verifications at OLS in the design state

Analyses	**State**	**$d_{D,OLS}$** [mm]	**$d_{C,OLS}$** [mm]	**$PGA_{D,OLS}$** [g]	**$PGA_{C,OLS}$** [g]	**$a_{PGA,OLS}$** [-]	**$TR_{D,OLS}$** [years]	**$TR_{C,OLS}$** [years]	**$a_{TR,OLS}$** [-]
1	ok	1.77	8.42	0.043	0.180	4.158	30.1	763.5	25.357
2	ok	1.73	7.60	0.043	0.171	3.956	30.1	677.1	22.489
3	ok	3.42	6.99	0.043	0.090	2.092	30.1	158.8	5.275
4	ok	3.53	7.36	0.043	0.092	2.131	30.1	164.9	5.475
5	ok	2.48	6.32	0.043	0.097	2.239	30.1	183.4	6.093
6	ok	2.43	6.61	0.043	0.101	2.342	30.1	201.8	6.703
7	ok	3.85	6.34	0.043	0.072	1.656	30.1	97.5	3.239
8	ok	3.99	6.57	0.043	0.071	1.653	30.1	97.2	3.228
9	ok	1.52	6.65	0.043	0.172	3.981	30.1	686.3	22.793
10	ok	1.47	6.47	0.043	0.173	3.997	30.1	693.2	23.023
11	ok	2.67	8.12	0.043	0.129	2.975	30.1	347.0	11.524
12	ok	2.76	8.00	0.043	0.123	2.839	30.1	311.9	10.360
13	ok	2.06	8.70	0.043	0.144	3.322	30.1	446.1	14.815
14	ok	2.11	8.64	0.043	0.141	3.267	30.1	429.3	14.257
15	ok	3.13	8.15	0.043	0.105	2.439	30.1	221.4	7.352
16	ok	3.14	8.57	0.043	0.109	2.517	30.1	237.7	7,896

6.5.6.2 Verification at DLS

As can be seen from the comparison of the data in Table 6.10 and Table 6.11, the building is largely verified at DLS in its actual state ($\zeta_{EG,SLD}$ = $a_{PGA,DLS}$ = 1.844 > 1.000).

Table 6.10. Verifications at DLS in the actual state

Analyses	State	$d_{D,DLS}$ [mm]	$d_{C,DLS}$ [mm]	$PGA_{D,DLS}$ [g]	$PGA_{C,DLS}$ [g]	$a_{PGA,DLS}$ [-]	$TR_{D,DLS}$ [years]	$TR_{C,DLS}$ [years]	$a_{TR,DLS}$ [-]
1	ok	2.12	9.62	0.052	0.198	3.769	50.3	958.8	19.066
2	ok	2.07	10.10	0.052	0.208	3.970	50.3	1095.8	21.789
3	ok	3.65	7.48	0.052	0.102	1.952	50.3	207.3	4.122
4	ok	3.65	7.83	0.052	0.106	2.018	50.3	223.1	4.436
5	ok	2.88	8.82	0.052	0.129	2.451	50.3	347.0	6.900
6	ok	2.86	9.19	0.052	0.133	2.542	50.3	378.0	7.516
7	ok	4.41	9.30	0.052	0.102	1.945	50.3	205.6	4.089
8	ok	4.68	9.12	0.052	0.097	1.844	50.3	183.4	3.648
9	ok	1.82	7.64	0.052	0.188	3.590	50.3	854.6	16.994
10	ok	1.77	8.42	0.052	0.204	3.881	50.3	1033.9	20.559
11	ok	3.13	9.36	0.052	0.142	2.707	50.3	435.1	8.652
12	ok	3.22	8.83	0.052	0.132	2.517	50.3	369.5	7.348
13	ok	2.50	11.64	0.052	0.183	3.494	50.3	800.7	15.923
14	ok	2.55	12.23	0.052	0.189	3.611	50.3	865.1	17.203
15	ok	3.67	11.26	0.052	0.140	2.670	50.3	422.7	8.404
16	ok	3.79	11.22	0.052	0.137	2.613	50.3	401.6	7.985

Table 6.11. Verifications at DLS in the design state

Analyses	**State**	**$d_{D,DLS}$** [mm]	**$d_{C,DLS}$** [mm]	**$PGA_{D,DLS}$** [g]	**$PGA_{C,DLS}$** [g]	**$a_{PGA,DLS}$** [-]	**$TR_{D,DLS}$** [years]	**$TR_{C,DLS}$** [years]	**$a_{TR,DLS}$** [-]
1	ok	2.13	11.19	0.052	0.221	4.217	50.3	1278.6	25.425
2	ok	2.09	10.98	0.052	0.222	4.238	50.3	1292.9	25.708
3	ok	4.12	8.89	0.052	0.111	2.117	50.3	249.2	4.956
4	ok	4.26	9.67	0.052	0.116	2.208	50.3	273.7	5.443
5	ok	2.99	8.72	0.052	0.125	2.380	50.3	325.3	6.468
6	ok	2.93	9.21	0.052	0.132	2.524	50.3	371.0	7.378
7	ok	4.64	9.23	0.052	0.099	1.881	50.3	190.8	3.793
8	ok	4.84	9.07	0.052	0.094	1.801	50.3	173.9	3.459
9	ok	1.83	8.97	0.052	0.209	3.993	50.3	1110.4	22.079
10	ok	1.78	8.75	0.052	0.210	4.002	50.3	1116.9	22.209
11	ok	3.22	11.42	0.052	0.167	3.183	50.3	639.0	12.706
12	ok	3.32	11.27	0.052	0.160	3.050	50.3	577.9	11.490
13	ok	2.49	12.13	0.052	0.190	3.622	50.3	873.1	17.361
14	ok	2.55	12.23	0.052	0.189	3.606	50.3	862.5	17.151
15	ok	3.77	11.25	0.052	0.138	2.634	50.3	408.8	8.129
16	ok	3.78	11.76	0.052	0.142	2.716	50.3	438.5	8.719

6.5.6.3 LSLS verification

As can be seen from the comparison of the data in Table 6.12 and Table 6.13, the building is largely verified at LSLS in its actual state ($\zeta_{EG,SLV}$ = $a_{PGA,LSLS}$ = 0.787 < 1.000). The reinforcement intervention appreciably improves the performance of the building, which in the design state is verified ($\zeta_{EG,SLV}$ = $a_{PGA,LSLS}$ = 1.052); in particular, the overall performance at LSLS allows for a seismic improvement greater than 30%.

Table 6.12. Verifications at LSLS in the actual state

Analyses	State	$d_{D,LSLS}$ [mm]	$d_{C,LSLS}$ [mm]	$PGA_{D,LSLS}$ [g]	$PGA_{C,LSLS}$ [g]	$a_{PGA,LSLS}$ [-]	$TR_{D,LSLS}$ [years]	$TR_{C,LSLS}$ [years]	$a_{TR,LSLS}$ [-]
1	ok	6.22	9.89	0.147	0.202	1.369	474.6	1009.2	2.127
2	ok	6.04	13.07	0.147	0.254	1.721	474.6	1868.7	3.938
3	ko	11.67	8.74	0.147	0.116	0.787	474.6	275.0	0.580
4	ko	11.71	10.53	0.147	0.135	0.914	474.6	386.5	0.814
5	ok	10.39	10.84	0.147	0.153	1.039	474.6	520.3	1.096
6	ko	10.35	10.29	0.147	0.147	0.996	474.6	469.3	0.989
7	ko	13.94	11.46	0.147	0.123	0.836	474.6	315.4	0.665
8	ko	14.50	11.17	0.147	0.116	0.787	474.6	274.4	0.578
9	ok	5.14	8.32	0.147	0.199	1.351	474.6	977.3	2.059
10	ok	4.99	9.97	0.147	0.229	1.556	474.6	1402.7	2.956
11	ok	9.83	10.38	0.147	0.154	1.046	474.6	527.2	1.111
12	ok	10.18	12.47	0.147	0.175	1.186	474.6	714.2	1.505
13	ok	9.00	14.74	0.147	0.225	1.530	474.6	1343.4	2.831
14	ok	9.12	15.07	0.147	0.228	1.546	474.6	1376.6	2.901
15	ok	11.94	14.13	0.147	0.172	1.167	474.6	686.3	1.446
16	ok	12.21	14.36	0.147	0.171	1.160	474.6	678.3	1.429

Table 6.13. Verifications at LSLS in the design state

Analyses	**State**	**$d_{D,LSLS}$** [mm]	**$d_{C,LSLS}$** [mm]	**$PGA_{D,LSLS}$** [g]	**$PGA_{C,LSLS}$** [g]	**$a_{PGA,LSLS}$** [-]	**$TR_{D,LSLS}$** [years]	**$TR_{C,LSLS}$** [years]	**$a_{TR,LSLS}$** [-]
1	ok	6.22	16.06	0.147	0.278	1.884	474.6	2475.0	5.215
2	ok	6.01	18.11	0.147	0.278	1.884	474.6	2475.0	5.215
3	ok	12.49	13.22	0.147	0.155	1.052	474.6	536.1	1.130
4	ok	12.85	16.92	0.147	0.190	1.288	474.6	871.7	1.837
5	ok	10.62	16.29	0.147	0.218	1.476	474.6	1224.4	2.580
6	ok	10.46	16.39	0.147	0.222	1.505	474.6	1287.5	2.713
7	ok	14.39	17.01	0.147	0.174	1.178	474.6	702.5	1.480
8	ok	14.80	17.80	0.147	0.177	1.200	474.6	733.2	1.545
9	ok	5.17	13.30	0.147	0.278	1.884	474.6	2475.0	5.215
10	ok	5.02	13.31	0.147	0.278	1.884	474.6	2475.0	5.215
11	ok	9.79	14.87	0.147	0.208	1.414	474.6	1099.0	2.316
12	ok	10.20	19.20	0.147	0.254	1.723	474.6	1877.6	3.957
13	ok	9.00	21.74	0.147	0.278	1.884	474.6	2475.0	5.215
14	ok	9.13	20.96	0.147	0.278	1.884	474.6	2475.0	5.215
15	ok	12.13	21.57	0.147	0.251	1.704	474.6	1813.3	3.821
16	ok	12.23	20.94	0.147	0.243	1.649	474.6	1640.9	3.458

6.5.6.4 Verification at CPLS

As can be seen from the comparison of the data in Table 6.14 and Table 6.15, the building is largely verified at CPLS in its actual state ($\zeta_{EG,SLC}$ = $a_{PGA,CPLS}$ = 0.739 < 1.000). The reinforcement intervention appreciably improves the performance of the building, which in the design state is verified ($\zeta_{EG,SLC}$ = $a_{PGA,CPLS}$ = 1.014); in particular, the overall performance at CPLS allows for a seismic improvement greater than 35%.

Table 6.14. Verifications at CPLS in the actual state

Analyses	State	$d_{D,CPLS}$ [mm]	$d_{C,CPLS}$ [mm]	$PGA_{D,CPLS}$ [g]	$PGA_{C,CPLS}$ [g]	$a_{PGA,CPLS}$ [-]	$TR_{D,CPLS}$ [years]	$TR_{C,CPLS}$ [years]	$a_{TR,CPLS}$ [-]
1	ok	9.71	13.19	0.199	0.251	1.263	974.8	1817.7	1.865
2	ok	9.49	17.42	0.199	0.278	1.396	974.8	2475.0	2.539
3	ko	16.25	11.66	0.199	0.147	0.739	974.8	472.8	0.485
4	ko	16.29	14.03	0.199	0.173	0.872	974.8	701.4	0.719
5	ok	14.46	14.46	0.199	0.199	1.001	974.8	975.8	1.001
6	ko	14.40	13.72	0.199	0.190	0.956	974.8	875.7	0.898
7	ko	18.98	15.29	0.199	0.161	0.810	974.8	587.3	0.602
8	ko	19.69	14.89	0.199	0.151	0.761	974.8	504.8	0.518
9	ok	8.30	11.09	0.199	0.244	1.229	974.8	1670.0	1.713
10	ok	8.14	13.29	0.199	0.278	1.396	974.8	2475.0	2.539
11	ko	14.07	13.84	0.199	0.196	0.986	974.8	942.1	0.967
12	ok	14.48	16.63	0.199	0.225	1.130	974.8	1334.3	1.369
13	ok	12.79	19.66	0.199	0.278	1.396	974.8	2475.0	2.539
14	ok	12.94	20.09	0.199	0.278	1.396	974.8	2475.0	2.539
15	ok	16.53	18.83	0.199	0.225	1.129	974.8	1330.7	1.365
16	ok	16.87	19.14	0.199	0.224	1.125	974.8	1318.0	1.352

Table 6.15. Verifications at CPLS in the design state

Analyses	State	$d_{D,DLS}$ [mm]	$d_{C,CPLS}$ [mm]	$PGA_{D,CPLS}$ [g]	$PGA_{C,CPLS}$ [g]	$a_{PGA,CPLS}$ [-]	$TR_{D,CPLS}$ [years]	$TR_{C,CPLS}$ [years]	$a_{TR,CPLS}$ [-]
1	ok	9.72	21.42	0.199	0.278	1.396	974.8	2475.0	2.539
2	ok	9.47	24.14	0.199	0.278	1.396	974.8	2475.0	2.539
3	ok	17.35	17.62	0.199	0.202	1.014	974.8	1009.2	1.035
4	ok	17.79	22.56	0.199	0.249	1.250	974.8	1761.2	1.807
5	ok	14.77	21.72	0.199	0.278	1.396	974.8	2475.0	2.539
6	ok	14.57	21.85	0.199	0.278	1.396	974.8	2475.0	2.539
7	ok	19.55	22.68	0.199	0.230	1.155	974.8	1410.2	1.447
8	ok	20.08	23.74	0.199	0.234	1.174	974.8	1469.3	1.507
9	ok	8.34	17.74	0.199	0.278	1.396	974.8	2475.0	2.539
10	ok	8.10	17.74	0.199	0.278	1.396	974.8	2475.0	2.539
11	ok	14.09	19.83	0.199	0.268	1.349	974.8	2227.2	2.285
12	ok	14.57	25.60	0.199	0.278	1.396	974.8	2475.0	2.539
13	ok	12.79	28.99	0.199	0.278	1.396	974.8	2475.0	2.539
14	ok	12.95	27.95	0.199	0.278	1.396	974.8	2475.0	2.539
15	ok	16.79	28.76	0.199	0.278	1.396	974.8	2475.0	2.539
16	ok	16.90	27.92	0.199	0.278	1.396	974.8	2475.0	2.539

As an example, a comparison of the verifications at the different limit states on the capacity curves for one of the critical analyses for the building in the actual state is shown in Figure 6.13. In particular, analysis #8 was considered, associated with the lowest safety index at LSLS (Table 6.12). The global response of the building in the actual state is shown in orange while that in the design state is in blue; the displacement capacities at the different limit states are represented with dots of corresponding colour on the curves and the corresponding displacement demands are indicated with vertical black lines of different hatching.

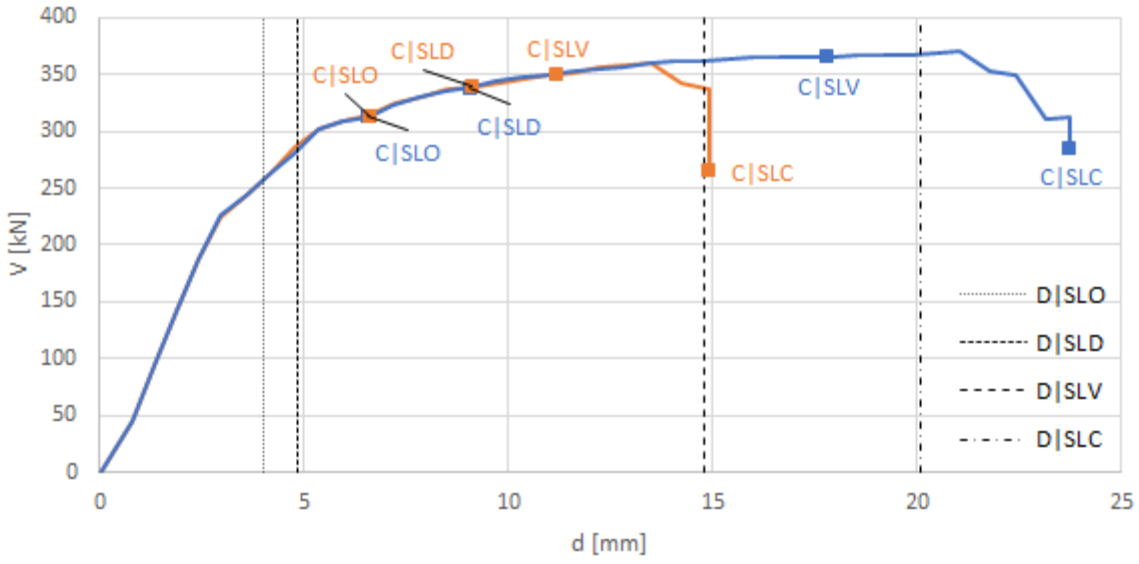

Figure 6.13 Example of safety checks on the capacity curves of the building in the actual state (in orange) and design state (in blue): analysis #8 [Y-|ea-|G1stat].

It can be observed that, in each of the analyses carried out, the activation of the OLS and DLS affects both the pier elements of the internal walls (stairwell) and of the perimeter walls in the actual state of the building, while the limit deformation in the design state is reached only by the internal, unreinforced walls. The differences in the overall displacement levels corresponding to the activation of each limit state in the elements of the two configurations relates to the irregularity in plan of the building and to the accidental eccentricity considered in the application of the seismic action. As an example, again with reference to the critical analysis considered above (analysis #8), Figure 6.14 and Figure 6.15 illustrate the different distribution of masonry elements that reached the limit deformation at the two limit states.

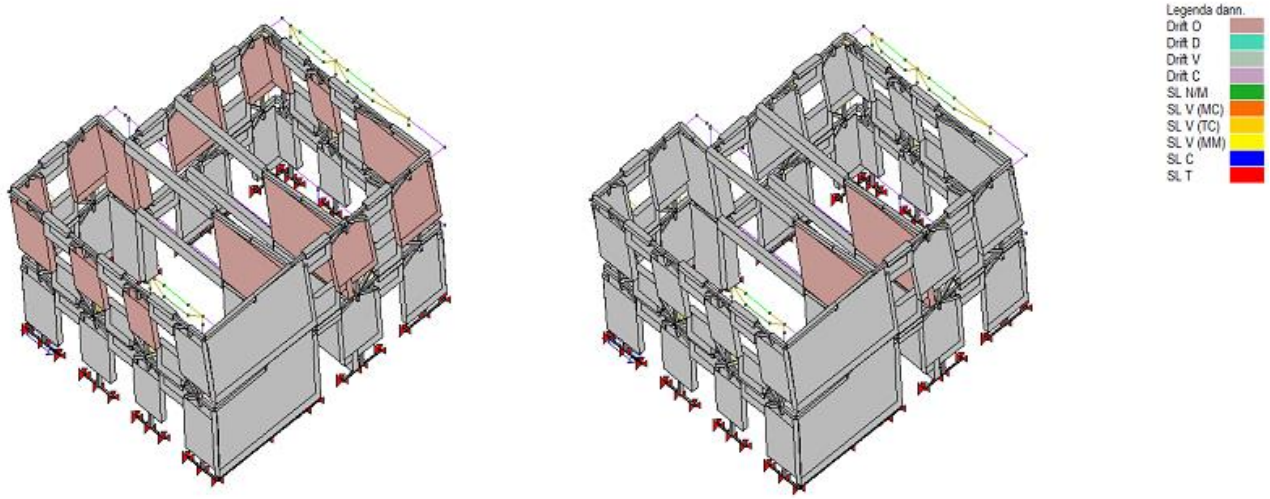

Figure 6.14 Reaching of the OLS in the pier elements of the building in the actual state (left) and in the design state (right): analysis #8 [Y-|ea-|G1stat].

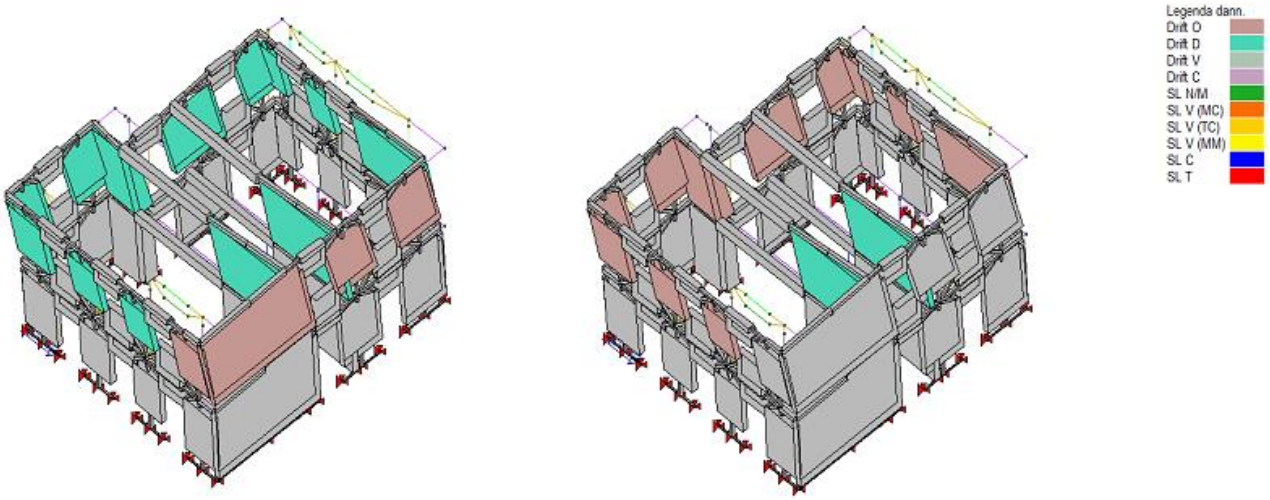

Figure 6.15 Reaching of the DLS in the pier elements of the building in the actual state (left) and in the design state (right): analysis #8 [Y-|ea-|G1stat].

In conclusion, as can be seen from the data reported in the previous Tables, the building, which was not verified at LSLS and CPLS in its actual state, is instead verified in its design state following reinforcement intervention using the Resisto 5.9 system, on the basis of the assumptions made regarding the increase in performance of the reinforced walls offered by it with respect to non-reinforced walls (§ 6.2).

BIBLIOGRAPHICAL REFERENCES

2Si. Pro_SAM (PRO_SAP, release 21.9.4). https://www.2si.it/it/pro_sam/ (https://www.2si.it/it/pro_sap/).

AMV - MasterSAP. https://www.amv.it/prodotti/mastersap/opere-muratura.

CSI. 3D-Macro. https://www.csi-italia.eu/software/3d-macro-2/.

Beolchini G. C., Milano L., Antonacci E., 2007. Modelli cinematici per l'analisi strutturale degli edifici in muratura, In: AA.VV., Regione Marche - Repertorio dei meccanismi di danno, delle tecniche d'intervento e dei relativi costi negli edifici in muratura. Sisma Marche 1997.

Circolare 21/01/2019 n.7 del Ministero delle Infrastrutture e dei Trasporti, 2019. Istruzioni per l'applicazione dell'aggiornamento delle "Norme tecniche per le costruzioni" (Circolare 7/2019), Gazzetta Ufficiale n.35 del 11/02/2019, Supplemento ordinario n.5.

Concrete. Sismicad Muratura. https://www.concrete.it/prodotti/sismicad/sismicad-muratura/.

D.M. 17/01/2018: Norme Tecniche per le Costruzioni (NTC 2018), Gazzetta Ufficiale, n. 42 del 20/02/2018 - Supplemento ordinario n.8.

Damiani N., Albanesi L., Manzini C.F., Magenes G., Morandi P., 2022. Studio del comportamento sismico di murature portanti rinforzate con rivestimento esterno modulare in acciaio - Rapporto numerico. Rapporto EUCENTRE, Pavia.

Dolce M., (1991). Schematizzazione e modellazione degli edifici in muratura soggetti ad azioni sismiche. L'industria delle Costruzioni. 25(242):44–57

EOTA, 2014. EAD 330076-00-0604: Metal injection anchors for use in masonry.

EOTA, 2016a. TR 053: Recommendations for job site tests of metal injection anchors in masonry.

EOTA, 2016b. TR 054: Design method for anchorages with metal injection anchors for use in masonry.

Manzini C.F., Albanesi L., Morandi P., 2021. Risposta sismica nel piano di murature portanti rinforzate con rivestimento esterno modulare in acciaio. Progettazione Sismica – Vol. 13, N.4:3-23, Anno 2021. DOI 10.7414/PS.13.1.4-https://doi.org/10.7414/PS.13.1.4

Manzini C.F., Albanesi L., Morandi P., 2022. Studio del comportamento sismico di murature portanti rinforzate con rivestimento esterno modulare in acciaio – Rapporto sperimentale. Rapporto EUCENTRE, Pavia.

Manzini, C.F., Morandi, P., Magenes, 2019. SAM-II: sviluppi del codice di calcolo a telaio equivalente per l'analisi sismica di edifici in muratura, Costruire in laterizio, vol. 180, p. 54-64, ISSN: 0394-1599

STADATA. 3Muri. www.3muri.com.

APPENDIX A. EVALUATION OF THE STRENGTH OF THE RESISTO 5.9 REINFORCEMENT SYSTEM

Below are the calculations for the strength assessment of the Resisto 5.9 reinforcement system to be used for the verification of local mechanisms according to the methods described in § 5.2. In particular, reference is made to the strength formulations in § 4.2.4 of NTC 2008, with the additions and modifications provided by Circular 7/2019 in § 4.2.12 for cold-formed profiles.

Figure A.1 shows the geometry of a standard-sized element of the modular reinforcement system. The dimensions (base and height) of the frame can vary, to be adapted to the geometry of the wall, while the position in relation to the outer edges of the frame of the holes for connecting the modules and for anchoring them to the masonry is fixed (see Figure A.2).

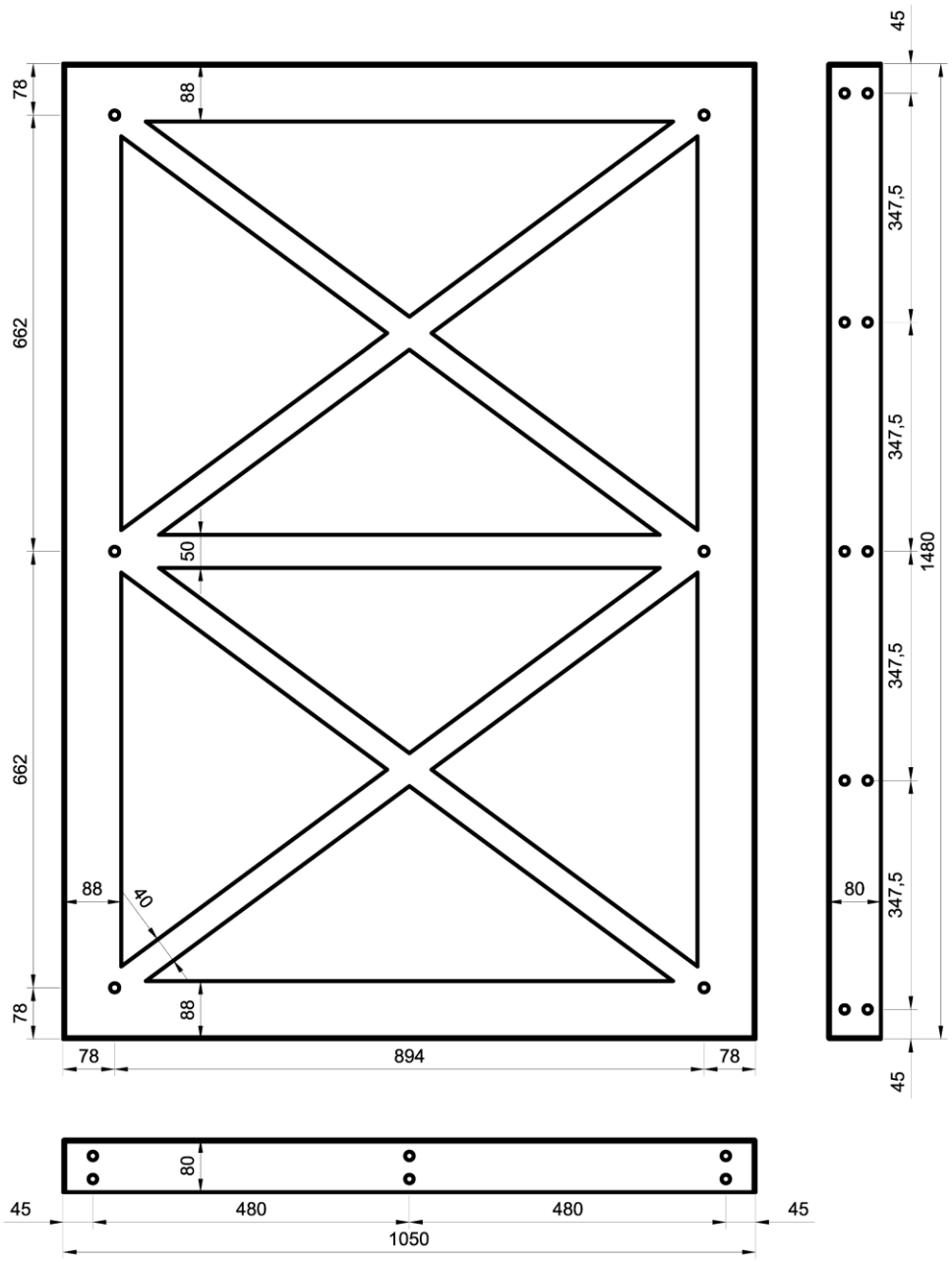

Figure A.1 Geometry of a modular element of the Resisto 5.9 reinforcement system.

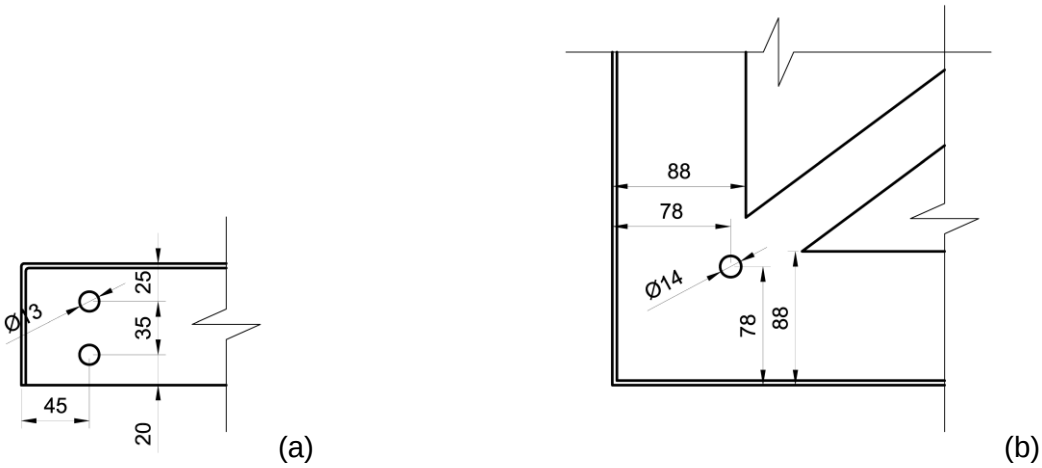

Figure A.2 Geometry of the holes in the frame elements for connecting the modular frames (a) and for anchoring to the masonry (b).

A.1. Maximum horizontal force that can be withstood by the connection between the orthogonal frames of the Resisto 5.9 system

The connection between the reinforcement frames of the perimeter walls of the building is realised by means of a system of metal plates connected by bolted joints, according to the detail illustrated in Figure A.3. For calculation purposes, it is assumed that the connection between the modular frame and the type 1 plate works predominantly in tensile and the connection between the type 1 and type 2 plates works predominantly in shear in the horizontal direction.

The plates in class 8.8 steel are 3 mm thick and 60 mm high and have holes with a diameter of 13 mm, according to the pattern of Figure A.4. Connections are made by means of class 8.8 M12/25 mm bolts and class 8M12 nuts and washers.

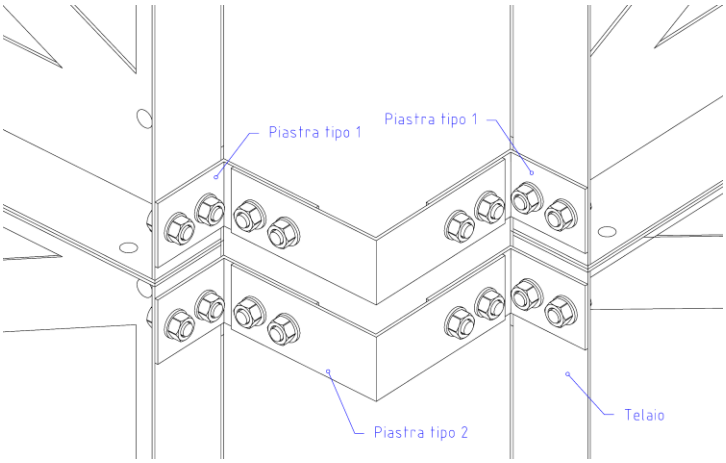

Figure A.3 Detail of the metal frame connection system.

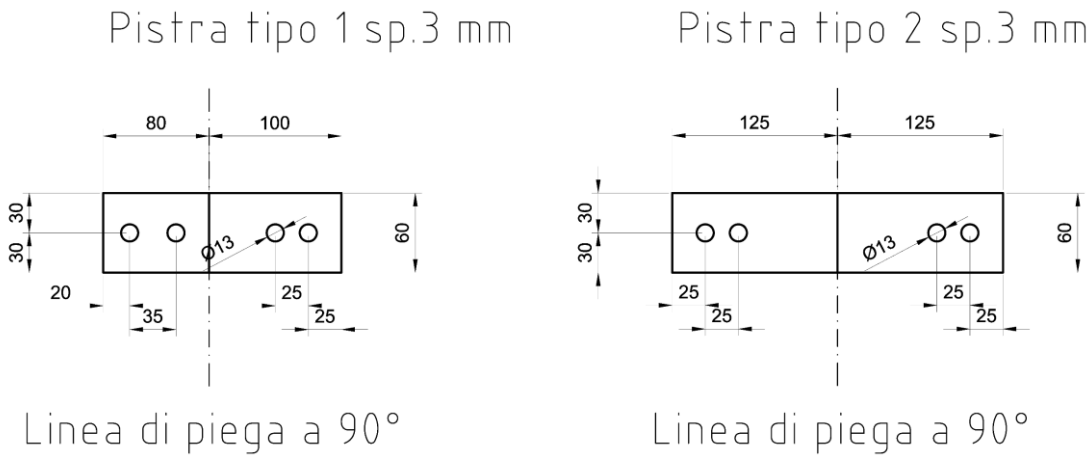

Figure A.4 Geometry of the plates of the metal frame connection system.

The maximum horizontal force $F_{c,Rd}$ that can be withstood by the connection can be evaluated as the minimum between:

- the tensile strength $\overline{F_{t,Rd}}$ of the bolted connection between the frame of the modular frame and the type 1 plate:

$$\overline{F_{t,Rd}} = n_b F_{t,Rd} = n_b \frac{0.9 f_{tbk} A_{res}}{\gamma_{M2}} \quad \text{(A.1)}$$

with $F_{t,Rd}$ evaluated, in accordance with § C4.2.12.1.7.4.2 of Circular 7/2019, using the expression [4.2.68] of NTC 2018, with n_b number of bolts constituting the connection, f_{tbk} characteristic breaking strength of the bolt, A_{res} resistant area of the bolt and γ_{M2} = 1.25 safety coefficient for verification of strength of bolts and contact plates;

- the puncture strength of the plate $\overline{B_{p,Rd}}$:

$$\overline{B_{p,Rd}} = n_b B_{p,Rd} = n_b \frac{0.6 \pi d_m t_p f_{tk}}{\gamma_{M2}} \quad \text{(A.2)}$$

with $B_{p,Rd}$ evaluated using the expression [4.2.70] of NTC 2018 with d_m minimum between nut diameter and average bolt head diameter, t_p plate thickness, f_{tk} plate steel breaking stress;

- the tensile strength $N_{t,Rd}$ of the gross plate cross-section A, evaluated by the expression [C4.2.113] of Circular 7/2019:

$$N_{t,Rd} = \frac{A f_{ymk}}{\gamma_{M0}} \quad \text{(A.3)}$$

with f_{ymk} average characteristic yield strength after forming of the steel of the plates (which can be evaluated using the expression [C4.2.101] but cautiously assumed in the calculation to be equal to the characteristic yield strength f_{yk}) and γ_{M0} = 1.05;

- the tensile strength $F_{n,Rd}$ of the net cross-section A_{net} at the connection holes, evaluated using the expression [C4.2.151] of Circular 7/2019:

$$F_{n,Rd} = \frac{\beta f_{tk} A_{net}}{\gamma_{M2}} \quad \text{(A.4)}$$

with f_{tk} characteristic breaking strength of plate steel and β coefficient defined by the expression [C4.2.152]:

$$\beta = 1 + 3r\left(\frac{d_0}{u} - 0.3\right) \leq 1 \quad \text{(A.5)}$$

with r ratio between the number of bolts in the net cross-section and the total number of bolts used for the connection, d_0 nominal diameter of the bolt hole and $u = min\{2e_2; p_2\}$, with $e_2$and p_2 descriptive parameters of the connection geometry, shown in Figure A.5;

- the tensile strength $\overline{F_{v,Rd}}$ of the bolted connection between the type 1 and type 2 plates:

$$\overline{F_{v,Rd}} = n_b F_{v,Rd} = n_b \frac{0.6 f_{tbk} A_{res}}{\gamma_{M2}} \quad \text{(A.6)}$$

with $F_{v,Rd}$ evaluated, for class 8.8 bolts, using the expression [4.2.63] of NTC 2018;

- the bearing strength $\overline{F_{b,Rd}}$ of the plates:

$$\overline{F_{b,Rd}} = n_b F_{b,Rd} = n_b \frac{2.5 \alpha_b k_t f_{tk} dt}{\gamma_{M2}} \quad \text{(A.7)}$$

with $F_{b,Rd}$ evaluated using the expression [C4.2.148] of Circular 7/2019, with d nominal diameter of the bolt, t thickness of the connected plate and α_b and k_t coefficients that depend on the geometry of the connection, defined by the expressions [C4.2.149] and [C4.2.150] respectively:

$$\alpha_b = min\left\{\frac{e_1}{3d}\ ;\ 1\right\} \quad \text{(A.8)}$$

with e_1 geometric parameter illustrated in Figure A.5;

$$k_t = \frac{0.8t + 1.5}{2.5} \quad \text{for } t \leq 1.25 \text{ mm}$$
$$k_t = 1.0 \quad \text{for } t > 1.25 \text{ mm} \quad \text{(A.9)}$$

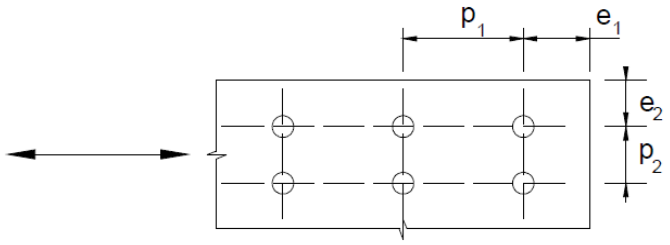

Figure A.5 Descriptive parameters of bolted connection geometry (from NTC 2018).

Noting the geometry of the metal elements of the connection, the details of the bolted joints and the strength classes of the materials, Table A.1 summarises the values of the different strength contributions considered. The minimum value corresponds to the maximum horizontal force the connection can withstand, $F_{c,Rd}$ = 32.4 kN.

In the evaluation of the activation multiplier α_0 of the kinematic mechanisms associated with the local mechanisms of simple overturning and vertical bending of walls reinforced with the Resisto 5.9 system (as described in § 5.2.1.2 and in § 5.2.3.2), a force $F_{roj} = F_{c,Rd}$ can therefore be assumed at each bracing wall connected to the wall under examination and at each horizontal reinforcement level.

Table A.1 Maximum force (in kN) that can be withstood by the connection between the orthogonal frames of the Resisto 5.9 system

$\overline{F_{t,Rd}}$	$\overline{B_{p,Rd}}$	$N_{t,Rd}$	$F_{n,Rd}$	$\overline{F_{v,Rd}}$	$\overline{F_{b,Rd}}$
97.1	32.4	46.3	32.6	64.7	33.0

A.2. Maximum force that can be withstood by the vertical members of the Resisto 5.9 system

When evaluating the activation multiplier α_0 of the kinematic collapse mechanism associated with the local vertical bending mechanism of a masonry wall reinforced with the Resisto 5.9 system (as described in § 5.2.3.2), a vertical force F_{rvj} acting in the metal elements of each of the vertical reinforcement positions arranged along the horizontal development of the wall must be taken into account. The value of this is assumed to be equal to the maximum tensile force that can be borne by the system, according to its characteristics, and which is therefore evaluated as the lower of:

- the tensile strength $\overline{F_{t,Rd}}$ of the bolted connection between the frame modules, defined by the above expression (A.1);
- the puncture strength $\overline{B_{p,Rd}}$ of connected plates, defined by the above expression (A.2);
- the tensile strength $N_{t,Rd}$ of the gross cross-section A of the profiles, defined by the above expression (A.3);
- the tensile strength $F_{n,Rd}$ of the net cross-section A_{net} of the profiles at the cross-section weakened by the connection holes, defined by the above expression (A.4).
- The strength in the vertical direction of the anchoring system between the reinforcement and masonry $\overline{V_{a,Rd}}$.

The maximum force that can be withstood by each anchoring is assumed to be the lesser of:

- The shear strength of the anchoring $V_{a,Rd}$ (to be determined by appropriate in situ tests or from the epoxy resin manufacturer's data sheets);
- the bearing strength $F_{b,Rd}$ of the member at the cross-section weakened by the anchoring hole, defined according to the above expression (A.7).

The strength in the vertical direction of the anchoring system between the reinforcement and masonry $\overline{V_{a,Rd}}$ is therefore determined by multiplying the strength of the single anchor by the smallest number $n_{a,min}$ of those present in the two rigid bodies into which the portion of wall involved in the kinematics is divided by the plastic hinge C. Unlike the previous contributions, the value of $\overline{V_{a,Rd}}$ therefore changes as the geometry of the rigid bodies participating in the kinematic motion changes due to the shift in the position of the plastic hinge C along the height of the portion of the wall considered.

In the case of experimental evaluation, the design value of the shear strength of anchorages must be determined from the characteristic value by adopting a material safety factor γ_M which can be defined, for example, according to § 2.2 of technical report EOTA TR-054 (EOTA 2016b). In particular, in the event of breakage of a steel bar:

$$\gamma_{Ms} = \frac{1.2}{f_{yk}/f_{uk}} \geq 1.4 \qquad \text{(A.10)}$$

(for anchoring by means of pieces of class 8.8 steel bars is, in particular $\gamma_{Ms} = 1.5$), while, in the event of anchor breakage:

$$\gamma_{Mm} = 2.5 \qquad \text{(A.11)}$$

Considering that, as illustrated in Figure A.2(b), the holes for housing the anchoring bars for connection of the metal frames to the masonry are located at the node areas, at the intersection of the vertical elements of the frame with the horizontal elements (L and flat profiles), it is considered insignificant to also take into account the tensile strength $F_{n,Rd}$ of the net cross-section, defined according to the above (A.4), when assessing the maximum force that each anchoring can withstand.

Noting the geometry of the cross-section of the vertical elements of the modular frame, the details of the bolted joints and the strength classes of the materials, the values of the various strength contributions considered are summarised in the following Table A.2; the lesser of these (also taking into account $\overline{V_{a,Rd}}$ which, as mentioned above, cannot be assessed a priori but is linked to the

properties of the anchorage and the geometry of the kinematic chain considered in the kinematic evaluation) can be taken in the calculation as the reference value of F_{rvj}..

Table A.2 Maximum force (in kN) that can be withstood by the vertical members of the Resisto 5.9 system

$\overline{F_{t,Rd}}$	$\overline{B_{p,Rd}}$	$N_{t,Rd}$	$F_{n,Rd}$	$\overline{V_{a,Rd}}$	
				$V_{a,Rd}$	$F_{b,Rd}$
97.1	32.4	117.9	110.1	*, **	27.7 **

Notes: * contribution to be assessed on a case-by-case basis; ** contribution to be multiplied by $n_{a,min}$ as the kinematic chain geometry varies

A.3. Maximum force that can be withstood by the horizontal members of the Resisto 5.9 system

When evaluating the activation multiplier α_0 of the kinematic collapse mechanism associated with the local vertical bending mechanism of a masonry wall reinforced with the Resisto 5.9 system (as described in § 5.2.4.2), a horizontal force F_{roj} acting in the metal elements of each of the continuous horizontal reinforcement levels (thus excluding those interrupted by the presence of any openings from the calculation) arranged in the wall, the value of which is assumed to be equal to the maximum tensile force that can be borne by the system, according to its characteristics, and which is therefore evaluated as the lower of:

- the tensile strength $\overline{F_{t,Rd}}$ of the bolted connection between the frame modules, defined by the above expression (A.1);
- the puncture strength $\overline{B_{p,Rd}}$ of connected plates, defined by the above expression (A.2);
- the tensile strength $N_{t,Rd}$ of the gross cross-section A of the profiles, defined by the above expression (A.3);
- the tensile strength $F_{n,Rd}$ of the net cross-section A_{net} of the profiles at the cross-section weakened by the connection holes, defined by the above expression (A.4).
- The strength in the horizontal direction of the anchoring system between the reinforcement and masonry $\overline{V_{a,Rd}}$;
- the maximum horizontal force that can be withstood by the connection between the orthogonal frames $F_{c,Rd}$, defined in previous § A.1.

The tensile strength $N_{t,Rd}$ of the gross cross-section of the profiles is to be evaluated by reference to the minimum horizontal section member (between plate and L-profile) identified along the development of the reinforcement at the level considered (to be assessed on the basis of the arrangement of the modules, conditioned by the geometry of the wall and, in particular, the presence of openings). An example of a reinforced wall is shown in Figure A.7 in which reinforcement line A, in which all members have an L-shaped cross-section (frame elements) and reinforcement line B, in which, due to the presence of openings, both frame and flat elements are present. At the top of the wall there is also a continuous kerb which is realised by means of a metal profile: at this reinforcement height, the strength $N_{t,Rd}$ must be evaluated considering the geometry of the element's cross-section.

The strength in the horizontal direction of the anchoring system between the reinforcement and the masonry $\overline{V_{a,Rd}}$ is determined by multiplying the strength of the single anchor (evaluated according to what is reported in the previous § A.2) by the smallest number $n_{a,min}$ of those present in the two rigid bodies into which the portion of wall involved in the kinematics is divided by the plastic hinge C. Unlike the previous contributions, the value of $\overline{V_{a,Rd}}$ cannot be assessed a priori since, in addition to depending on the strength of the anchors (to be assessed by means of in situ tests or to be

obtained from the epoxy resin manufacturer's data sheets), it varies as the geometry of the rigid bodies involved in the kinematic motion changes, depending on the inclination of the diagonal hinges and the position of the vertical hinge assumed in the iterative calculation of the minimum activation multiplier.

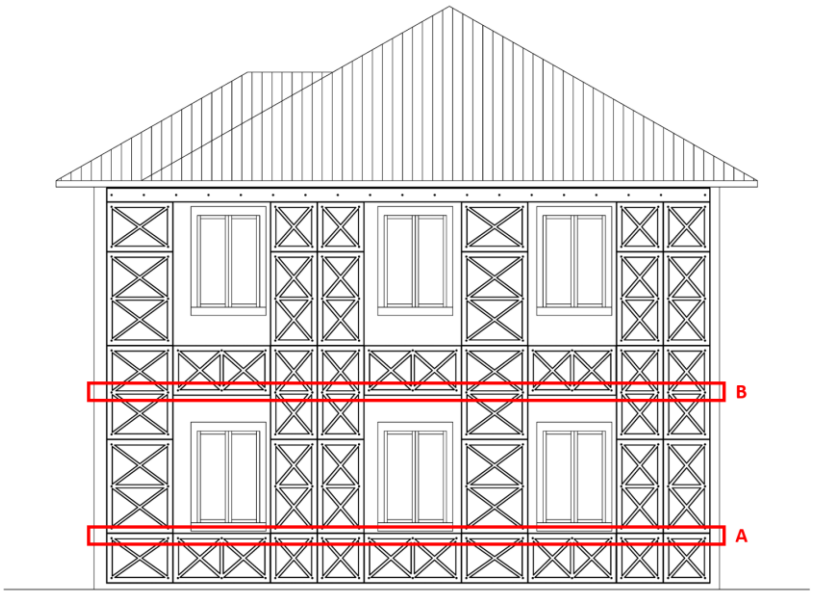

Figure A.6 Example of a wall reinforced with the Resisto 5.9 modular system.

Note the geometry of the cross-section of the horizontal elements of the modular frame at the level of the reinforcement level considered, the details of the bolted connections and the strength classes of the materials; the values of the various strength contributions considered are summarised in the following Table A.2; the lesser of these (also taking into account values not shown, since these are to be evaluated on a case-by-case basis) can be taken in the calculation as the reference value of F_{roj}.

Table A.3 Maximum force (in kN) that can be withstood by the horizontal members of the Resisto 5.9 system

$\overline{F_{t,Rd}}$	$\overline{B_{p,Rd}}$	$N_{t,Rd}$		$F_{n,Rd}$		$\overline{V_{a,Rd}}$		$F_{c,Rd}$
						$V_{a,Rd}$	$F_{b,Rd}$	
97.1	32.4	frame	117.9	frame	110.1	*, **	27.7 **	32.4
		plate	35.7	plate	***			
		kerb	*	kerb	*			

Notes: * contribution to be assessed on a case-by-case basis; ** contribution to be multiplied by $n_{a,min}$ as the kinematic chain geometry varies, *** assessment not necessary given the geometry of the frame.

A.4. Maximum out-of-plane bending moment that can be withstood by the Resisto 5.9 system applied to a gable wall

The maximum bending moment $M_{S,r}$ that can be withstood by each vertical frame element of the modular Resisto 5.9 system applied to reinforce a gable wall is evaluated as the minimum between:

- the resistant moment $M_{Rd,L}$ of the L-profile:

$$M_{Rd,L} = \frac{W_{el} f_{yk}}{\gamma_{M0}} \tag{A.12}$$

- the bending moment $M_{Rd,c}$ corresponding to the maximum tensile strength of the bolted connection between the reinforcing elements at the base of the gable wall and the modular frames arranged at the lower level, in turn defined as the lower of the tensile strength of the individual bolt $F_{t,Rd}$ and the puncture strength $B_{p,Rd}$ of the frame plate of the modular frame resulting from the above expressions (A.1) and (A.2):

$$M_{Rd,c} = p \cdot min\{F_{t,Rd}\ ;\ B_{p,Rd}\} \tag{A.13}$$

with p distance between the bolts.

The resistant moment $M_{Rd,L}$ of the upright is evaluated with reference to the elastic modulus of strength W_{el}. With reference to the symbols shown in Figure A.7 in which the cross-section of the metal element is depicted, W_{el} it can be evaluated as specified below.

$$y_G = \frac{BH^2 - bh^2}{2(BH - bh)} \tag{A.14}$$

$$I_x = \frac{BH^3 - bh^3}{3} - \frac{(BH^2 - bh^2)^2}{4(BH - bh)} \tag{A.15}$$

$$\begin{cases} W'_x = \dfrac{I_x}{y_G} \\ W''_x = \dfrac{I_x}{H - y_G} \end{cases} \tag{A.16}$$

Given the dimensions of the cross-section, they are W'_x = 5025 mm^3 and W''_x = 15444 mm^3. Taking into account the direction of deflection of the metal profile due to the tilting of the gable wall, which is expected towards the outside of the building, it is assumed in the calculation $W_{el} = W''_x$ that, given the class of steel, it follows$M_{Rd,L}$ = 3.68 kNm.

Given the geometry of the connection, illustrated in Figure A.2(a) and the class of materials (frame and bolts), the maximum moment that can be withstood by the single bolted connection at the base of the reinforcement is $M_{Rd,c}$ = 0.95 kNm.

In conclusion, when evaluating the overturning mechanism of the gable wall reinforced by means of the Resisto 5.9 system, it is assumed that the stabilising moment increase offered by each of the n_{rt} vertical framing elements of the metal modules is $M_{S,r}$ = 0.95 kNm.

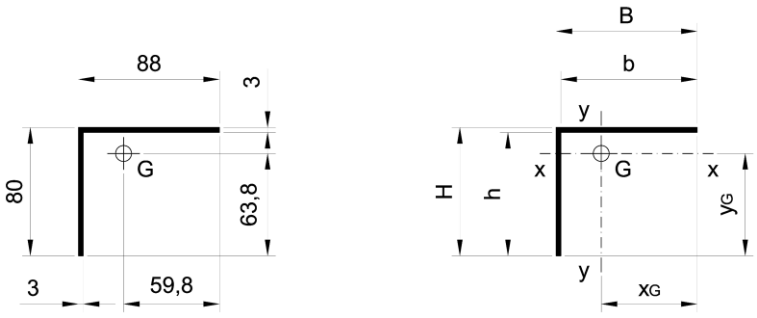

Figure A.7 Geometry of the L-profile cross-section of the vertical frame element of the modular frame.